Photoinduced electron transfer in model systems of photosynthesis

Promotor: dr. T. J. Schaafsma,
hoogleraar in de moleculaire fysica

Ulbert Hofstra

Photoinduced electron transfer in model systems of photosynthesis

Proefschrift
ter verkrijging van de graad van
doctor in de landbouwwetenschappen,
op gezag van de rector magnificus,
dr. C. C. Oosterlee,
in het openbaar te verdedigen
op woensdag 25 mei 1988
des namiddags te vier uur in de aula
van de Landbouwuniversiteit te Wageningen

NN08201, 1223

STELLINGEN

1. De snelheid van "through-bond" electron transport door een keten, die een electron-donor en -acceptor verbindt, is afhankelijk van het electronenzuigend karakter van de groepen, waaruit de keten bestaat.

   Dit proefschrift, hoofdstuk 4.2 en 6.

2. Onder bepaalde omstandigheden wordt de electronische configuratie van de laagste aangeslagen toestanden van een porfyrine bepaald door de omgeving.

   Dit proefschrift, hoofdstuk 4.1.

3. Bij donor-acceptor verbindingen met een flexibele keten is de fluorescentielevensduurmeting geen geschikte techniek voor de bepaling van de electron overdrachtssnelheid, als deze even groot of sneller is dan de snelheid, waarmee de conformatie van de keten verandert.

4. De spectroscopische veranderingen in een oplossing van porfyrine en benzochinon in chloroform bij belichting met blauw licht moeten niet worden verklaard door complexvorming, maar door een fotochemische omzetting.

   T.Ueda, A.Tanaka en M.Iqarashi, Spectrochim.Acta 42A (1986) 209.

5. Sigvardson et al. beweren ten onrechte dat pentafluoropropionzuur geschikter is als derivatiseringsreagens voor electron capture detectie dan trifluorazijnzuuranhydride.

   K.W.Sigvardson, J.M.Kennish en J.W.Birks, Anal.Chem. 56 (1984) 1096.

6. Het feit dat het M13 mantel eiwit in de geaggregeerde irreversibele β-structuur moet worden beschouwd als gedenatureerd eiwit wordt onvoldoende erkend als belangrijk voor de fysiologische relevantie van de fysische metingen aan dit eiwit.

   P.K.Walber en B.S.Hudson, Biophys.J. 37 (1982) 253.
   L.M.Smith, B.A.Smith en H.M.McConnell, Biochemistry 18 (1979) 2256.

7. SQL en andere, vergelijkbare, vraagtalen voor relationele databases zullen niet geschikt zijn als hulpmiddel voor eindgebruikers, zolang queries volgens een strakke syntax geformuleerd moeten worden en zolang voor het beantwoorden van een vraag meerdere queries mogelijk zijn.

8. Gezien het feit dat arbeidsbureau's niet bemiddelen om academici in hun eigen vakgebied te plaatsen, is het merkwaardig dat pas afgestudeerden reeds na een maand een oproep tot omscholing ontvangen. Deze oproep dient als prematuur te worden aangemerkt.

9. De sterk verlaagde aanvangssalarissen van beginnende promovendi zullen de mobiliteit van pas afgestudeerden tussen de instellingen niet bevorderen.

10. Een waterstofeconomie die gebaseerd is op waterstofgas productie in kolloidale systemen is gebouwd op drijfzand.

11. Bij vervanging van de militaire dienstplicht door een beroepsleger kan veel creativiteit, gericht op het verkrijgen van vrijstelling, aangewend worden voor maatschappelijk nuttige toepassingen.

14. Na invoering van de verplichte OV-kaart voor studenten kan nog een aanzienlijke bezuiniging op de kosten van de studentenhuisvesting worden behaald door uitbreiding van de nachtdienstregeling van de Nederlands Spoorwegen.

Ulbert Hofstra

Photoinduced electron transfer in model systems of photosynthesis

Wageningen, 25 mei 1988

Aan mijn ouders
Aan Els

VOORWOORD

Velen hebben in de afgelopen vier jaar bijgedragen tot de totstandkoming van dit proefschrift. Allereerst wil ik iedereen van de vakgroep Moleculaire Fysica, tappers en wp'ers, studenten, binnen- en buitenlandse medewerkers en alle quantum jumpers, hartelijk danken voor hun steun en voor de sfeer op de vakgroep, waardoor het er goed toeven was.

Enkele mensen wil ik met name noemen, waaronder mijn promotor prof. T.J.Schaafsma. Tjeerd, ik wil je hartelijk danken voor de manier, waarop je vaak een heldere lijn zag in duistere meetresultaten en voor de flitsende, al dan niet juiste, verklaringen voor waargenomen fenomenen.

De schier onbegrensde synthetische capaciteiten van Rob Koehorst hebben in hoge mate bijgedragen aan dit proefschrift. Rob, jouw enthousiasme en creativiteit hebben mij veel nieuwe mogelijkheden geboden. De structuren die uit plastic bolletjes waren geboren bleken vaak ook uit de kolf te kunnen komen.

Mijn andere mede-fotosynthetici, Bert Benthem (in het prille begin), Hans-Walter Krüger, Fred van Wijk, Peter Gast, Raymond Verhaert en Geoff Searle bedank ik voor experimentele hulp en voor stimulerende discussies. Geoff, ik wil je ook bedanken voor je NMR berekeningen, waar ik dankbaar op voort kon bouwen

De sterk gegroeide samenwerking met de organici Geoske Sanders, Rien van Dijk en Fred Roeterdink heb ik bijzonder op prijs gesteld. Beb van Veldhuizen wil ik bedanken voor de kundige wijze, waarop hij porfyrine NMR spectra heeft gemeten.

Doctoraal studenten hebben een gewaardeerde bijdrage aan dit onderzoek geleverd. In chronologische volgorde wil ik Marinette van der Graaf, die nog een prettig lang negenmaands vak deed, Alfred Koetsier, die zich een onsterfelijke reputatie verwierf, Marleen de Bueger, Theo Roelofs en Frank Vergeldt, die allen met de transient absorptie opstelling stoeiden en Dirk Huckriede, onze computer-expert, bedanken.

I want to thank Mike Wasielewski and Doug Johnson (Argonne National Laboratory) for our cooperation and for their hospitality during my

stay in Argonne.

Jannie Bijl en Riet Mes, jullie wil ik vooral bedanken voor het vervelende corrigeren van ↑ en ↓ op een onwillige tekstverwerker.

De fotografen en de mensen van de tekenkamer, met name Arie Bergwerff dank ik voor de reproductie van vrijwel alle tekeningen.

De hulp van Adrie de Jager en Arie van Hoek was onmisbaar voor vele van de in dit boekje beschreven experimenten. Jullie optische en electronische kennis is een rots in de branding van elk promotieonderzoek.

Tot slot wil ik mijn vriendin Els Rijnierse bedanken dank zij wie niet zozeer het onderzoek als wel ik zelf op de been bleef gedurende de afgelopen jaren.

Ik vraag allen die ik niet met name bedankt heb mij dit niet kwalijk te nemen. Mijn dank is groot.

Ulbert Hofstra, maart 1988

CONTENTS

		page
1	INTRODUCTION	1
2	THEORY OF PHOTOINDUCED ELECTRON TRANSFER PROCESSES	13
2.1	Introduction.	13
2.2	Electronic factors.	14
2.3	Nuclear factors.	20
3	EXPERIMENTAL METHODS	29
3.1	EPR spectra.	29
3.2	ODMR spectra and fluorescence fading experiments.	29
3.3	Fluorescence lifetime measurements.	30
3.4	Transient absorption measurements.	31
	1. ms - μs region.	31
	2. ns - ps region.	33
4	MODEL COMPOUNDS WITH A DIPHENYLETIOPORPHYRIN AS PHOTOSENSITIZER AND ANTHRAQUINONE AS ELECTRON ACCEPTOR	35
4.1	Optical and FDMR spectroscopy of diphenyletioporphyrin. (Chem. Phys. Lett. 144 (1988) 125)	35
4.2	Picosecond charge separation and triplet formation in a closely spaced photosynthetic model system.	41
4.3	A comparison of electron transfer between free and linked donor and acceptor compounds.	59
5	DIMERS OF OPPOSITELY CHARGED WATER-SOLUBLE PORPHYRINS	65
5.1	Excited state properties of water-soluble porphyrin dimers. (Chem. Phys. Lett. 130 (1986) 555)	65

5.2 Solution structure of porphyrin aggregates determined by ^{1}H NMR ring current shifts. I. Heterodimers of oppositely charged porphyrins. (Magn. Res. Chem. 25 (1987) 1069) 71

5.3 II. Conformations of dimers and higher aggregates of water-soluble porphyrins. (Magn. Res. Chem. 26 (1988) 167) 77

5.4 Extension of water-soluble porphyrin dimers towards modular model systems for photoinduced electron transfer. 83

6 PHOTOINDUCED ELECTRON TRANSFER IN DONOR-PORPHYRIN-ACCEPTOR MODEL SYSTEMS AND THEIR COMPONENTS. 97

6.1 Introduction. 97

6.2 Experimental. 99

6.3 Determination of the solution structure by ^{1}H NMR. 101

6.4 Redoxpotential and fluorescence lifetime measurements. 107

6.5 Discussion. 110

6.6 Donor-porphyrin-acceptor triads. 112

7 EXCITED STATE KINETICS OF PARAMAGNETIC PORPHYRIN DIMERS. 115

7.1 Introduction. 115

7.2 Experimental. 117

7.3 Zn-porphyrin with a nearby Cu(II)-ion. 118

7.4 Oppositely charged porphyrin dimers. 121

7.5 Covalently linked porphyrin dimers. 122

7.6 Ligated porphyrin dimers. 125

7.7 Conclusion. 131

8 SUMMARY 135

Chapters 4.1, 5.1, 5.2 and 5.3 are reproduced with kind permission of The North-Holland Publishing Company (Chemical Physics Letters) and John Wiley and Sons Limited (Magnetic Resonance in Chemistry).

CHAPTER 1

Introduction

Light energy from the sun is captured in photosynthesis and stored in energy-rich compounds. The process involves the separation of an electron from a photoexcited donor and the transfer of this electron to suitable acceptors to produce high-energy redox intermediates. In artificial solar energy systems light energy is transformed into electrical energy or chemical energy, using transfer of electrons from a photoexcited donor into an electrical circuit or to an electron acceptor molecule.

Photoinduced electron transfer (ET) is the common factor in natural and artificial solar energy systems. The factors affecting the electron transfer rates are not all well-understood. It is therefore of importance to study this process and a wide body of research is devoted to this subject [1]. A fruitful way to study photoinduced electron transfer is the synthesis of model systems, containing an electron donor and an electron acceptor molecule, exhibiting electron transfer from the donor to the acceptor after photoexcitation of one of the components. By using different model systems several properties of these model systems , e.g. geometry, medium, distance and energy, can be varied to study their effect on the electron transfer rate.

The study of model systems for photoinduced electron transfer is the subject of this Thesis, and serves two purposes. Firstly, model systems are used to understand how photosynthetic electron transfer in natural systems works and secondly, they are used to devise efficient artificial solar energy systems.

The primary ET steps in photosynthesis occur between a number of different pigments, which are organized as a unit in a membrane protein. This unit is called the photosynthetic reaction centre. The structure of the reaction centres of some photosynthesizing bacteria is now known from X-ray crystallography [2-4] (figure 1). Also much progress has been made in elucidating the kinetics of the various ET steps [5-14]. Excitation energy is transferred to the reaction centre after absorption of a light photon by an antenna system of chlorophylls [5,6]. At the reaction centre highly efficient charge

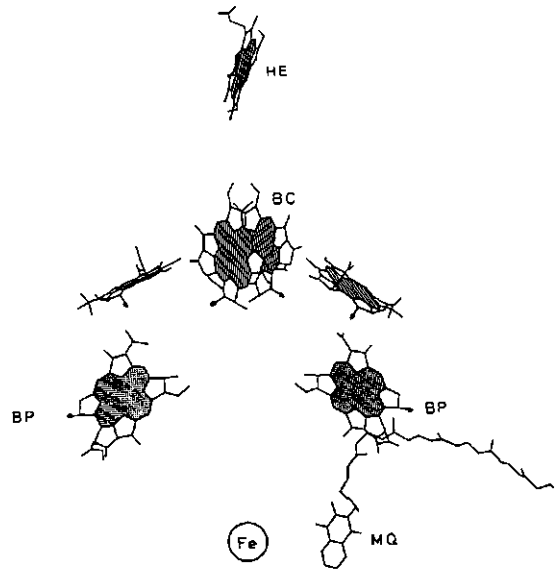

Figure 1: Position of the chromophores in the reaction centre of the bacterium R.Viridis. BC is the primary electron donor, a dimer of bacteriochlorophyll BP is the primary electron acceptor, bacteriopheophytin, MQ is the secondary electron acceptor menaquinone, Fe is an Fe^{2+}-atom and HE is one of the four heme groups in the secondary donor cytochrome c. Adapted from ref.2.

separation occurs, starting from the so-called primary donor. For the bacterial reaction centres the ET from the primary donor, a bacteriochlorophyll dimer, to the primary acceptor pheophytin, a chlorophyll-like molecule occurs in a few picoseconds [10], possibly preceded by ET on a femtosecond time scale within the dimer [11,12]. The subsequent ET step from pheophytin to a secondary electron acceptor quinone takes place in 200 ps [10]. The electron hole on the bacteriochlorophyll dimer is filled by an electron from the electron donor cytochrome, a protein located on top of the reaction centre (figure 1), in 0.5 - 20 μsec, depending on the bacterial species [13].

Several artificial solar energy systems like semiconductor photovoltaic cells which convert light into electricity, and thermal

systems which convert light into heat, are already commercially available [14-18]. Unfortunately, this is not true for photochemical solar energy systems, which are designed to produce electricity or fuels, e.g. hydrogen (figure 2) [19-21]. Artificial solar energy systems as energy producers have to compete with another solar energy converting system, namely photosynthesis, which produces biomass as an energy source. The application of highly-efficient, energy-rich crops as solar energy converting systems is a promising source of non-limited energy [22]. Other applications of artificial solar energy systems have also become increasingly important, like the stereospecific synthesis of fine chemicals, e.g. by driving enzymatic reactions [23].

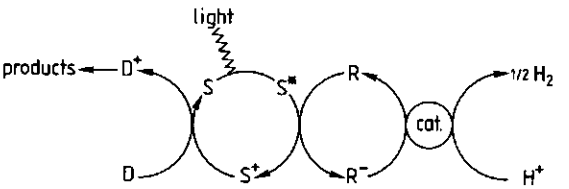

Figure 2: Scheme for the photoproduction of hydrogen. S is the photosensitive compound, e.g. a porphyrin, R is the electron acceptor, cat is a catalyst, D is the secondary electron donor, which is converted to waste products. Reproduced from ref.22.

Porphyrins, which have the same macrocycle as the natural chlorophylls, are widely used as photosensitizers in artificial solar energy systems, because they exhibit very efficient light absorption in the visible part of the spectrum, where the solar energy spectrum has a maximum. Some reviews are given in refs.24-34.

Most artificial photochemical systems, based on porphyrins as electron donors with several electron acceptors, consist of components, which are freely diffusing in solution [29,34-55]. The diffusion process may then be the rate-limiting factor for the ET process from the light-excited porphyrin to the primary electron acceptor [56]. Due to the limited rate of the diffusion process ET can not

proceed from the excited singlet state of the porphyrin, which exists only several nanoseconds in the absence of quenchers. The reaction then proceeds from the lowest excited triplet state, of which the unperturbed lifetime is in the millisecond range. The triplet state is, however at much lower energy and a considerable amount of energy is lost in the singlet-triplet conversion. ET can occur from the lowest excited singlet state for systems, in which the porphyrin and the acceptor are held at close distance, so that ET occurs sufficiently fast.

Research on linked model systems, containing porphyrins as photosensitizers has greatly expanded in recent years [59-96]. Most studies focus on ET from the porphyrin to an electron acceptor, only a few treat ET from a electron donor to the porphyrin [57,58]. The electron acceptor is in the majority of the studies benzoquinone, but also other acceptors, e.g. methylviologen [59-62], pyromellitimide [63], nitrobenzene [64] have been used. Several factors, influencing the electron transfer rate constants have been studied, e.g. distance [60,62,65,66], energy [67,68], conformation [63,69,70] and solvent [71-73]. In a few studies the porphyrin-acceptor model system has been extended, either with a second acceptor [73] or with an electron donor carotene [75,76] or N,N-dimethylaniline [77] to study multi-step electron transfer reactions. The latter two systems are of great importance, because in these systems two very fast forward ET steps on a picosecond timescale are followed by a slow recombination on a microsecond timescale.

There are far less studies of electron transfer in dimers of porphyrins and porphyrin-like molecules [97-105]. Especially noteworthy are the picosecond studies of Netzel et al. on covalently linked magnesiumporphyrin-free base porphyrin dimers [97-101].

This thesis treats several porphyrin-acceptor and porphyrin-donor systems, where the acceptor or donor can also be a porphyrin, held together by covalent linkages, by electrostatic interactions or by metal-ligand interactions. Several aspects relevant to the possible electron transfer in these compounds are studied, such as the struc-

ture of the compounds in solution, the electronic properties of the photoexcited states and the rate constants for electron transfer.

The experimental techniques, which are applied to the model systems are mainly spectroscopic techniques. NMR has been used to determine the solution structures, ESR and ODMR yield information about the electronic properties of the excited states. Time-resolved optical techniques, such as picosecond and microsecond absorption measurements as well as picosecond fluorescence measurements are used to determine electron transfer rate constants.

The contents of this Thesis are organized in the following way:

Chapter 2 contains a discussion of the theory of photoinduced electron transfer, emphasizing the factors that enhance the forward ET and minimize the backward ET.

Chapter 3 gives a description of the experimental spectroscopic techniques.

Chapter 4 treats the electron transfer in substituted diphenyletioporphyrins. It is divided in 3 parts: in § 4.1 the electronic properties of the excited singlet and triplet states of diphenyletioporphyrin are discussed; in § 4.2 the ET processes for this porphyrin to anthraquinone are treated and in § 4.3 measurements on separate porphyrin and anthraquinone molecules are compared with those on covalently linked porphyrins.

Chapter 5 deals with dimers of watersoluble porphyrins. In § 5.1 the spectroscopic properties of the excited states of the dimers are discussed. In §§ 5.2 and 5.3 the structure of the dimers in solution is determined by NMR. In § 5.4 ET in these dimers and in dimers, substituted with extra donor and acceptor groups is discussed.

Chapter 6 treats ET between tetraphenylporphyrin and several covalently linked substituents, resulting in the synthesis of a donor-prophyrin-acceptor complex.

In Chapter 7 the quenching mechanisms are discussed, which are operative between diamagnetic free base or zinc porphyrins and paramagnetic copper porphyrins.

Finally a summary of the results of this Thesis is given in Chapter 8.

References

1. Proceedings of "The Sixth International Conference on Photochemical Conversion and Storage of Solar Energy", New J. Chem. vol.11 (1987).
2. J.Deisenhofer, O.Epp, K.Miki, R.Huber and H.Michel, J. Mol. Biol. 180 (1984) 385.
3. C.H.Chang, D.Tiede, J.Tang, U.Smith, J.R.Norris and M.Schiffer, F.E.B.S. Lett. 205 (1986) 82.
4. J.P.Allen, G.Feher, T.O.Yates, D.C.Rees, J.Deisenhofer, H.Michel and R.Huber, Proc. Natl. Acad. Sci. USA 83 (1986) 8589.
5. R.M.Pearlstein, in "Photosynthesis: Energy conversion by plants and bacteria", Acad. Press Inc. 1982, vol.1, p.293.
6. R.van Grondelle, Biochim. Biophys. Acta, 811 (1985) 147.
7. W.W.Parson and R.J.Cogdell, Biochim. Biophys. Acta 415 (1975) 105.
8. D.Holten, M.W.Windsor and D.Holten, Phil. Trans. R. Soc. Lond. A 298 (1980) 335.
9. J.P.Thornber, R.J.Cogdell, B.K.Priester and R.E.B.Sefta, J. Cell. Biochem. 23 (1983) 159.
10. W.W.Parson, Ann. Rev. Biophys. Bioeng. 11 (1982) 57.
11. J.Breton, J.L.Martin, A.Migus, A.Antonetti, and A.Orszag, Proc. Natl. Acad. Sci. U.S.A. 83 (1986) 5121.
12. S.R.Meech, A.J.Hoff and D.Wiersma, Chem. Phys. Lett. 121 (1985) 287.
13. R.E.Blankenship and W.W.Parson, in "Photosynthesis in Relation to Model Systems", J.Barber ed., Elsevier, Amsterdam, 1979.
14. G.Porter, New J. Chem. 11 (1987) 173.
15. M.Claverie, New J. Chem. 11 (1987) 175.
16. J.R.Bolton and M.D.Archer in "Intersol 85", Proc.9th Bienn. Congr. Int. Sol. Energy Soc., E.Bilgen and K.G.T.Hollands eds., Pergamon, New York, 1986, p.1843.

17. S.Wagner in "Photochemical conversions", Presses Polytechniques Romandes, Lausanne, 1983, p.235.
18. A.van Heereveld, Ph.D. thesis, Groningen, 1988.
19. J.R.Bolton, Science 202 (1978) 105.
20. "Photogeneration of Hydrogen", A.Harriman and M.A.West eds., Acad. Press, London, 1983.
21. J.R.Biddle, D.B.Peterson, T.Fujita, Int. J. Hydr. Energy 10 (1986) 633.
22. M.Kleijn, Ph.D. thesis, Wageningen, 1987.
23. "Energy from Biomass: 3rd E. C. Conference", Elsevier Applied Science Publishers, London (1985).
24. C.Laane and R.Verhaert, Isr. J. Chem. 28 (1987/88) 17.
25. M.D.Archer, Proc. 3rd General Conf. European Physical Society, Bucharest, 1975
27. J.S.Connolly, Proc. Conf. Photochemical Conversion and Storage of Solar Energy, J.Rabani ed., Weizmann Science Press of Israel, Jerusalem 1982, p.175.
28. M.R.Wasielewski, Mol. Biol. Biochem. Biophys. 35, F.K.Fong ed., Springer Verlag, Berlin Heidelberg, 1982, p.234.
29. P.A.Loach, J.A.Runquist, J.L.Y.Kong, T.J.Dannhauser, K.G.Spears, Adv.Chem.Ser.210, K.M.Kadish ed., 1982, p.516.
30. A.A.Krasnovsky, Physiol. Veg. 23 (1985) 611.
31. J.H.Fendler, J.Phys. Chem. 89 (1985) 2730.
32. S.G.Boxer, Biochim. Biophys. Acta, 726 (1983) 265.
33. K.N.Ganesh, Proc. Indian Acad. Sci. (Chem. Sci.) 93 (1984) 647.
34. V.Krishnan, Current Science 54 (1985) 207.
35. A.Harriman, J. Photochem. 25 (1984) 33.
36. W.Schuhmann, H.-P.Josel and H.Parlar, Angew. Chem. 99 (1987) 264.
37. F.Castelli, NATO ASI Ser.,Ser.B 105, Laser Appl. Chem. (1984) 225.
38. K.C.Cho, C.M.Che, K.M.Ng and C.L.Choy, J. Phys. Chem. 92 (1987) 3690.
39. Z.B.Alfassi, A.Harriman, S.Mosseri and P.Neat, Int. J. Chem. Kinet. 18 (1986) 1315.
40. K.Maruyama, H.Furuta and A.Osuka, Tetrahedr. 42 (1986) 6149.
41. M.Hoshino, H.Seki and H.Shizuka, J. Phys. Chem. 89 (1985) 470.

42. N.Mataga, A.Karen, T.Okada, S.Nishitani, N.Kurata, Y.Sakata and S.Misumi, J. Phys. Chem. 88 (1984) 4650.
43. N.Mataga, A.Karen, T.Okada, S.Nishitani, N.Kurata, Y.Sakata and S.Misumi, J. Phys. Chem. 88 (1984) 5138.
44. T.K.Chandrasekhar and V.Krishnan, Can. J. Chem. 62 (1984) 475.
45. D.Holten, M.W.Windsor, W.W.Parson and M.Gouterman, Photochem. Photobiol. 28 (1978) 951.
46. L.A.Margulis, I.V.Khudyakov and V.A.Kuzmin, Chem. Phys. Lett. 124 (1986) 483.
47. R.Livingston, L.Thompson and M.V.Ramarao, J. Am. Chem. Soc. 74 (1952) 1073.
48. D.Huppert, P.M.Rentzepis and G.Tollin, Biochim. Biophys. Acta 440 (1976) 356.
49. K.Maruyama, H.Furuta and T.Otsuki, Chem. Lett. (1980) 857.
50. L.V.Natarajan, L.R.Humphreys and R.Chang, Spectr. Lett. 18 (1985) 219.
51. K.Maruyama and H.Furuta, Chem. Lett. (1986) 473.
52. S.M.B.Costa and R.Brookfield, J. C. S. Faraday Trans. 2 82 (1986) 991.
53. I.Okura, S.Aono, M.Hoshino and A.Yamada, Inorg. Chim. Acta 86 (1984) L55.
54. G.S.Nahor and J.Rabani, J. Phys. Chem. 89 (1985) 2468.
55. P.Neta, A.Scherz and H.Levanon, J. Am. Chem. Soc. 101 (1979) 3624.
56. Maillard, S.Gaspard, P.Krausz and C.Gianotti, J. Organomet. Chem. 212 (1981) 185.
57. G.J.Kavarnos and N.Turro, Chem. Rev.86 (1986) 401.
58. S.Kojo, K.Morimitsu and I.Tabushi, Chem. Lett. (1987) 2095.
59. A.Harriman and R.J.Hosie, J. Photochem. 15 (1981) 163.
60. G.Blondeel, D.de Keukeleire, A.Harriman and L.R.Milgrom, Chem. Phys. Lett. 118 (1985) 77.
61. A.Harriman, Inorg. Chim. Acta 88 (1984) 213.
62. A.Harriman, G.Porter and A.Wilowska, J. C. S. Faraday Trans. 2 80 (1984) 191.
63. Y.Kanda, H.Sato, T.Okada and N.Mataga, Chem. Phys. Lett. 129 (1986) 306.

64. R.J.Harrison, B.Pearce, G.S.Beddard, J.A.Cowan and J.K.M.Sanders, Chem. Phys. 116 (1987) 429.

65. G.Bhaskar Marya and V.Krishnan, J. Phys. Chem. 89 (1985) 5225.

66. A.D.Joran, B.A.Leland, G.G.Geller, J.J.Hopfield and P.B.Dervan, J. Am. Chem. Soc. 106 (1984) 6090.

67. S.Nishitani, N.Kurata, Y.Sakata, S.Misumi, M.Migita, T.Okada and N.Mataga, Tetrahedr. Lett. 27 (1981) 2099.

68. A.D.Joran, B.A.Leland, P.M.Felker, A.H.Zewail, J.J.Hopfield and P.B.Dervan, Nature 327 (1987) 508.

69. M.P.Irvine, R.J.Harrison, G.S.Beddard, P.Leighton and J.K.M.Sanders, Chem. Phys. 104 (1986) 315.

70. J.S.Connolly, K.L.Marsh, D.R.Cook, J.R.Bolton, A.R.McIntosh, A.Siemiarczuk, A.C.Weedon and T.-F. Ho, Sci. Pap. Inst. Phys. Chem. Res. 78 (1984) 118.

71. A.R.McIntosh, J.R.Bolton, J.S.Connolly, K.L.Marsh, D.R.Cook, T.-F.Ho and A.C.Weedon, J. Phys. Chem. 90 (1986) 5640.

72. M.D.Archer, V.Y.Gadzepko, J.R.Bolton, J.A.Schmidt and A.C.Weedon, J. C. S. Faraday Trans. 2 82 (1986) 2305.

73. J.L.Y.Kong, K.G.Spears and P.A.Loach, Photochem. Photobiol. 35 (1982) 545.

74. J.R.Bolton, T.-F.Ho, S.Liauw, A.Siemiarczuk, C.S.K.Wan and A.C.Weedon, J. C. S. Chem. Comm. (1985) 559.

75. S.Nishitani, N.Kurata, Y.Sukata, S.Misumi, A.Karen, T.Okada and N.Mataga, J. Am. Chem. Soc. 105 (1983) 7771.

76. D.Gust, T.A.Moore, P.A.Liddell, G.A.Nemeth, L.R.Makings, A.L.Moore, D.Barrett, P.J.Pessiki, R.V.Bensasson, M.Rougee, C.Chachaty, F.C.De Schrijver, M.Van der Auweraer, A.R.Holzwarth and J.S.Connolly, J. Am. Chem. Soc. 109 (1987) 846.

77. T.A.Moore, D.Gust, P.Mathis, J.-C.Mialocq, C.Chachaty, R.V.Bensasson, E.J.Land, D.Doizi, P.A.Liddell, W.R.Lehman, G.A.Nemeth and A.L.Moore, Nature 307 (1984) 630.

78. M.R.Wasielewski, M.P.Niemczyk, W.A.Svec and E.B.Pewitt, J. Am. Chem. Soc. 107 (1985) 5562.

79. E.I.Kapinus, M.M.Alekantina, V.P.Staryi, V.I.Boghillo and I.I.Dilung, J. C. S. Faraday Trans.2 81 (1985) 631.

80. M.Migita, T.Okada, N.Mataga, S.Nishitani, N.Kurata, Y.Sakata and S.Misumi, Chem. Phys. Lett. 84 (1981) 263.
81. M.R.Wasielewski and M.P.Niemczyk, J. Am. Chem. Soc. 106 (1984) 5043.
82. T.-F Ho, A.R.McIntosh and A.C.Weedon, Can. J. Chem.62 (1984) 967.
83. M.A.Bergkamp, J.Dalton and T.L.Netzel, J. Am. Chem. Soc. 104 (1982) 253.
84. N.Mataga, A.Karen, T.Okada, S.Nishitani, N.Kurata, Y.Sakata and S.Misumi, J. Phys. Chem.88 (1984) 5138.
85. J.L.Y.Kong and P.A.Loach, Frontiers of Biol.Energ. 1, Acad. Press. Inc. (1978).
86. J.S.Lindsey, D.C.Mauzerall and H.Lindschitz, J. Am. Chem. Soc. 105 (1983) 6528.
87. A.R.McIntosh, A.Siemiarczuk, J.R.Bolton, M.J.Stilman, T.-F.Ho and A.C.Weedon, J. Am. Chem. Soc. 105 (1983) 7215.
88. A.Siemiarczuk, A.McIntosh, T.-F.Ho, M.J.Stillman, K.J.Roach, A.C.Weedon, J.R.Bolton and J.S.Connolly, J. Am. Chem. Soc. 105 (1983) 7224.
89. T.-F.Ho, A.R.McIntosh and J.R.Bolton, Nature 286 (1980) 254.
90. Y.Sakata, S.Nishitani, N.Nishimizu, S.Misumi, A.R.McIntosh, J.R.Bolton, Y.Kanda, A.Karen, T.Okada and N.Mataga, Tetrahedr. Lett. 26 (1985) 5207.
91. J.S.Lindsey, D.C.Mauzerall, J. Am. Chem. Soc. 104 (1982) 4498.
92. J.Weiser and H.A.Staab, Angew. Chem. 23 (1984) 623.
93. P.Leighton and J.K.M.Sanders, J. C. S. Chem. Comm. (1985) 24.
94. J.A.Schmidt, A.Siemiarczuk, A.C.Weedon and J.R.Bolton, J. Am. Chem. Soc. 107 (1985) 6112.
95. J.Dalton and L.R.Milgrom, J. C. S. Chem. Comm. (1979) 609.
96. G.Krieger, J.Weiser and H.A.Staab, Tetrahedr. Lett. 26 (1985) 6055.
97. G.S.Nahor, J.Rabani and F.Grieser, J. Phys. Chem. 85 (1985) 697.
98. T.L.Netzel, P.Kroger, C.K.Chang and I.Fujita, Chem. Phys. Lett. 67 (1979) 223.
99. T.L.Netzel, M.A.Bergkamp, C.K.Chang, J. Am. Chem. Soc. 104 (1982) 1952.

100.I.Fujita, J.Fajer, C.K.Chang, C.-B.Wang, M.A.Bergkamp and T.L.Netzel, J. Phys. Chem. 86 (1982) 3754.

101.I.Fujita, T.L.Netzel, C.K.Chang and C.-B.Wang, Proc. Natl. Acad. Sci. USA 79 (1982) 413.

102.M.A.Bergkamp, C.K.Chang and T.L.Netzel, J. Phys. Chem. 87 (1983) 4441.

103.P.Neta, J. Phys. Chem. 85 (1981) 3678.

104.Gitzel, H.Ohno, E.Tsuchida and D.Woehrle, Polymer 27 (1986) 1781.

105.M.J.Perlin, K.J.Kaufmann and M.R.Wasielewski, Nature 278 (1979) 54.

106.J.E.Hunt, J.J.Katz, A.Svirmickas, J.C.Hindman, J. Am. Chem. Soc. 106 (1984) 2242.

CHAPTER 2

Theory of photoinduced electron transfer processes

2.1 Introduction

This chapter treats the theory of photoinduced electron transfer (ET) with an emphasis on donor-acceptor (D-A) model systems of photosynthetic reaction centres.

For the construction of an effective model system the first forward ET step should not be followed by a fast recombination to the ground state for two reasons: (i) in practically usable systems the stored chemical energy from the first ET step should be used in subsequent reactions and (ii) if subsequent reactions are blocked, preferably a true model system should exhibit the recombination to the donor triplet state, as occurs in photosynthetic reaction centres. Several factors, affecting the forward and backward rates of ET processes will be discussed in this chapter, some of which are well understood by now, but many are not.

If the Born-Oppenheimer approximation is valid, i.e. the configuration of the nuclei does not change at the moment that the electron transfer takes place, the equation governing the rate constant for transfer of an electron for a pair of molecules at a distance r, can be separated into an electronic part and a nuclear part:

$$k_{ET}(r) = 2\pi/h.V(r)^2.FC \qquad (1)$$

V(r) is the electronic coupling between the initial and final states, D*-A and D^+-A^- and FC is the Franck-Condon weighted density of vibronic and solvent modes, which expresses the difference in equilibrium nuclear configuration for D*-A and D^+-A^-. V is given by:

$$V = (1-S^2)^{-\frac{1}{2}}.(\langle\Phi_f|\, H^{int}\,|\Phi_i\rangle - S.\langle\Phi_i|\, H^{int}\,|\Phi_i\rangle) \qquad (2)$$

S is the overlap integral $\langle\Phi_i|\,\Phi_f\rangle$. The second right hand term results from the non-orthogonality of the initial and final states Φ_i and Φ_f.

If interactions of the transferred electron with other electrons are not explicitly included in the hamiltonian, H^{int} is equal to V_A, the interaction of the electron with the acceptor.

Equation (1) is valid for molecules with a fixed donor-acceptor distance r. If the donor and the acceptor are free in solution or are linked by a flexible chain, the donor and the acceptor have to diffuse to within a distance at which ET can occur and the observed rate constant is given by: $1/k_{ET}^{obsd} = 1/k_{diff} + 1/k_{act}$, [1] where k_{diff} is the diffusion controlled rate constant for the formation of the precursor complex [D*,A] and k_{act} is the activation controlled rate constant. This rate constant would be observed, if the rate constants for formation and dissociation of [D*,A] are much larger than k_{ET}, i.e. during ET the precursor complex [D*,A] remains always in equilibrium with the separated reactants [1].

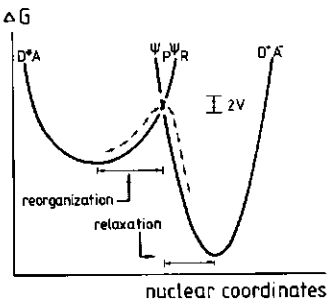

Figure 1:
A potential energy description of ET from a photoexcited donor D to an acceptor A. V is the electronic coupling matrix element for the interaction between the reactant and product potential surfaces.

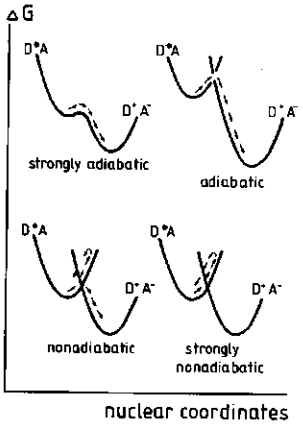

Figure 2:
Cross-section through potential energy surfaces for adiabatic and non-adiabatic ET (after ref.13).

2.2 Electronic factors

The magnitude of the electronic coupling depends on a large number

of factors, such as distance [2-4], mutual orientation [5,6], nature of the bridge [7-11] and solvent modes [3]. Also the spin dynamics exert an effect on the ET pathway [12].

The importance of the electronic coupling can be pictured in a potential energy surface description of photoinduced electron transfer (figure 1) [13].
$2|V|$ is equal to the splitting between the upper and lower potential energy levels at the crossing point. At large V the ET reaction is adiabatic and the process goes smoothly from the potential energy surface of the initial state to that of the final state. If V is much smaller than the difference between the energy of the initial state at its minimum and the energy at the crossing point, the reaction is non-adiabatic. Then an energy level-crossing has to take place from the reactant potential energy surface to the product potential energy surface and ET does not occur every time that the system reaches the crossing point (figure 2).

The matrix element of the electronic coupling V is related to the spin-exchange interaction J, described by the hamiltonian $-J.S_1.S_2$, where S_1 and S_2 are the electron spin operators for the two spins on D^+ and A^- in the final state D^+-A^- [14-17]. The configuration interaction between the singlet state of the photoexcited donor D*-A and that of the radical pair D^+-A^- contributes to the energy splitting J between the singlet and triplet states of the radical pair. For ET from D*-A to D^+-A^- J is directly related to V, only if the main contribution to J arises from the configuration interaction between the initial state Φ_i (D*-A) and the final state Φ_f (D^+-A^-) [17]:

$$J = -2V^2/U \qquad (3)$$

where U represents the electronic energy difference between the two states Φ_i and Φ_f.

Distance dependence

V strongly depends on the distance between the donor and the accep-

tor and has a maximum for ET from D*-A to D^+-A^-, if the overlap between the donor LUMO and acceptor LUMO also has a maximum. Consequently, charge separation via an exciplex pathway is very rapid, because of the large donor-acceptor orbital overlap [13]. V depends exponentially on the donor-acceptor distance r [2]:

$$V = V_0 . e^{-\alpha(r-r_0)/2} \qquad (4)$$

r_0 is the distance of closest approach between donor and acceptor; V_0 is the electronic coupling at r_0. Combining (1) and (4) gives:

$$k_{ET} = k_0 . e^{-\alpha(r-r_0)} \qquad (5)$$

where k_0 is the maximum rate constant for ET at the passage point. k_0 is $\approx 10^{13}$ (sec^{-1}), limited by vibrational motions. Some illustrative cases for the distance dependence, represented by α (eqn.5), are given in Table I.

Table I: The ET rate constant at several values of α and $r-r_0$

k_{ET} (sec^{-1})	α (A^{-1})	$r-r_0$ (A)
10^3	2.0	5
10^5	1.2	15
10^8	1.2	10
10^9	1.2	5
10^9	0.9	10

The factor α strongly depends on the medium. In the absence of a medium α is determined by the direct orbital overlap between donor and acceptor orbitals. At large distance, such that the orbital shapes can be neglected, α is typically 2.6 $Å^{-1}$ [18]. In a rigid medium α decreases to ca. 1.1 $Å^{-1}$ [19]. In a rigid medium ET has been observed over distances up to 34 Å [3]. In a solvent the orbitals of the solvent

molecules between the donor and the acceptor molecule can contribute to V. This so-called superexchange mechanism leads to a decrease of α w.r.t. its value in the absence of a medium. Both filled and unfilled solvent orbitals contribute to the electron superexchange coupling. An expression can be derived for α, using the superexchange model of McConnell [3]:

$$\alpha = d^{-1}\ln(B/\beta) \qquad (6)$$

where d is the spatial distance between two solvent molecules, participating in the ET process, β is the interaction between the adjacent solvent states and B is the energy required to transfer the electron from the donor to an empty solvent orbital or from a filled solvent orbital to the acceptor (depending on which orbitals of the solvent contribute to the superexchange mechanism) (figure 3).

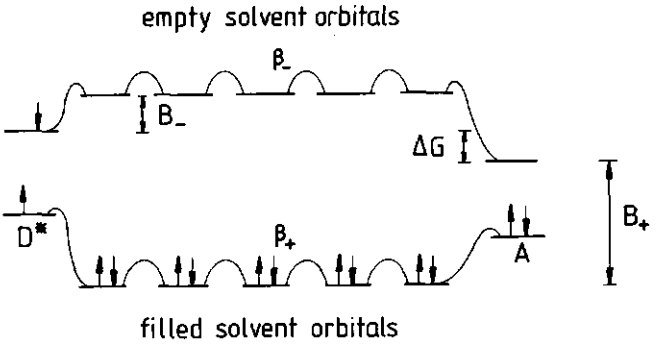

Figure 3: Energy level diagram for the superexchange model for photoinduced ET from D*-A to D^+-A^- (adapted from ref.2).

Linking bridge

In the presence of a bridge between donor and acceptor the through-bond coupling is usually stronger than the abovementioned through-solvent coupling. Even saturated hydrocarbon spacers contribute significantly to through-bond interactions [8-10,20-22]. For a norborane-

linked model system α was found to be 20 % smaller than found for ET between identical free donor and acceptor molecules in a rigid solvent [2,9,22]. For dienes separated by σ-bonds V(r) was calculated to decrease only a factor 200, upon a change from a 5-bond diene (6.2 Å) to a 17-bond diene (21 Å) [23], resulting in α = 0.5 $Å^{-1}$. The through-bond interactions may be substantially higher, when the spacer contains π orbitals. In a linking chain, consisting of several phenyl groups the addition of extra phenyl groups causes only a slight attenuation of the ET rate constants [24,25]. The energies of the molecular orbitals of the spacer w.r.t. those of the donor and acceptor are also important. The replacement of a 1,4-phenyl in the linking bridge by a 1,4-naphthalene, having lower orbital energies, leads to a significant increase of the ET rate [24,25].

Conformation

The conformation of a donor-acceptor system influences the ET rate constant. In covalently linked donor-acceptor molecules the ET rate constant can be very different for different conformations and the observed rates may be controlled by conformational interconversion [26,27].

A high value of V for forward ET is mostly accompanied by a similar high value of V for backward ET. But there are differences, because V for both processes represents the coupling between different states. The rate constant for forward ET depends on the electronic coupling between the LUMO's of donor and acceptor, whereas the recombination rate constant is determined by the coupling between the acceptor LUMO and the donor HOMO. A large difference was found between forward ET from a photoexcited magnesium porphyrin to a free base porphyrin ($>10^{11}$ s^{-1}) and backward ET in the reverse direction ($\approx 10^{9}$ s^{-1}) in a cofacial porphyrin dimer [28], as opposed to the similar rate constants for both processes for a "jawed" dimer ($\approx 10^{9}$ s^{-1}) [29]. Using π-orbitals of the type Φ_m = cos(mϕ) or sin(mϕ), for m = 4 yielding the HOMO (4,π) and for m = 5 the LUMO (5,π) orbitals, a high value of V is calculated for cofacial (5,π) -> (5,π) forward ET and a low value of V

for (5,π) -> (4,π) backward ET due to the orthogonality or near orthogonality of the orbitals involved in the recombination process in the cofacial arrangement [30,31]. For the "jawed" dimer no difference was calculated between V for (5,π) -> (5,π) and for (5,π) -> (4,π) ET. The geometry of the porphyrin dimer is thus of importance for the ET rates.

Stereoelectronic effects have also been found to be important in molecules like 2-biphenyl-6-naphthyl-decalin, which shows different ET rates for its stereoisomers [8].

Spin dynamics

In the bacterial reaction centre the radical pair can recombine to the donor triplet state [32]. This recombination pathway is possible, because of spin dephasing in the radical pair due to hyperfine interactions and differences in g-values. The formation of the donor triplet state from the radical pair state by spin dephasing results in a very characteristic triplet ESR spectrum. The triplet ESR spectrum is specifically "anomalously" spin polarized, because only the $m_S = 0$ level of the radical pair triplet state and, subsequently, of the donor triplet state is populated [33]. Typical lifetimes of the radical pair necessary to allow for hyperfine dephasing are 10^{-9}-10^{-8} sec [34]. The exchange interaction J between the singlet and triplet radical pair states must be smaller than the hyperfine and g-value differences for the preferential recombination into the radical pair $m_S = 0$ triplet state to occur. In the bacterial reaction centre $J \approx 1 \times 10^{-4}$ eV [35].

To model the triplet recombination due to hyperfine dephasing in a model system the donor-acceptor distance should be quite large to minimize J. As shown above, J is related to the value of the electron coupling matrix element, however. If J is small, generally V is also small and ET is slow or does not occur. Triplet recombination by hyperfine dephasing has been found for flexibly linked dimethylaniline-pyrene molecules [36]. The first ET step in these compounds occurs, when the acceptor is folded back to the donor. Then the

chain unfolds, increasing the donor-acceptor distance, allowing for spin dephasing and, thereby, for recombination to the triplet state. The flexibility of the linking chain is essential for this sequence of events. No anomalously polarized triplet ESR spectrum could be detected, because triplet ESR is limited to rigid matrices at low temperature.

More-component systems

A very important method to achieve a recombination rate constant, which is much smaller than that for the charge-separation is to use systems, containing more than two components. The first ET step from the donor D to the acceptor A is then followed by an ET step to a secondary acceptor A_2 or by ET from a secondary donor D_2:

$$D^*\text{-}A\text{-}A_2 \rightarrow D^+\text{-}A^-\text{-}A_2 \rightarrow D^+\text{-}A\text{-}A_2^+$$

$$D_2\text{-}D^*\text{-}A \rightarrow D_2\text{-}D^+\text{-}A^- \rightarrow D_2^+\text{-}D\text{-}A^-$$

Chemically linked three-component molecules of the second type were examined by Moore, Gust et al. and by Wasielewski et al. [37,38]. The electronic coupling between the neighbouring molecules D and A and between D_2 and D is large, whereas the coupling between D_2 and A, which are well separated is small, slowing down the recombination rate. In a model system with more components the exchange interaction between the singlet and triplet states of the secondary or higher order radical pairs might be sufficiently low to allow hyperfine spin dephasing. In the above mentioned triad systems it does not occur, probably because J is still too large, as compared to the hyperfine interaction and g-value differences.

2.3 Nuclear factors

Most developments in ET theory focus on the Franck-Condon density in equation (1). In the Born-Oppenheimer approximation it is assumed,

that the nuclear coordinates do not change at the instant of electron transfer. The equilibrium nuclear coordinates of the vibrational states in the product of the ET process will generally differ, however, from those of the reactants and a change in nuclear coordinates is required before the ET process can take place. In addition, the solvation of the product differs from that of the reactant. Consider a charge separating step in a non-charged donor-acceptor pair: the product of the ET step is a radical pair, containing a positive and a negative charge, which polarize the surrounding solvent. Therefore, both a vibrational reorganization energy, λ_v, and a solvation reorganization energy, λ_s, are contributing to the energy required for ET to take place. The highest ET rate constant is found, when the free energy of the reaction equals the sum, λ, of both reorganization energies ($\lambda = \lambda_v + \lambda_s$). Three situations are depicted in figure 4 : (a,b) - $\Delta G < \lambda$; (c) - $\Delta G = \lambda$ and (d) - $\Delta G > \lambda$.

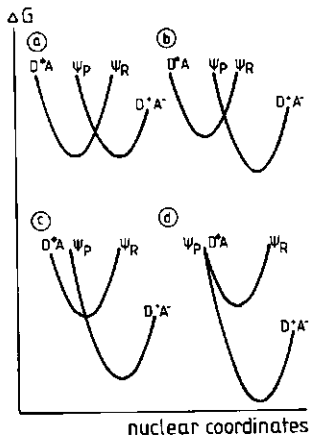

Figure 4:
Potential energy surface descriptions for ET if (a) $\Delta G = 0$; (b) $\Delta G > -\lambda$. (c) $\Delta G = -\lambda$; (d) $\Delta G < -\lambda$. Cases a-c show ET in the normal region. Case d pertains to ET in the inverted region.

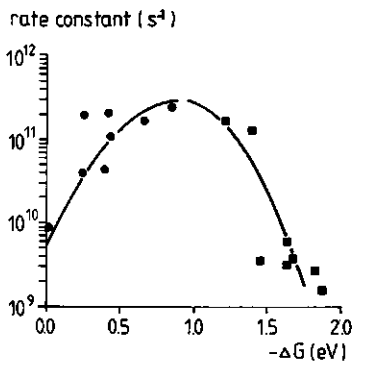

Figure 5:
Rate constant vs free energy ΔG for the reactions $D^*-A \rightarrow D^+-A^-$ (•); and $D^+-A^- \rightarrow D-A$ ( ). D represents a porphyrin and A a quinone. Reproduced from ref.42.

The value of λ can directly be determined from figure 4c. If the free energy ΔG of the ET process is small, the rate constant increases with increasing ΔG. But if ΔG exceeds λ, the rate constants decrease with increasing ΔG (this is called the "inverted region"), as can be seen from the classical Marcus expression for the ET rate constant [39] (figure 5):

$$k_{ET} = 2\pi/h.V(r)^2.(4\pi\lambda k_BT)^{-\frac{1}{2}}.\exp[-(\Delta G+\lambda)^2/4\pi\lambda k_BT] \qquad (7)$$

where ΔG is the change in free energy in the ET process, k_B is Boltzmann's constant and T is the absolute temperature. The ET rate constant k_{ET} is a maximum, if $\Delta G = -\lambda$. This effect has been predicted many years ago and has been confirmed only recently by several groups [7,19,40]. The reason for its late confirmation is, that in the past research was focussed on separated bimolecular systems, for which the magnitude of the diffusion constants of the donor and the acceptor often was the rate-limiting factor.

The expression for the free energy change, ΔG, includes the oxidation potential of the donor, $E_{ox}(D)$, the reduction potential of the acceptor, $E_{red}(A)$, the energy of the lowest excited state, from which ET occurs, $E(D^*)$, and the Coulombic attraction between the donor cation radical and the acceptor anion radical, $e^2/\epsilon r$, where r is the donor-acceptor distance [41].

$$\Delta G = E_{ox}(D) - E_{red}(A) - E(D^*) - e^2/\epsilon r \qquad (8)$$

Equation (8) must be corrected if the redoxpotentials are measured in a different solvent:

$$\Delta G = E_{ox}(D) - E_{red}(A) - E(D^*) - e^2/\epsilon r - (e^2/2)(1/r_D+1/r_A)(1/\epsilon_R-1/\epsilon) \qquad (9)$$

where ϵ_R and ϵ are the dielectric constant of the solvent, in which the redoxpotentials are measured and that of the solvent in which the ET process occurs, respectively. r_D and r_A represent the ionic radii of the donor radical cation and the acceptor radical anion. Equation

(8) reflects the macroscopic properties of the solvent and it may not be valid in close-distance complexes, where only several or even no solvent molecules can be present between the donor and the acceptor, which form a contact-ion pair. The solvent contribution to ΔG is then different and equation (8) has to be corrected by:

$$-\mu^2/a^3((\epsilon-1)/(2\epsilon+1)) - e^2/r(1-1/\epsilon) + e^2(1/r_D+1/r_A) \qquad (10)$$

where μ is the induced dipolemoment in the contact ion pair and a is the distance between the positive and negative centres of μ.

In complexes, where donor and acceptor are not at a close distance λ is between 0.5 and 1 eV [40,42,43]. For the TCNQ/naphthalene system λ_S was calculated, using known vibrations, to be 0.31 eV [44].

In equation (7) both the solvent and the vibrations are treated classically. A second model for calculating the nuclear factor in the ET rate constant treats the solvent classically, but the vibrations quantum-mechanically. The donor is assumed to be in the vibrational ground state and a single high-frequency vibrational mode of the acceptor is included in the expression for k_{ET}. The vibrational reorganization energy is taken to be that of a shifted harmonic oscillator: $\lambda_v = \frac{1}{2}.\Delta Q^2$, where ΔQ is the shift of the equilibrium positions of the normal coordinates between product and reactant. The expression is summed over m vibrational levels [45]:

$$k_{ET} = (\pi/h^2\lambda_S k_B T)^{-\frac{1}{2}}.V(r)^2.\Sigma(e^{-S}S^m/m!).\exp[-(\lambda_s+\Delta G^0+mh\upsilon)^2/4\lambda_S k_B T] \qquad (11)$$

$$S = \lambda_v/h\upsilon$$

where S is the vibrational electronic coupling strength. $h\upsilon$ can be calculated from known vibrational spectra of the acceptor. Vibrational energies representing carbon skeletal motions of the acceptor for an organic molecule of 1500 cm^{-1} [40] and 1600 cm^{-1} [46] have been used, resulting in a λ_v of 0.3 eV.

To maximize forward ET and to minimize backward ET, to achieve a high ET yield in a specific model system the reorganization parameter

should be determined for that system and then the ΔG values for forward and backward ET should be chosen by varying the acceptor in a homolog series or by varying the solvent.

The parameters in equation (11) are specific for a certain model system and a certain solvent. λ depends on the charge-solvent interactions, which are small if the radii of the reactants are large [47] as in porphyrin dimers resulting in a small λ for ET in these compounds.

Solvent reorientation

Normally it is assumed, that the reorientation of the solvent molecules occurs on a very fast time scale. The dielectric relaxation time of the solvent (a few picoseconds) does not limit the rate of the ET process [48]. For very fast ET processes, however, and for processes in very low viscosity solvents [24] the electron transfer rate is limited by the solvation time of the solvent. In a dielectric continuum model for solvation, the solvation time is equal to τ_L, the longitudinal relaxation time [49]. For a solvent which does not have a Debije relaxation distribution the rate is found to depend on $\tau_L^{-\beta}$, where β is a parameter of the frequency distribution function. The theory has been extended to solvents with two characteristic relaxation times and it was proposed, that the electron transfer rate may be limited by either of these relaxation times [50]. The relation between the ET rate and the solvent relaxation times appears, however, to be valid only for specific solvents.

Polarity of the medium

The reorganization parameter λ shifts to smaller values for apolar media, because the apolar solvent molecules hardly care to adapt to the change in charge distribution in the donor-acceptor complex upon photoinduced charge-separation [8]. For more apolar systems the curve in figure 5 shifts to the left. This shift is appropriate for ET optimalization, because i) the required free energy for the maximum for-

ward ET is small, resulting in a small loss of energy for this step and ii) if the forward ET has a small ΔG the recombination ET has a large ΔG, thereby taking place in the "inverted region", resulting in a low backward ET rate constant.

Concluding remarks

The concepts, reviewed in this chapter, have been applied to the experimental data treated in this thesis. Application is made to the effects of (i) solvent polarity (Chapters 4.2 and 6), (ii) redoxpotentials of the donor and acceptor (Chapters 6 and 7), (iii) conformation of the D-A compounds and the nature of the bridge (Chapters 4.2 and 6), (iv) freezing out the solvent motion (Chapter 5.4), (v) D-A distance (Chapter 6) and (vi) spin polarization (Chapter 4.2) on the ET rate constants.

References

1. M.D.Newton and N.Sutin, Ann. Rev. Chem. 35 (1984) 437.
2. J.R.Miller, New J. Chem. 11 (1987) 83.
3. J.R.Miller and J.V.Beitz, J. Chem. Phys. 74 (1981) 6746.
4. B.A.Leland, A.D.Joran, P.M.Felker, J.J.Hopfield, A.H.Zewail and P.B.Dervan, J. Phys. Chem. 89 (1985) 5571.
5. R.J.Cave, S.J.Klippenstein and R.A.Marcus, J. Phys. Chem. 90 (1986) 1436.
6. W.Rettig, Angew. Chem. 25 (1986) 971.
7. J.R.Miller, L.T.Calcaterra and G.L.Closs, J. Am. Chem. Soc. 106 (1984) 3047.
8. G.L.Closs, L.T.Calcaterra, N.J.Green, K.W.Penfield and J.R.Miller, J. Phys. Chem. 90 (1986) 3673.
9. J.M.Warman, M.P.de Haas, M.N.Padden-Rowe, E.Cotsaris, N.S.Hush, H.Oevering and J.W.Verhoeven, Nature 320 (1986) 615.
10. S.Larsson and A.Volosov, J. Chem. Phys. 85 (1986) 2548.
11. S.Larsson, J. Am. Chem.Soc. 103 (1981) 4834.

12. A.Ogrodnik, H.W.Kruger, H.Orthuber, R.A.Haberkorn, M.E. Michel-Beyerle and H.Scheer., Biophys. J. 39 (1982) 91.
13. G.J.Kavarnos and N.Turro, Chem. Rev. 86 (1986) 401.
14. R.Haberkorn, M.E.Michel-Beyerle and R.A.Marcus, Proc. Natl. Acad. Sci. USA 76 (1979) 4185.
15. M.Y.Okamura, R.A.Isaacson and G.Feher, Biochim. Biophys. Acta 546 (1979) 394.
16. M.Redi and J.J.Hopfield, J. Chem. Phys. 72 (1980) 6651.
17. P.Bertrand, Chem. Phys. Lett. 113 (1985) 104.
18. R.A.Marcus and P.Siders, J. Phys. Chem. 86 (1982) 622.
19. J.R.Miller, J.V.Beitz and R.Kurt Huddleston, J. Am. Chem. Soc. 106 (1984) 5057.
20. N.S.Hush, M.N.Padden-Row, E.Cotsaris, H.Oevering, J.W.Verhoeven and M.Heppener, Chem. Phys. Lett. 117 (1985) 8.
21. J.Warman, Nature 372 (1987) 462.
22. N.S.Hush, M.N.Paddon-Rowe, E.Cotsaris, H.Oevering, J.W.Verhoeven and M.Heppener, Chem. Phys. Lett. 117 (1985) 8.
23. V.Balaji, L.Ng, K.D.Jordan, M.N.Paddon-Row and H.K.Patney, J. Am. Chem. Soc. 109 (1987) 6957.
24. H.Heitele, M.E.Michel-Beyerle and P.Finckh, Chem. Phys. Lett. 134 (1987) 273.
25. H.Heitele and M.E.Michel-Beyerle, J. Am. Chem. Soc. 107 (1985) 8286.
26. R.J.Cave, S.J.Klippenstein and R.A.Marcus, J. Chem. Phys. 84 (1986) 3089.
27. B.M.Hoffman and M.A.Ratner, J. Am. Chem. Soc. 109 (1987) 6240.
28. T.L.Netzel, M.A.Bergkamp and C.K.Chang, J. Am. Chem. Soc. 104 (1982) 1952.
29. R.E.Overfield, A.Scherz, K.J.Kaufman and M.R.Wasielewski, J. Am. Chem. Soc. 105 (1983) 4256.
30. R.J.Cave, P.Siders and R.A.Marcus, J. Phys. Chem. 90 (1986) 1436.
31. R.A.Marcus, New J. Chem. 11 (1987) 79.
32. A.J.Hoff in "Triplet state ODMR Spectroscopy", R.H.Clarke ed., Wiley New York (1982), pp.367-425.
33. R.E.Blankenship, Acc. Chem. Res. 14 (1981) 163.
34. R.Kaptein in Biological Magnetic Resonance, L.J.Berliner and

J.Reuben Eds., Plenum Press, New York (1982) 145.

35. A.J.Hoff and P.Gast, J. Phys. Chem. 83 (1979) 3355.
36. A.Weller, H.Staerk and R.Treichel, Faraday Discuss. Chem. Soc. 78 (1984) 271.
37. T.A.Moore, D.Gust, P.Mathis, J.-C.Mialocq, C.Chachaty, R.V.Bensasson, E.J.Land, D.Doizi, P.A.Liddell, W.R.Lehman, G.A.Nemuth and A.L.Moore, Nature 307 (1984) 630.
38. M.R.Wasielewski, M.P.Niemczyk, W.A.Svec and E.P.Pewitt, J. Am. Chem. Soc. 107 (1985) 5562.
39. R.A.Marcus, J. Chem. Phys. 24 (1956) 966.
40. R.J.Harrison, B.Pearce, G.S.Beddard, J.A.Cowan and J.K.M.Sanders, Chem. Phys. 116 (1987) 429.
41. A.Weller, Z. Phys. Chem NF 133 (1982) 93.
42. M.R.Wasielewski, M.P.Niemczyk, W.A.Svec and E.B.Pewitt, J. Am. Chem. Soc. 107 (1985) 1080.
43. M.P.Irvine, R.J.Harrison,G.S.Beddard, P.Leighton and J.K.M.Sanders, Chem. Phys. 104 (1986) 315.
44. S.F.Fischer and R.P.Van Duyne, Chem. Phys.26 (1977) 9.
45. J.Jortner, J. Chem. Phys. 64 (1976) 4860.
46. A.D.Joran, B.A.Leland, P.M.Felker, A.H.Zewail, J.J.Hopfield and P.B.Dervan, Nature 327 (1987) 508.
47. R.A.Marcus and N.Sutin, Biochim. Biophys. Acta 811 (1985) 265.
48. J.Jortner, J. Am. Chem. Soc 102 (1980) 6676.
49. I.Rips and J.Jortner, Chem. Phys. Lett 133 (1987) 410.
50. L.D.Zusman, Chem.Phys. 119 (1988) 51.

CHAPTER 3

Experimental methods

This chapter treats the spectroscopic techniques, used in the experiments described in this thesis. The preparation and purification of the compounds is described in the separate chapters.

3.1 EPR spectra

EPR spectra were recorded on a X-band VARIAN E-6 spectrometer, equipped with a rectangular cavity (VARIAN E-213). The modulation frequency was 100 kHz, the modulation amplitude 0.8-2.5 mT and the microwave power 0.5-10 mW. Low temperature spectra were obtained with a liquid nitrogen flow cryostat (VARIAN E-257) (100K $\leq$ T $\leq$ 300K> or an Oxford Instruments ESR-9 flow cryostat (5K $\leq$ T $\leq$ 100 K).

Light excitation of the sample was obtained by irradiation with a cw argon-ion laser (Coherent Radiation CR 4), a 150 W Xe-lamp (ILC) filtered through 5 cm water or with a 900 W Xe-lamp (Osram), filtered via a saturated $CuSO_4$ solution and a UV cut-off filter (Schott GG 395). Light induced spectra in the presence of strong steady state signals were obtained by chopping the exciting light with a mechanical chopper and detecting the output of the ESR apparatus with a lock-in analyzer (EG&G 5204), using for the reference signal deflected light detected by a photodiode.

3.2 ODMR spectra and fluorescence fading experiments

Two set-ups were used for the ODMR spectra, one equipped with a Leybold-Heraeus cryostat [1] and the other with a l'Air Liquide liquid helium vessel and an optical light guide [2]. The sample, immersed in liquid helium, was optically excited by a cw argon-ion laser (Coherent Radiation CR 4) or by a dye laser (Coherent Radiation CR 590), which was pumped by the argon-ion laser, using rhodamine 6G as dye. Microwave power was obtained from a Hewlett-Packard 8620 C sweep oscillator with 86220 A plug-in (10-1300 MHz) or from a Hewlett-Packard 8690 B sweep oscillator with 8699B plug-in (1000-2000 MHz). Fluores-

cence emitted by the sample passed a suitable cut-off filter, focussed on the entrance slit of a monochromator (Spex Minimate, f=0.25 m; or Jarrel-Ash model 182.001, f=0.5 m) and detected by a photomultiplier (RCA C 31034 A). The signal from the photomultiplier was AC coupled to a signal averager (PAR model 4203) and transferred to a DEC MINC-11 minicomputer or to a MicroVax II computer.

The same set-ups were used for fluorescence fading experiments, in which the triplet state kinetic parameters are determined without the need to invoke a microwave source [3]. Multi-exponential fits to digitally recorded experimental fluorescence fading curves were determined, using a weighted least squares approximation method [4]. The true triplet rate constants were found by extrapolating the observed kinetic parameters to zero light intensity [1].

3.3 Fluorescence lifetime measurements

The fluorescence lifetime measurements were performed with a single photon counting apparatus, described in [5].

For the excitation of the sample a mode-locked argon-ion laser (Coherent Radiation CR 18 UV) was used. The 100 ps, 514.5 nm pulses of the laser were used for excitation or for pumping a dye laser (Coherent Radiation CR 590), using rhodamine 6G as dye, resulting in 5 ps pulses. The repetition rate of the pulses is decreased from 38 MHz to 600 kHz by using an electro-optic modulator. The fluorescence is detected perpendicularly to the excitation direction and the detection polarization was under the magic angle with respect to the polarization direction of the excitation. For wavelength selection proper interference filters were used. The photomultiplier, detecting the emission photons, is a Philips PM 2254B or a Hamamatsu R1645U. For the registration of the fluorescence decay curves time correlated single photon counting is used [6]. Data were collected in a ND66 multichannel analyzer and were transferred to a MicroVax II computer. The fluorescence decay curves were deconvoluted, using the decay of a reference compound, oxazine in methanol, having single exponential decay, to correct for the instrumental respons [7].

3.4 Transient absorption measurements

3.4.1 ms - µs region

The set-up for the transient absorption measurements is given in figure 1. For excitation of the sample a Q-switched Nd-Yag laser is used. The Nd-Yag laser (JK lasers System 2000) is used in the frequency doubled configuration producing 12 ns, 532 nm pulses. The probe light stems from a 250 W tungsten lamp (Osram) with a highly stabilized power supply. Wavelength selection is performed by one or two monochromators (Spex Minimate f=0.25 m). The probe light is detected by a Hamamatsu R 928 photomultiplier in a PFR TE-234RF housing. The

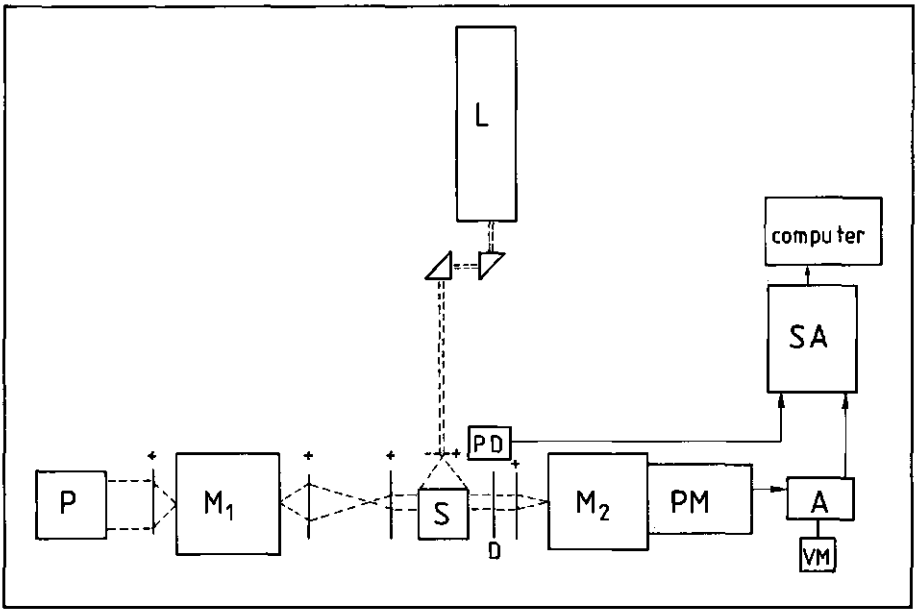

Figure 1: Experimental set-up for transient absorption measurements. L: Nd-Yag pulselaser; P: 250 W lamp; M1,M2: monochromators; D: diaphragm; PM: photomultiplier; S: sampleholder; PD: photodiode to trigger the signal analyzer; A: amplifier; VM: DC voltmeter; SA: signal analyzer.

current from the photomultiplier (PM) is converted to a voltage drop over a 2.2 kΩ or a 50 Ω resistor and this voltage is amplified by a Ithaco 1201 amplifier or the amplifier of a Philips PM 3055 oscilloscope with Y-out option. The output is fed via a LeCroy 6102 amplifier into a transient recorder (LeCroy TR 8818). The data are stored in a LeCroy 3500 SA signal analyzer. For analyzing the kinetic curves the data are transfered to a MicroVax II computer. The kinetic parameters are determined by analyzing the data with a Fortran 77 program for analyzing exponential curves (SPLMOD, EMBL Heidelberg).

The transient decay curves were recorded with 5 nm intervals, using either AC or DC coupling. In the AC-mode the average PM output was recorded with a DC voltmeter.

The transient absorption difference, ΔA, is calculated from Lambert-Beer's law:

$$\Delta A(t) = -^{10}\log(I_2(t)/I_1) = -^{10}\log[(\Delta I(t)/I_1)+1] \qquad (1)$$

where I_1 and $I_2(t)$ are the light intensities before and after the exciting pulse at $t = 0$, respectively, and $\Delta I(t) = I_2(t) - I_1$. The output voltage from the PM is chosen to be linearly dependent on the probe light intensity and (1) can be rewritten as:

$$\Delta A(t) = -^{10}\log[(\Delta V(t)/V_{pp})+1] \qquad (2)$$

where V_{pp} is the prepulse PM output and $\Delta V(t)$ is the detected voltage difference upon light excitation.

For kinetic analyses of the data the absorption difference, ΔA, must be small to be able to fit the data directly with exponentials:

$$\Delta V(t) = V_{pp}.(10^{-\Delta A(t)} - 1) \qquad (3)$$

For small ΔA (3) can be rewritten in a Taylor series. Keeping only the linear term:

$$\Delta V(t) = -2.303\ V_{pp}.\Delta A(t) \qquad (4)$$

For $\Delta A = 0.03$ the error in this approximation is 4 %.

The spectral range of the apparatus is 360-860 nm, limited by the UV absorption of some glass components and by the red wavelength limit of the PM. The time resolution of the apparatus is 10 ns. The detection of fast transients is perturbed by spurious signals, lasting 0.2 μsec, caused by electromagnetic noise from the firing of the flashlamp of the Nd-Yag laser and the discharge of the capacitor of the Nd-Yag laser. The sensitivity at short time ranges is limited by the photon noise due to the low light level of the probe light, which is limited by the maximum anode current of the photomultiplier. At a time resolution of 0.1 μsec the photon noise is 20 % in a single scan. The signal-to-noise ratio is improved by averaging 250 or 500 scans.

Low temperature spectra were measured, using an Oxford Instruments CF 204 flow cryostat.

3.4.2. ns-ps region

The picosecond absorption measurements were performed with dr. M.R.Wasielewski at Argonne National Laboratory. The apparatus, described in [8], produced 610 nm, 0.5-3 ps, 1.5 mJ pulses for excitation. Continuum probe pulses were used in a double beam configuration to detect the transient absorption spectra at various time intervals, determined by the optical delay line.

References

1. L.Benthem, Ph.D.Thesis, Wageningen Agricultural University (1984).
2. S.J.van der Bent, P.A.de Jager and T.J.Schaafsma, Rev. Sci. Instrum. 47 (1976) 117.
3. R.Avarmaa, Mol. Phys. 37 (1979) 441.
4. S.W.Provencher, J. Chem. Phys. 64 (1976) 2772.
5. A.van Hoek, J.Vervoort and A.J.W.G.Visser, J. Biochem. Biophys. Meth. 7 (1983) 243.
6. D.V.O'Connor and D.Phillips, "Time correlated single photon coun-

ting", Acad. Press, FL, USA (1984).

7. K.Vos, A.van Hoek, A.J.W.G.Visser, Eur. J. Biochem. 165 (1987) 55.
8. M.R.Wasielewski and M.P.Niemczyk, J. Am. Chem. Soc. 106 (1984) 5043.

CHAPTER 4.1

Volume 144, number 2 CHEMICAL PHYSICS LETTERS 19 February 1988

OPTICAL AND FDMR SPECTROSCOPY OF DIPHENYLETIOPORPHYRIN

U. HOFSTRA, M. VAN DER GRAAF and T.J. SCHAAFSMA
Department of Molecular Physics, Agricultural University, De Dreijen 11, 6703 BC Wageningen, The Netherlands

Received 23 November 1987; in final form 15 December 1987

The triplet state of 5,15-diphenyl-2,8,12,18-tetraethyl-3,7,13,17-tetramethylporphyrin was investigated at 4.2 K by fluorescence-detected magnetic resonance (FDMR). Two clearly distinct sites (site I: $D=462\times10^{-4}$ cm^{-1} and $E=20\times10^{-4}$ cm^{-1}; site II: $D=442\times10^{-4}$ cm^{-1} and $E=16\times10^{-4}$ cm^{-1}) can be distinguished in a solid octane matrix. The triplet-state properties and the absorption spectra of diphenyletioporphyrin can be rationalized by the four-orbital model of Gouterman. From the triplet-state decay parameters and the D and E values, it is concluded that the FDMR spectra of the two sites originate from triplet states with different degrees of configuration interaction.

1. Introduction

Diphenyl-substituted porphyrins are suitable photosensitizers in model systems of photosynthetic reaction centres. Understanding the electronic properties of these porphyrins, in particular the electronic distribution and orbital symmetry of the excited states, is essential for designing such models [1–3]. Therefore, we have studied the excited singlet and the lowest triplet state of diphenyletioporphyrin free base by optical and fluorescence-detected magnetic resonance (FDMR) spectroscopy. Unexpectedly, it was found that diphenyletioporphyrin in frozen *n*-octane at low temperature shows a Shpolskii spectrum and two widely different FDMR spectra for the two main sites in the *n*-octane matrix. The compound studied in this work is 5,15-diphenyl-2,8,12,18-tetraethyl-3,7,13,17-tetramethylporphyrin (diphenyletioporphyrin II free base), abbreviated as H_2DPEP (fig. 1a).

Solutions of unsubstituted porphin, H_2P, in *n*-alkanes form single-crystal Shpolskii matrices [4]. Solutions of tetraphenylporphyrin, H_2TPP, do not form a Shpolskii matrix in *n*-alkanes [5,6], but site-selective spectra have been obtained in non-crystalline solids [6] and nitrobenzene appeared to be a suitable Shpolskii host [7].

The combined substituent effects of alkyl groups at the pyrrole rings and phenyl groups at the meso positions on the electronic properties have been investigated for H_2DPEP via the optical absorption spectra and the triplet state parameters in a polycrystalline Shpolskii matrix, as studied by FDMR. The substituent effects for porphyrins can be satisfactorily explained by Gouterman's four-orbital model [8], as has been convincingly illustrated for optical spectra [9–11]. Its validity for the lowest excited states has been justified by various quantum-mechanical calculations [12–15].

The two highest occupied molecular orbitals (HOMOs) and the two lowest unoccupied molecular orbitals (LUMOs) of H_2DPEP are presented in fig. 1b. In porphyrins with D_{4h} symmetry the two possible singlet transitions ($a_{1u}\rightarrow e_g$) and ($a_{2u}\rightarrow e_g$) are degenerate. These transitions mix through configuration interaction (CI), resulting in a weak Q-band transition and a strong Soret-band transition [8]. In H_2P, which has D_{2h} symmetry, the transitions are no longer degenerate, but mix sufficiently to result in weak *x*- and *y*-polarized Q bands and strong *x*- and *y*-polarized Soret bands. The degree of CI is directly related to the energy difference between the two *x* transitions and the two *y* transitions, respectively. The energy differences depend on the energies of the HOMOs and LUMOs, which shift on substitution of H_2P. The shift depends on the electron density of the orbital at the substitution position.

The intensity ratio between the Soret and the Q

0 009-2614/88/$ 03.50

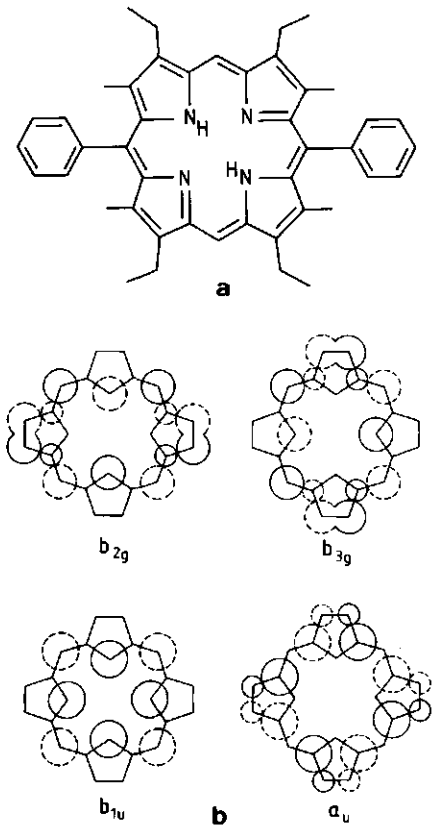

Fig. 1. (a) Molecular structure of H_2DPEP. (b) The HOMOs (b_{1u} and a_u) and LUMOs (b_{2g} and b_{3g}) used in Gouterman's four-orbital model [16]. The atomic orbital coefficients are proportional to the circles; solid and dashed circles indicate the sign of the wavefunction. The orbitals are given in D_{2h} notation.

bands in the porphyrin spectra is determined by the degree of CI in the singlet state. For a small amount of CI, the Q bands gain intensity from the Soret band.

On the other hand, it is to be expected that CI would affect the zero-field splitting (ZFS) parameters of the triplet state [17], as well as its population and decay kinetics. Surprisingly, optical spectra as well as FDMR of H_2DPEP demonstrate that the electronic configurations of the excited singlet and the lowest triplet state of this compound are very similar to those of unsubstituted free-base porphin.

2. Experimental

H_2DPEP has been synthesized according to the method of Gunter and Mander [18]. The purity was checked by ^1H NMR and by thin-layer chromatography, *n*-octane (Fluka p.a.) was used as solvent after drying over aluminium oxide. The absorption spectra were recorded on a Kontron Uvikon spectrometer.

The emission spectra and the FDMR spectra were measured at 4.2 K on our ODMR apparatus which has been described previously [19]. The excitation source was a cw CR590 dye laser, using rhodamine 6G, pumped by a CR4 Ar^+ ion laser. On the detection side we used a Jarrell–Ash 82.001 monochromator and a RCA C 31034A photomultiplier.

Measurements of the triplet state kinetics by FDMR were carried out by switching the microwave power at resonance on and off. The microwave power used in the kinetic experiments was 40 mW, well above saturation of the transitions between the triplet sublevels.

The microwave experiments were done at such low light intensity, that the triplet yield as determined from fluorescence fading experiments [20] was linearly dependent on the excitation light intensity and was less than 10%.

3. Results and discussion

3.1. The absorption spectrum of H_2DPEP

The absorption spectrum of H_2DPEP in *n*-octane (fig. 2) demonstrates that the $Q_x(0,0)$ and $Q_y(0,0)$ transitions have a low intensity as compared to the (1,0) transitions. This is characteristic of a so-called phyllo-type absorption spectrum [8]. The spectrum of H_2DPEP is surprising, because both octaalkylporphyrins, H_2OAP, and tetraphenylporphyrins, H_2TPP, show an etio-type spectrum. H_2DPEP is expected to combine the substituent effects of the alkyl groups of H_2OAP and the phenyl groups of H_2TPP. H_2DPEP, however, has a phyllo-type absorption

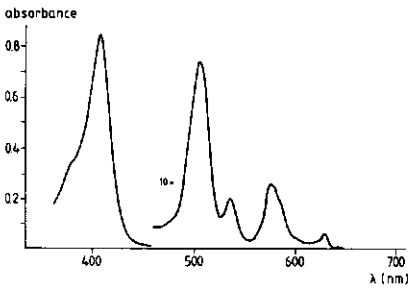

Fig. 2. Absorption spectrum of 2.0×10^{-5} M H_2DPEP in *n*-octane.

spectrum as does free-based porphin, H_2P.

An etio-type spectrum arises if the Q bands can borrow intensity from the very intense Soret band by a decrease in the CI of $(b_{1u} \rightarrow b_{2g})$ with $(a_u \rightarrow b_{3g})$ for the *y*-polarized transitions and of $(b_{1u} \rightarrow b_{3g})$ with $(a_u \rightarrow b_{2g})$ for the *x*-polarized transitions in D_{2h} notation. The decrease in the degree of CI in H_2OAP is the result of an upward shift of the a_u energy level due to the substitution of eight electron-donating groups on positions which mainly affect this orbital [8]. The b_{2g} and b_{3g} orbitals also have an upward shift, but their relative positions remain the same. The energy gap between the b_{1u} and a_u orbitals increases, thereby decreasing the CI in H_2OAP [8] (fig. 3). In H_2TPP the electron-donating phenyl groups, which are situated on the meso positions, mainly affect the b_{1u} orbital, resulting in an upward shift. It has indeed been calculated that the b_{1u} level is higher than the a_u level in H_2TPP and that their separation is increased with respect to that in H_2P [12]. The degree of configuration interaction in H_2TPP is therefore less than in H_2P.

In H_2DPEP both substituent effects are combined. The methyl and ethyl groups on the pyrrole rings destabilize the a_u energy level, whereas the two phenyl groups on the meso positions destabilize the b_{1u} energy level. Since the substituent effects on the spectra of H_2OAP and H_2TPP are very similar, we expect that the combined effect of both types of substituents in H_2DPEP results in an energy gap between the a_u and b_{1u} orbitals very similar to that in unsubstituted H_2P. The CI in H_2DPEP is therefore much larger than in either H_2OAP or H_2TPP, resulting in a phyllo-type absorption spectrum for H_2DPEP.

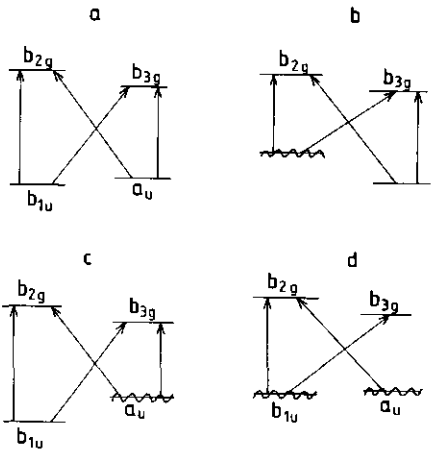

Fig. 3. Energy level diagrams of (a) H_2P, (b) H_2TPP, (c) H_2OAP and (d) H_2DPEP. The levels that have shifted most with respect to those of H_2P are marked by ~ ~ (see text).

3.2. The FDMR spectrum of H_2DPEP

The fluorescence spectrum of H_2DPEP in *n*-octane at 77 K is presented in fig. 4a. The 0–0 emission band is split into two bands at 625 and 632 nm. The relative amplitudes of these bands depend on the freezing rate of the solution. At a low freezing rate the short-wavelength band gains intensity with respect to that at higher wavelength. The splitting of the 0–0 fluorescence band in *n*-octane at 77 K is therefore due to the occurrence of different sites for the porphyrin in *n*-octane. At 4.2 K the fine structure of the spectrum has increased, as is shown in fig. 4b. The peak positions in the spectrum do not change on varying the excitation wavelength, demonstrating that a polycrystalline Shpolskii matrix has been formed. For zinc etioporphyrin, which lacks the two phenyl groups, a high-resolution Shpolskii spectrum has also been reported [21], but not for H_2TPP. The formation of a Shpolskii matrix for H_2DPEP in *n*-octane is probably facilitated by the rod-like structure of H_2DPEP, which can replace several octane chains in the polycrystalline matrix.

In fig. 4b the resolved site emissions are centered around 624.6 and 632.8 nm. Each site emission exhibits a 54 cm^{-1} doublet splitting assigned to the two

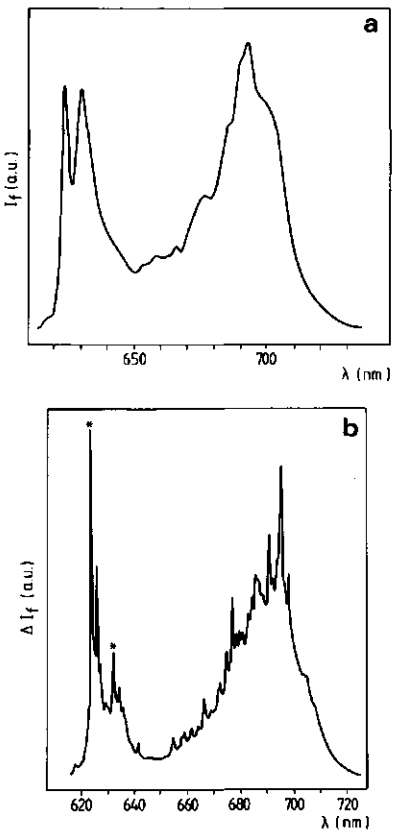

Fig. 4. Fluorescence spectrum of 5×10^{-6} M H_2DPEP in *n*-octane (a) at 77 K, $\lambda_{exc}=588$ nm; (b) at 4.2 K, $\lambda_{exc}=570.5$ nm. In (b) the detection wavelengths for the FDMR spectra have been marked.

N–H tautomers in a low-symmetry site, similar to the tautomeric splitting observed for H_2P [22].

For FDMR we have selected the resolved emissions at 623.5 and 631.7 nm, marked in fig. 4b.

The FDMR spectra detected at 623.5 and at 631.7 nm are completely different (fig. 5). The ZFS parameters were calculated from these spectra (table 1). They are in agreement with the ZFS parameters of H_2DPEP in toluene and in dimethylformamide (DMF), which were determined by triplet ESR at

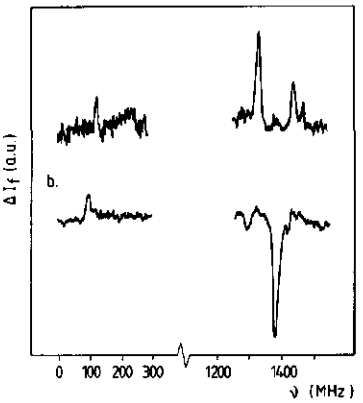

Fig. 5. FDMR spectra of a 5×10^{-6} M H_2DPEP solution in *n*-octane at 4.2 K. The excitation wavelengths are (a) 570.5 nm and (b) 586.7 nm. The detection wavelengths are (a) 623.5 nm and (b) 631.7 nm.

100 K (toluene: $D=0.0454$ cm^{-1} and $E=0.0033$ cm^{-1}; DMF: $D=0.0451$ cm^{-1} and $E=0.0013$ cm^{-1}).

The D value in H_2DPEP is lower than the 0.048 cm^{-1} observed for free-base etioporphyrin [23]. This is to be expected on delocalization of the π electrons into the phenyl groups [24].

At a low light intensity and with microwave saturation the change in fluorescence intensity upon switching on the microwaves at the resonance frequency of the transition between the triplet sublevels i and j is given by [25]

$$\Delta I_f(t)=k_f K[(k_i-k_j)/(k_i+k_j)](n_i-n_j)\times\{\exp[-\tfrac{1}{2}(k_i+k_j)t]-1\}, \quad (1)$$

where k_i and k_j are the decay constants of the triplet

Table 1
D and E values of a 5×10^{-6} M H_2DPEP solution in *n*-octane; $T=4.2$ K

Site	Detection wavelength (nm)	D (10^{-4} cm^{-1})	E (10^{-4} cm^{-1})
I	623.5	462.4±0.7	20.0±0.7
II	631.7	442.0±0.7	15.7±1.0

Table 2
Triplet decay constants of H_2DPEP (5×10^{-6} M solution in *n*-octane); $T=4.2$ K. *x* and *y* refer to two in-plane axes, *z* is out of the plane. The estimated error is 20%

Site	k_x (s^{-1})	k_y (s^{-1})	k_z (s^{-1})
I	112	134	69
II	32	214	5

sublevels *i* and *j*, k_f is the fluorescence rate constant, n_i and n_j are the populations at $t=0$ of the sublevels *i* and *j*, and *K* is a constant. The change in fluorescence on steady-state illumination is therefore given by

$$\Delta I_f(t) = -k_f K[(k_i-k_j)/(k_i+k_j)](n_i-n_j). \quad (2)$$

When the microwaves are switched off, the microwave-induced change of fluorescence at a later time *t* is given by

$$I_f(t) = k_f K[k_i k_j/(k_i+k_j)](n_i-n_j) \times [k_i^{-1}\exp(-ik_i t) - k_j^{-1}\exp(-k_j t)]. \quad (3)$$

The triplet decay constants of H_2DPEP in both sites of *n*-octane were determined using the above-mentioned method, by fitting the rise and decay curves to eqs. (1) and (3), respectively (table 2).

By combining the decay constants with the sign of the FDMR transitions, the relative populations of the triplet sublevels of H_2DPEP were determined. The order for site I is $n_z>n_x>n_y$; for site II $n_x>n_y>n_z$. The steady-state populations and decay constants for the two sites are schematically depicted in fig. 6.

The relative populations of the triplet sublevels of H_2DPEP in site II are similar to those of H_2P in *n*-octane. In addition, the decay rates k_x, k_y and k_z are almost identical to those of H_2P ($k_x=75\ s^{-1}$, $k_y=230\ s^{-1}$ and $k_z=6\ s^{-1}$ [24]). Finally, the *D* values are very similar (for H_2P in *n*-octane $D=(435\text{–}440)\times10^{-4}\ cm^{-1}$ [4]). In view of this striking agreement we assume that H_2DPEP in site II, like H_2P, has a nearly pure $(b_{1u}\rightarrow b_{3g})$ configuration in the lowest triplet state [4].

The populations of the *x* and *y* sublevels of H_2DPEP for site I are smaller than for site II (fig. 6). By combining this result with the decay constants in table 2, it is concluded that the relative populating rates p_x and p_y of the *x* and *y* sublevels of the lowest triplet state of H_2DPEP in site I have decreased with respect to those for site II. p_x and p_y are largely determined by the coupling of the corresponding triplet sublevels with singlet states containing p orbitals on the central nitrogen atoms [8]. Apparently, the triplet state of H_2DPEP in site II has a smaller coupling with these singlet states. If we assume that the site II triplet state has significant $(a_u\rightarrow b_{2g})$ character, we can explain the smaller coupling, because the a_u orbital has no electron density on the nitrogen atoms (fig. 1b). In the triplet state the $(a_u\rightarrow b_{2g})$ state can mix with the $(b_{1u}\rightarrow b_{3g})$ state with the same symmetry by CI. This also explains the larger value of *D* for this site as compared to site II, because *D* is known to increase with increasing CI [17].

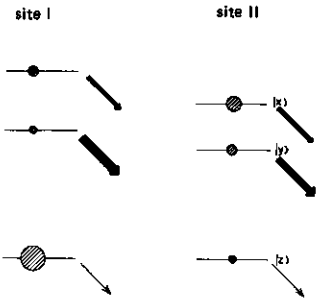

Fig. 6. Population densities and decay kinetics of the triplet sublevels of H_2DPEP for site I and site II. The relative population densities for each site and the decay kinetics are proportional to the size of the circles and arrows, respectively.

We conclude that the site II triplet state has a pure $(b_{1u}\rightarrow b_{3g})$ configuration and the site I triplet state is the result of CI between $(b_{1u}\rightarrow b_{3g})$ and $(a_u\rightarrow b_{2g})$ configurations.

Our results indicate that the electronic distribution in porphyrins may be affected by their environment through configuration interaction. This, in turn, is an important factor on the efficiency of photoinduced electron transfer in photosynthetic model systems.

Acknowledgement

We thank Dr. G.M. Sanders and Mr. M. van Dijk of the Organic Chemistry Department for the synthesis of H_2DPEP. This investigation was supported by the Netherlands Foundation for Chemical Research (SON) with financial help from the Netherlands Organization for the Advancement of Pure Research (ZWO).

References

[1] H. Kuhn, Phys. Rev. A34 (1986) 3409.
[2] P. Bertrand, Chem. Phys. Letters 140 (1987) 57.
[3] S. Larsson, J. Am. Chem. Soc. 103 (1981) 4034.
[4] W.G. van Dorp, M. Soma, J.A. Kooter and J.H. van der Waals, Mol. Phys. 28 (1974) 1551.
[5] I.J. Aronowitz and M. Gouterman, J. Mol. Spectry. 64 (1977) 267.
[6] L.A. Bykovskaya, R.I. Personov and Y.V. Romanovskii, Zh. Prikl. Spektroskopii 31 (1979) 910.
[7] R. Tamkivi, I. Renge and R. Avarmaa, Chem. Phys. Letters 103 (1983) 103.
[8] M. Gouterman, in: The porphyrins, Vol. 3, ed. D. Dolphin (Academic Press, New York, 1978) p. 1.
[9] M.-Y. Rachel Wang and B.M. Hoffman, J. Am. Chem. Soc. 106 (1984) 4235.
[10] J.A. Shelnutt and V. Ortiz, J. Phys. Chem. 89 (1985) 4733.
[11] C. Djerassi, Y. Lu, A. Wakeh, A.Y.L. Shu, R.A. Goldbeck, L.A. Kehres, C.W. Crandell, A.G.H. Wee, A. Knierzinger, R. Gaete-Holmes, G.H. Loew, P.S. Clezy and E. Bunnenberg, J. Am. Chem. Soc. 106 (1984) 4241.
[12] S.J. Chantrell, C.A. McAuliff, R.W. Munn, A.C. Pratt and R.F. Weaver, Bioinorg. Chem. 7 (1977) 283.
[13] H. Sekino and H. Kobayashi, J. Chem. Phys. 75 (1981) 3477.
[14] J.D. Pettke, G.M. Maggiora, L.L. Shipman and R.E. Cristoffersen, J. Mol. Spectry. 71 (1978) 64.
[15] M.B. Masthay, L.A. Findsen, B.M. Pierce, D.F. Bocian, J.S. Lindsey and R.R. Birge, J. Chem. Phys. 84 (1986) 3901.
[16] M. Gouterman, J. Mol. Spectry. 6 (1961) 138.
[17] J.F. Kleibeuker, R.J. Platenkamp and T.J. Schaafsma, Chem. Phys. 27 (1978) 51.
[18] M.J. Gunter and L.N. Mander, J. Org. Chem. 46 (1981) 4792.
[19] L. Benthem, Ph.D. Thesis, Agricultural University, Wageningen (1984) p. 38.
[20] R. Avarmaa, Mol. Phys. 37 (1979) 441.
[21] S.R. Langhoff, E.R. Davidson, M. Gouterman, W.R. Leenstra and A.L. Kwiram, J. Chem. Phys. 62 (1975) 169.
[22] G. Jansen, M. Noort, N. van Dijk and J.H. van der Waals, Mol. Phys. 39 (1980) 865.
[23] Z.P. Gribova and L.P. Kayushin, Russian Chem. Rev. 41 (1972) 154.
[24] J.H. van der Waals, W.G. van Dorp and T.J. Schaafsma, in: The porphyrins, Vol. 4, ed. D. Dolphin (Academic Press, New York, 1978) p. 257.
[25] R.H. Clarke, in: Triplet state ODMR spectroscopy, ed. R.H. Clarke (Wiley, New York, 1982) pp. 25–42.

CHAPTER 4.2

Picosecond charge separation and triplet formation in a closely spaced photosynthetic model system.

U. Hofstra and T.J. Schaafsma
Department of Molecular Physics, Agricultural University Wageningen
De Dreyen 11, 6703 BC Wageningen, The Netherlands.

G.M. Sanders, M. van Dijk and H.C. van der Plas
Department of Organic Chemistry, Agricultural University Wageningen,
Wageningen, The Netherlands

D.G. Johnson and M.R.Wasielewski
Chemistry Division, Argonne National Laboratory,
Chicago, U.S.A.

Abstract

Intramolecular electron transfer has been investigated for three diphenyletioporphyrins covalently linked to an anthraquinone via a sulfonyloxy bridge at the ortho, meta or para substitution position of the phenyl groups of the porphyrin. The ortho-linked porphyrin is strongly folded and exhibits extremely fast charge separation (CS) and recombination (CR) between porphyrin and anthraquinone (k_{CS} >$3x10^{11}$ sec^{-1} and k_{CR} = $5.9x10^{10}$ sec^{-1} in CH_2Cl_2). The less-folded meta- and para-linked porphyrins have smaller, but similar electron transfer rate constants, presumably because electron transfer occurs through the sulfonyloxy-bridge in both compounds.

For the ortho-linked compound the triplet state is formed in high yield in toluene via fast intersystem crossing in the charge-separated state.

Introduction

The first photoinduced electron transfer steps in photosynthesis following the excitation of the reaction centre involve charge separation between a chlorophyll donor and nearby electron acceptors on a picosecond time scale [1]. A vast amount of research has been dedicated to mimic these electron transfer (ET) steps using model systems containing a porphyrin molecule along with a donor and/or an acceptor molecule covalently linked to the porphyrin moiety [2-5]. One of the main objectives for this type of research is to design a model system, which undergoes fast forward electron transfer and slow back electron transfer, resulting in a high quantum yield for charge separation.

We present the results of fluorescence and picosecond, as well as microsecond transient absorption measurements for three compounds, denoted as 1, 2 and 3. Each compound consists of 5,15-diphenyl-2,8,12,18-tetraethyl-3,7,13,17-tetramethylporphyrin (P) with an electron acceptor anthraquinone (AQ) and an electron donor dimethyl-aniline (DMA) both covalently linked to the phenylgroups of the porphyrin via a sulfonyloxy-bridge (figure 1a). AQ is linked to the ortho-, meta- or para-position of the 5-phenyl group (compounds 1, 2 and 3, respectively). DMA is linked to the ortho-position of the 15-phenyl group in all three compounds. Compound 4, which has two tosyloxy groups linked to the ortho positions of the phenyl groups, is used as reference compound.

Using the redoxpotentials of anthraquinone and N,N-dimethylaniline [6,7], the free energy changes for the two electron transfer steps: i) $DMA\text{-}P^{*}\text{-}AQ \rightarrow DMA\text{-}P^{+}\text{-}AQ^{-}$ and ii) $DMA\text{-}P^{+}\text{-}AQ^{-} \rightarrow DMA^{+}\text{-}P\text{-}AQ^{-}$ are i) ΔG = -0.15 eV, for ii) ΔG = -0.13 eV, neglecting Coulombic interactions. In addition to the free energy of reaction other factors, contributing to the ET rate constants are the conformation of the compound, as well as the chemical nature of the linking bridges [8,9]. Our experiments show, that the linking bridges can not be considered to be inert. The conformations of 1 - 3 turn out to play a significant rôle in the ET mechanism.

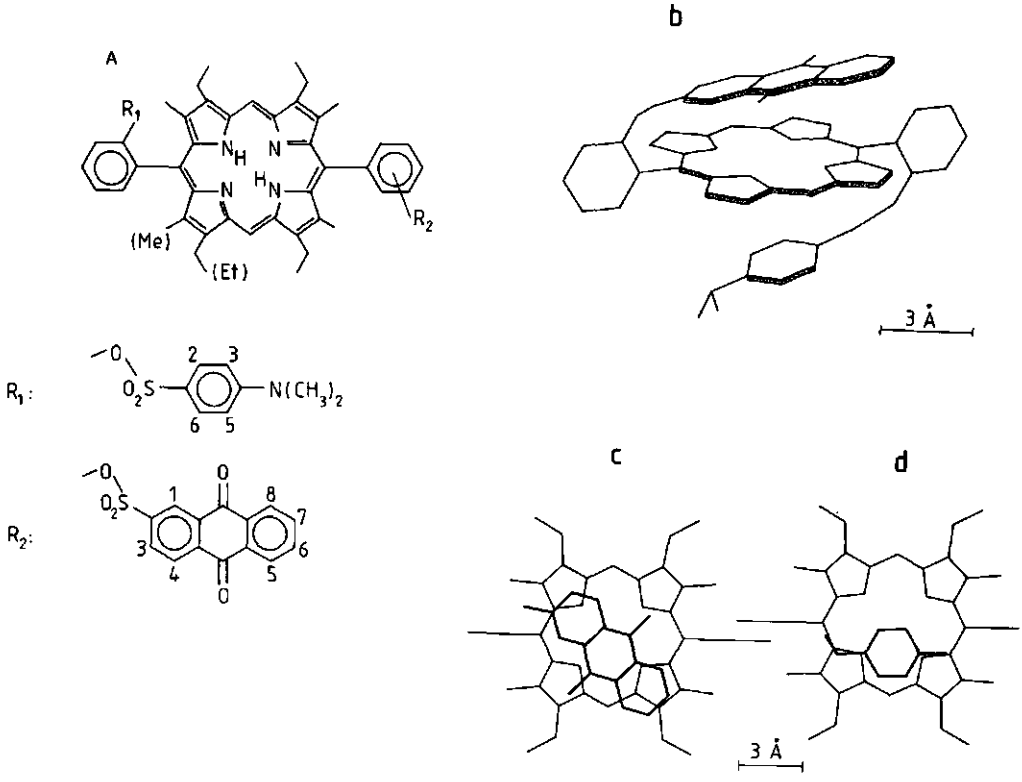

Figure 1: a) Molecular structure of 1, 2 and 3: 1: R_2 at ortho position; 2: R_2 at meta position. 3: R_2 at para postion; 4: R_1 and R_2 are 4-(sulfonyloxy)tolyl groups at ortho positions. Me = methyl, Et = ethyl.

b) Conformation of 1 (side view) in $CDCl_3$, calculated from ^1H NMR ring current shifts.

c) P-AQ part (top view);

d) DMA-P part (bottom view).

The phenyl groups have been assumed to be perpendicular to the porphyrin plane.

The conformations can be controlled by varying the position of the linking sulfonyloxy-bridge on the porphyrin phenyl groups. We used this as a means to discriminate between through-bond and through-space ET. Since 2 and 3 have a similar linking chain but widely different centre-to-centre donor acceptor distances the through-space ET mechanism would give rise to quite different rate constants for these compounds, whereas through-bond ET is expected to give rise to similar rate constants. The centre-to-centre donor-acceptor distance for 1 is strikingly small as compared to 2 and 3 and other model systems [2,3,4], resulting in considerable orbital overlap and extremely fast charge separation as well as recombination to the ground state by a through-space mechanism.

The pathways immediately following the primary forward ET step can be controlled by choosing various solvents. As an example, under suitable conditions 1 exhibits formation of porphyrin triplets via radical pair states.

Experimental

The compounds were prepared as described in ref.5 and checked for purity by thin layer chromatography, C,H,N microanalyses, ^{1}H NMR and mass spectroscopy.

The ^{1}H NMR spectra were recorded at 300 MHz, using a Bruker CXP-300 spectrometer. Redox potentials were measured by AC voltammetry at a platinum disk electrode versus SCE in CH_2Cl_2/0,1 M tetra-n-butylammoniumperchlorate. Fluorescence quantum yields were determined on a Perkin Elmer LS5 fluorimeter and measured relative to tetraphenylporphyrin (H_2TPP) in degassed benzene (0.13 [10]).
The optical density at the excitation wavelength was less then 0.2. The 10^{-5} M solutions were made oxygen-free by bubbling deoxygenated argon through the solutions for about 15 minutes.

Fluorescence lifetimes were determined, using a single photon counting apparatus, as described in ref.11. The sample was excited with 580 nm, 5 ps pulses. The recorded decay curves were deconvoluted with the decay of the reference compound oxazine in methanol to

correct for the instrumental respons.

The apparatus for picosecond absorption measurements [12] produced 600 nm, 0.5 psec, 1.5 mJ pulses for excitation. Continuum probe pulses were used in a double beam configuration to detect the transient absorption difference spectra at various time intervals, determined by an optical delay line.

The microsecond transient absorption spectra were measured using a frequency doubled Nd-Yag laser (532 nm, 12 nsec, 30 mJ pulses) for the excitation and a 250 W tungsten lamp as a probe source. The probe wavelength was selected by two Spex 25 monochromators and detected with a Hamamatsu R928 photomultiplier. After amplification by an Ithaco amplifier the photomultiplier output was digitized with a LeCroy 3500 transient recorder.

ESR spectra were recorded at 20 and 100 K on a Varian E-6 spectrometer, using a 150 W Xenon lamp for optical excitation.

Results

Solution structure

The solution structure of 1 (figure 1b) in $CDCl_3$ was calculated from the ^1H NMR spectra, using the effect of the porphyrin ring currents on the chemical shifts of the protons of the AQ and DMA-groups [13]. The conformation was calculated by systematically varying the coordinates of the substituents with respect to the porphyrin and minimizing the absolute difference between calculated and experimental ring current shifts (Table I). Details of the calculation will be presented in a forthcoming paper.

From these calculations the anthraquinone plane was found to be 3.2 Å above the porphyrin plane making an angle of 17° with the porphyrin plane, whereas DMA is situated 3.3 Å below the porphyrin plane with an angle of 15° with the porphyrin plane. In toluene the experimental ring current shifts are considerably smaller than in $CDCl_3$ indicating a less folded average conformation. The conformation

Table I: Experimental and calculated ring current shifts, δ_{exp} and δ_{calc}, (in ppm) of 1 and 3 in $CDCl_3$ (T = 213 K) and calculated ring current shifts.

proton[a]	1 δ_{exp}[b,c]	1 δ_{calc}	3 δ_{exp}[b,c]	3 δ_{calc}
AQ-1	-2.22	-2.27	+0.19	+0.19
AQ-3	-3.23	-3.23	+0.24	+0.13
AQ-4	-5.20	-5.09	+0.11	+0.17
AQ-5	-1.39	-1.60	+0.04	+0.07
AQ-6	-0.39	-0.43	+0.05	+0.03
AQ-7	-0.39	-0.43	+0.05	+0.03
AQ-8	-0.93	-0.88	+0.04	+0.04
DMA-2,6	-2.15	-2.15		
DMA-3,5	-3.32	-3.05		
DMA-$N(CH_3)_2$	-2.37	-2.51		

a: For the numbering of the protons see figure 1a.

b: Experimental ring current shifts of the anthraquinone protons were calculated from the chemical shifts relative to the reference compound 2-(anthraquinone-2-sulfonyloxy)benzaldehyde for 1 and 4-(anthraquinone-2-sulfonyloxy)benzaldehyde for 3.

c: The reference compound for the dimethylaniline protons is 2-(4-dimethylaminobenzenesulfonyloxy)benzaldehyde.

of 1 in this solvent can not be calculated with satisfactory precision, because the aromatic shift due to the solvent molecules can not be easily separated from the intramolecular ring current shifts.

The ring current shifts for the AQ group of 2 are much smaller (<0.5 ppm), because the AQ groups are further away from the porphyrin ring. The porphyrin-anthraquinone distance of 8.8 Å for 2 was taken from the structure of the analogously substituted tetraphenylporphyrin [14]. The ring current shifts for the AQ group of 3 are small and of opposite sign to those of 1 and 2. A centre-to-centre distance of 13 Å was calculated from teh ring current shifts.

1 in CH_2Cl_2 has a unique conformation, whereas 2 and 3 may have a

relatively narrow distribution around the average conformation, as follows from molecular models.

Redox potentials

The redox potentials of 1 and two analogs containing either two DMA- (5) or two AQ (6) moieties attached to the ortho phenyl position via a sulfonyloxy bridge, were measured in dichloromethane (Table II). From the oxidation potential of the isopropylester of dimethylaniline sulfonic acid at 1.27 eV vs. SCE in CH_2Cl_2 we conclude that the oxidation of DMA in 1 is hidden under the oxidation peak $E_{ox}(2)$ at 1.33 eV. Using the results of Table II, we calculate for the process
$DMA\text{-}P^*\text{-}AQ \rightarrow DMA\text{-}P^+\text{-}AQ^-$: $\Delta G = -0.29$ eV and for
$DMA\text{-}P^+\text{-}AQ^- \rightarrow DMA^+\text{-}P\text{-}AQ^-$: $\Delta G = +0.36$ eV. The second process is strongly endothermic and therefore does not occur.

Table II Redox potentials of the compounds[a] 1, 5 and 6 *in* CH_2Cl_2 vs SCE.

compound	$E_{ox}(2)$	$E_{ox}(1)$	$E_{red}(1)$	$E_{red}(2)$
1	1.33	0.91	-0.75	-1.10
5	1.29	0.87	-1.28	
6	1.28	0.97	-0.77	-1.20

a: For structure of 1, see fig. 1a; for 5 and 6, see text.

Fluorescence

The fluorescence of diphenyletioporphyrin is strongly quenched, when anthraquinone is covalently linked to the porphyrin. The fluorescence

Table III: Fluorescence quantum yields, ϕ_f, and lifetimes, τ_f, of substituted diphenyletioporphyrins (figure 1) in toluene.

compound	r[a] (Å)	ϕ_f	τ_f(ns)
1	3.2	$(2.6\pm0.3)\times10^{-3}$	0.18±0.02
2	8.8	$(5.5\pm0.3)\times10^{-3}$	0.25±0.02
3	13	$(1.1\pm0.1)\times10^{-2}$	0.21±0.02
4		0.11±0.01	14.31±0.02

a: r is the centre-to-centre distance from the porphyrin to the anthraquinone, determined from ^{1}H NMR ring current shifts.

quantum yields and lifetimes are given in Table III.

The fluorescence lifetimes of 1, 2 and 3 are similar. Assuming, that the radiative rate constants are similar for 1 - 4, a rate constant for charge separation $k_{CS} \approx 5\times10^9$ sec^{-1} is calculated for 1 - 3 in toluene.

Transient absorption

The picosecond transient absorption spectra of 1 - 3 in dichloromethane and in toluene show fast ET from the porphyrin to the anthraquinone, giving rise to the radical pair P^+-AQ^-. A typical transient spectrum for 1 in dichloromethane is shown in figure 2a. The characteristic difference absorption bands of P^+ can be seen at 480 and 650 nm [15]. The transient absorption band of AQ^- at 560 nm [16] is obscured in dichloromethane by the bleaching of the porphyrin ground state absorption. The rise and decay of the P^+ transients were monitored at 656 nm and 480 nm. Figure 2b shows the P^+ transient for 1 in dichloromethane at 656 nm. The formation of the radical pair P^+-AQ^-

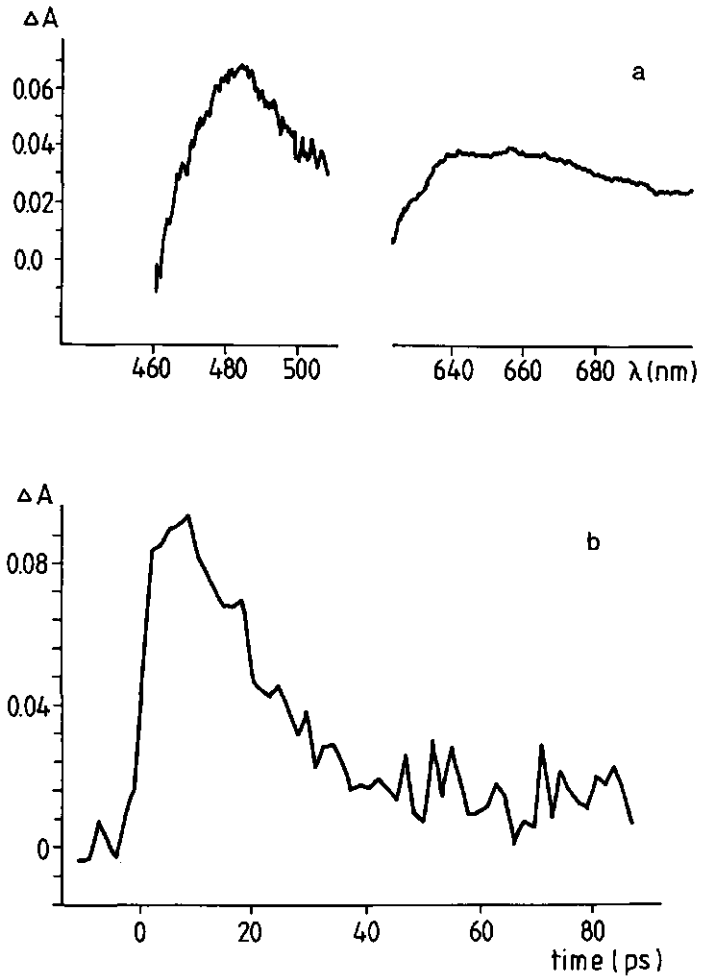

Figure 2: a) Transient absorption difference spectrum of 1 in dichloromethane 3 picoseconds after a 0.5 ps, 610 nm excitation pulse. Regions of strong ground state absorption have been omitted.

b) Time dependence of the transient absorption difference at 656 nm of 1 in dichloromethane, following a 0.5 ps 610 nm excitation pulse.

for 1 - 3 in dichloromethane follows the excitation pulse, which in practice means $k_{CS} \geq 3x10^{11}$ sec^{-1}. Table IV summarizes the experimental values of k_{CS} and k_{CR} for charge separation and charge recombination in dichloromethane and toluene.

Table IV: Formation and decay constants, k_{CS} and k_{CR}, (sec^{-1}) of the transient absorption at 470 nm of $1x10^{-4}$M solutions of 1, 2 and 3 in dichloromethane and in toluene.

compound	dichloromethane		toluene	
	k_{CS}	k_{CR}	k_{CS}	k_{CR}
1	$>3x10^{11}$	$(5.9\pm0.2)x10^{10}$	$>3x10^{11}$ a	$(2.1\pm0.2)x10^{10}$
			$(3.2\pm0.4)x10^{9}$	$< 10^{9}$ b
2	$>3x10^{11}$	$(4.4\pm0.4)x10^{9}$	$(4.5\pm0.5)x10^{9}$	$1.0x10^{9}$
3	$>3x10^{11}$	$(2\pm0.5)x10^{9}$	c	c

a: In toluene two transients are observed (fig. 4).

b: The decay rate constant of the second transient could not be determined due to the timewindow (1 ns) of the experiment.

c: Not measured due to low solubility.

In toluene two P^+ transients for 1 are observed with very similar absorption spectra for two different time-windows : (i) a fast transient with k_{CS} and k_{CR} similar to those of the transient in dichloromethane and (ii) a slow transient with significantly smaller rate constants (figure 3a). The time dependence of the transient absorption is given in figure 4.

The rate constant for formation, k_{CS}, of the second P^+ transient is very similar to the fluorescence decay rate constant found for 1 (Table III). The spectra of the fast and the slow transient species are different from the T-T transient absorption spectrum of the ^3P state (figure 3b). We can explain the experimental results by assuming, that 1 in toluene exists in two conformations with very dif-

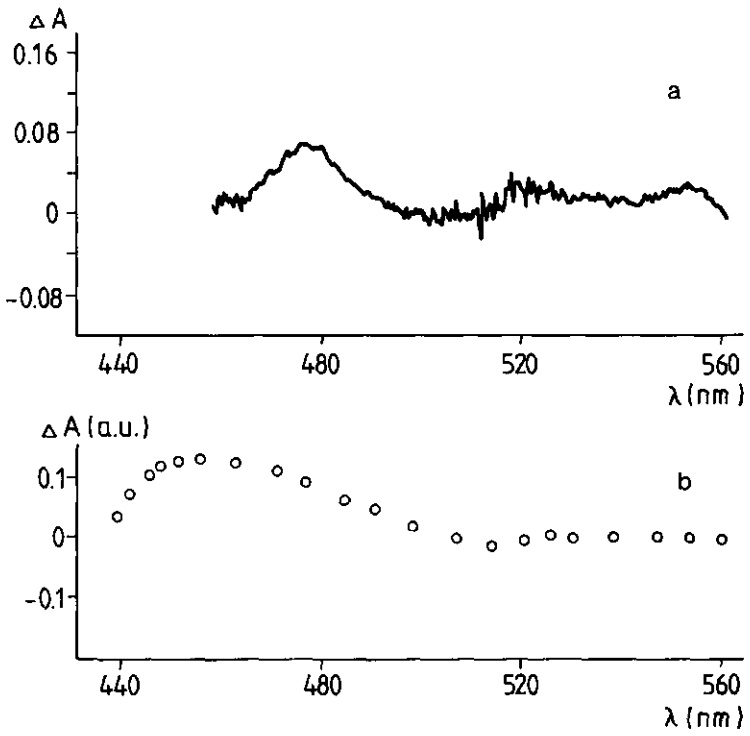

Figure 3: Transient absorption difference spectrum of 1 in toluene. a) 600 picoseconds after a 0.5, ps 610 nm excitation pulse; b) 20 microseconds after a 12 ns, 532 nm excitation pulse.

ferent values of k_{CS} and k_{CR}. Only a single fluorescence lifetime, associated with the longer living species, can be detected. Obviously, the fluorescence lifetime of the shorter lived species is too short to be detected by our apparatus. The existence of two conformations of 1 in toluene is confirmed by the fluorescence excitation spectrum detected at 697 nm, for which the lowest Q-band is 2 nm blue-shifted with respect to the absorption spectrum, since the fluorescence mainly stems from the less folded conformation. Also, the ^1H NMR chemical shifts of 1 in toluene demonstrate, that the average conformation in toluene is less folded than in $CDCl_3$. Since a separate rise of a

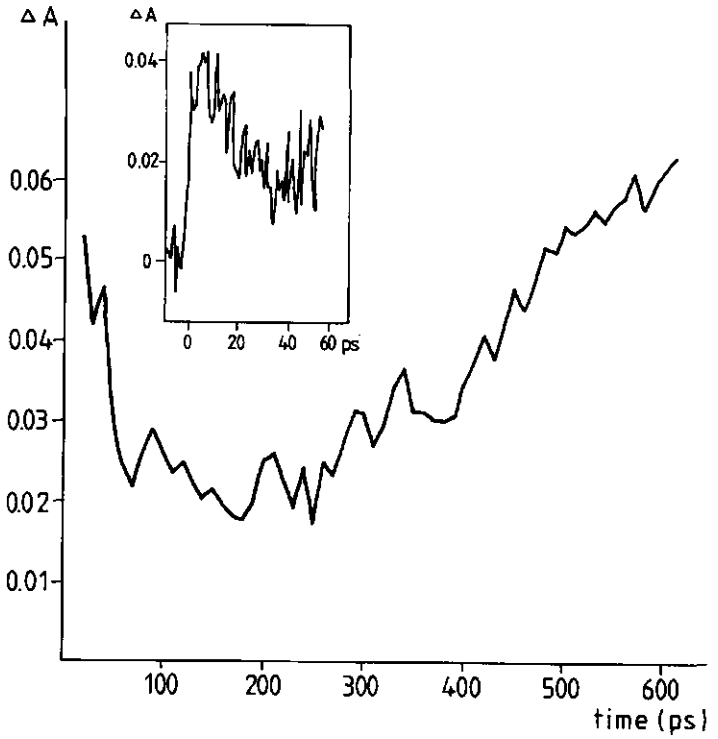

Figure 4: Time dependence of the transient difference absorption spectrum at 478 nm of 1 in toluene, following a 0.5 ps, 610 nm excitation pulse. Insert: 0 - 30 psec transient.

second transient is observed (fig.4), the interconversion between the two conformations must be slower than the formation of the charge separated states P^+-AQ^-.

Triplet formation

For 1 in toluene a transient spectrum was detected on a microsecond (μs) time scale. No μs transients were detected for solutions of 1 in dichloromethane. The transient spectra for 1 in toluene at 600 ps

and at 20 μs are given in figures 3a and b. The μs transient absorption of the toluene solution was shown to be due to a triplet state, because it was quenched by ethyl iodide and oxygen. These data, combined with the position of the μs transient absorption band at 460 nm, corresponding to a typical porphyrin T-T absorption band, identifies this transient as due to the porphyrin triplet state. The triplet quantum yield, determined from the T-T absorption at 700-800 nm, is 30 % of that of the reference compound 4 ,if it is assumed, that the extinction coefficients of the triplet states of these compounds are approximately equal in the 700-800 nm wavelength region.

The $\Delta m = \pm 1$ ESR spectrum of the porphyrin triplet state of 1 in toluene glass at 20 K was recorded to determine its electron spin polarization pattern [17]. This pattern was found to be AAAEEE (A= absorptive, E=emissive) for the six orientations, for which the magnetic field is parallel to the principle axes of the zero field splitting tensor of this triplet state.

Discussion

The folded model system 1 has unusually small distances between porphyrin and anthraquinone, as compared to other covalently linked model systems. In several recently reported model systems [2,3,4,], as well as in bacterial reaction centres, the distances between the redox components is ~10 Å [18], quite different from those in 1. On the other hand the donor-acceptor distance in 1 compares quite well with the distance between the bacteriochlorophyll monomers in the dimeric primary donor of the bacterial reaction centre. Photochemical hole-burning and photon-echo experiments indicate ultrafast ET within the donor [19]. It is therefore of interest to consider the consequences of the close folding of 1 for its photophysical properties.

The non-negligible π-orbital overlap leads to a very efficient through-space electron transfer for 1, as is evident from Table III. The charge recombination rate constants, k_{CR}, in CH_2Cl_2 and the charge separation rate constants, k_{CS}, in toluene show a marked difference between the folded compound 1 on one hand and the non-folded compounds

2 and 3 on the other hand. For the latter two the distance between porphyrin and anthraquinone is larger and the π-orbital overlap between porphyrin and anthraquinone is much smaller than in 1, resulting in smaller rate constants for through space ET.

The rate constants for 2 and 3 are very similar (Table IV) although the porphyrin-anthraquinone distances are different (8.8 Å for 2 vs 16 Å for 3). We propose, that electron transfer occurs mainly through the phenyl-O-SO_2- bridge. The distance through the bridge is similar for 2 and 3, so that a through-bond ET process is expected to have similar rate constants, in agreement with experimental results. Through-bond coupling via the sulfonyloxy bridge is facilitated by the partial π-orbital character of the bonds between the S-and the O-atoms. The presence of the -O-SO_2- group in the bridge has a considerable effect on the redox potentials of the DMA and AQ moieties. For the DMA-P^+-AQ^- -> DMA^+-P-AQ^- process introduction of the sulfonyloxygroup into the bridge between DMA and P changes ΔG from -0.13 eV to +0.53 eV, thereby preventing this process. For the DMA-P-AQ -> DMA-P^+-AQ^- process a change of ΔG from -0.15 to -0.29 eV results, enhancing the charge separation.

At first sight, the high yield of ^3P for 1 in toluene is surprising, because the ISC rate constant of the reference compound 4 ($\leq 5x10^7$ sec^{-1}, derived from the data of Table II) can not compete with the ET rate constants, quoted in Table III, both for the folded and for the unfolded conformation of 1. The former decays directly to the ground state (fig.4), whereas for the latter the observed porphyrin triplet state is not formed by the direct ISC process $^1P^*$-AQ -> ^3P-AQ, but via the triplet radical pair state, i.e. by the process $^1P^*$-AQ -> $^1(P^+-AQ^-)$ -> $^3(P^+-AQ^-)$ -> ^3P-AQ (fig.5). Nevertheless, the characteristic electron spin polarization (ESP) pattern of the $\Delta m_s = \pm 1$ triplet ESR spectrum, arising from exclusive population of the $m_s = 0$ spin level by hyperfine interaction in the radical pair, observed for bacterial reaction centres [17], is not found for 1, obviously because the exchange interaction between the unpaired electrons on P^+ and AQ^- in the radical pair dominates the hyperfine interaction [20].

The conversion of the radical pair singlet state to the correspon-

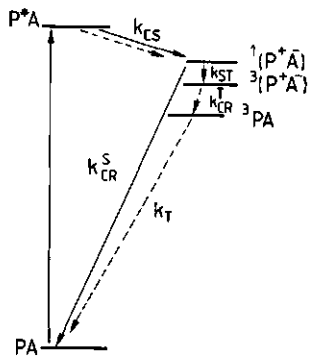

Figure 5: Kinetic scheme for charge separation and recombination in 1 in toluene. (——) folded conformation; (---) unfolded conformation. Fully drawn arrows also apply to the kinetic processes in dichloromethane. The positions of the radical pair energy levels have been calculated, using the data of Table II. Coulombic attraction has been neglected. The energy gap between $^1(P^+-AQ^-)$ and $^3(P^+-AQ^-)$ has been magnified for reasons of clarity. For definition of rate constants k, see text.

ding triplet state is enhanced for 1, because i) the energy gap between both states is much smaller than between localized singlet and triplet states and ii) the anthraquinone oxygen atoms may contribute to the ISC process, due to π-orbital overlap. Figure 5 summarizes the pathways for electron transfer and triplet formation for 1 in both

Acknowledgements

We thank Mr.B.van Veldhuizen for recording the NMR spectra, Mr.A.van Hoek for fluorescence lifetime measurements and Mr.T.A.Roelofs for microsecond transient absorption measurements.
This investigation was supported by the Netherlands Organization for Chemical Research (S.O.N.) with financial aid from the Netherlands Organization for Scientific Research (N.W.O.).

Work at Argonne National Laboratory was supported by the Division of Chemical Sciences, Office of Basic Energy Sciences, U.S. Department of Energy under contract W-31-109-ENG-38.

References

1. W.W.Parson, Ann. Rev. Biophys. Bioeng. 11 (1982) 57.
2. M.R.Wasielewski, M.P.Niemczyk, W.A.Svec and E.Bradley Pewitt, J. Am. Chem. Soc., 107 (1985) 5562.
3. R.J.Harrison, B.Pearce, G.S.Beddard, J.A.Cowan and J.K.M.Sanders, Chem.Phys. 116 (1987) 429.
4. D.Gust, T.A.Moore, P.A.Liddell, G.A.Nemeth, L.R.Makings, A.L..Moore, D.Barrett, P.J.Pessiki, R.V.Bensasson, M.Rouge, C.Chachaty, F.C.DeSchrijver, M.Van der Auweraer, A.R.Holzwarth and J.S.Connolly, J. Am. Chem. Soc. 109 (1987) 846.
5. G.M.Sanders, M.van Dijk, A.van Veldhuizen and H.C.van der Plas, J. Chem. Soc., Chem. Comm. (1986) 1311 and references therein.
6. S.Hayano and M.Fujihira, Bull.Chem.Soc.Jap. 44 (1971) 1496.
7. E.T.Seo, R.F.Nelson, J.M.Fritsch, L.S.Marcoux, D.W.Leedy and R.N.Adams, J. Am. Chem. Soc. 88 (1966) 3498.
8. G.L.Closs, L.T.Calcaterra, N.G.Green, K.W.Penfield and J.R.Miller, J. Phys. Chem. 90 (1986) 3673.
9. H.Heitele, M.E.Michel-Beyerle and P.Finckh, Chem. Phys. Lett. 134 (1987) 273.
10. A.Harriman, J. Chem. Soc., Faraday Trans. II 77 (1981) 1695.
11. K.Vos, A.van Hoek and A.J.W.G.Visser, Eur. J. Biochem. 165 (1987) 55.
12. M.R.Wasielewski, M.P.Niemczyk, J. Am. Chem. Soc. 106 (1984) 5043.
13. R.J.Abraham, K.M.Smith, D.A.Goff and Ian-Li Lai, J. Am. Chem. Soc. 104 (1982) 4332.
14. R.B.M.Koehorst, et.al., manuscript in preparation.
15. R.Bonnet, C.Lambert, E.J.Land, P.A.Sourides,R.S.Sinclair and T.G.Truscott, Photochem. Photobiol. 38 (1983) 1.

16. M.Fujihira and S.Hayano, Bull. Chem. Soc. Japan 45 (1972) 644.
17. R.E.Blankenship, Acc. Chem. Res. 14 (1981) 163.
18. J.Deisenhofer, O.Epp, K.Miki, R.Huber and H.Michel, J. Mol. Biol. 180 (1984) 385.
19. S.R.Meech, A.J.Hoff and D.A.Wiersma, Proc. Natl. Acad. Sci. USA, 83 (1986) 9464.
20. A.Weller, H.Staerk and R.Treichel, Faraday Discuss. Chem. Soc. 78 (1984) 271.

CHAPTER 4.3

A comparison of electron transfer between free and linked donor and acceptor molecules.

Until recently the majority of studies on photoinduced electron transfer (ET) reactions was performed on bimolecular systems, containing loose donor and acceptor molecules, which meet through diffusion in solution. For very fast ET reactions the diffusion of the reactants becomes the rate limiting step [1].

In this Chapter we compare the ET rate constants of a bimolecular system with those for a covalently linked system to determine under which conditions the diffusion of the donor and the acceptor to form the precursor complex is the rate-limiting step for the ET process. In both systems the donor is a diphenyletioporphyrin and the acceptor is an anthraquinone molecule. The porphyrins in the bimolecular systems are diphenyletioporphyrin, H_2DPEP and bis(2-tosylatephenyl)etioporphyrin, Tol-H_2P-Tol (§§ 4.1 and 4.2 (fig.1), respectively). The covalently linked molecules consist of free base or zinc diphenyletioporphyrin, sandwiched between two anthraquinone molecules, which are linked to the porphyrin via a sulfonyloxybridge, AQ-H_2P-AQ and AQ-ZnP-AQ.

Bimolecular system

The fluorescence of H_2DPEP and Tol-H_2P-Tol is quenched by the electron acceptor anthraquinone. If the diffusion is not the rate-limiting step the fluorescence quenching of Tol-H_2P-Tol is expected to be smaller than that for H_2DPEP, because the accessibility of the porphyrin ring is hindered by the tolylgroups above and below the porphyrin plane. The fluorescence quenching experiments were performed on a Perkin-Elmer (HPF-2a) spectrometer. A typical Stern-Volmer plot of the quenching of H_2DPEP by anthraquinone is given in figure 1. At high concentrations the decrease of the fluorescence is no longer linearly dependent on the concentration of the quencher. The Stern-Volmer constants, K, were determined by linear regression (Table

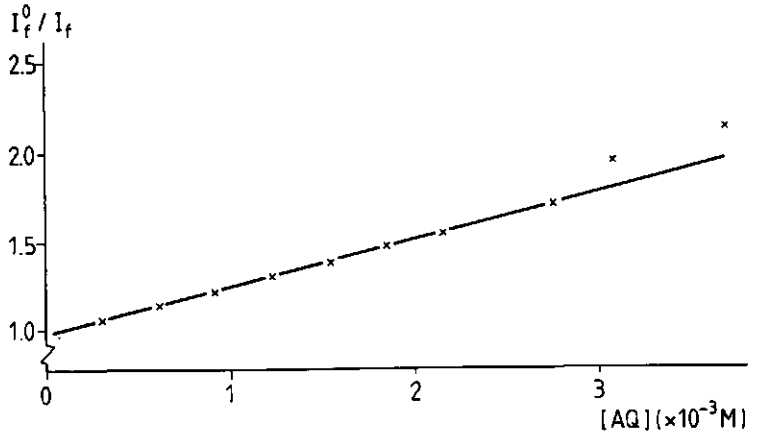

Figure 1: Stern-Volmer plot of the fluorescence quenching of 1.46×10^{-6} M H_2DPEP in toluene by anthraquinone. The straight line is determined by linear regression of the data in the anthraquinone concentration range < 3×10^{-3} M.

Table I: Stern-Volmer constants K and bimolecular quenching rate constants kq of the fluorescence quenching of 1×10^{-6} M solutions of H_2DPEP[a] and Tol-H_2P-Tol[a] in toluene and in dichloromethane.

compound	solvent	K (l/mol)	k_q (l/mol.sec) [b]
H_2DPEP	dichloromethane	283	2.3×10^{10}
	toluene	259	1.8×10^{10}
Tol-H_2P-Tol	dichloromethane	277	2.3×10^{10}
	toluene	256	1.8×10^{10}

a: The porphyrins were excited in the S_2-S_0 band at ≈ 408 nm and the emission was detected at 695 nm.

b: The estimated error for k_q is 10 %.

I). From the Stern-Volmer constants the bimolecular quenching rate constants, k_q, can be calculated by $K = k_q \times \tau_f$, where τ_f is the fluorescence lifetime of the porphyrin in the absence of quencher. The fluorescence lifetimes of Tol-H_2P-Tol in toluene and in dichloromethane were determined by the method of single photon counting: τ_f= 14.3 ns in argon-flushed toluene and 11.9 ns in argon-flushed CH_2Cl_2. The same values were used for H_2DPEP, because both porphyrins have identical fluorescence quantum yields. The calculated bimolecular quenching rate constants are included in Table I.

The quenching rate constants are very near to the diffusional limit. The rate constant for diffusion limited dynamic fluorescence quenching, assuming two spherical molecules, is given by $k_D = 8000RT/3\eta$, where T is the absolute temperature, η is the viscosity and R is the universal gas constant. In toluene, at 20°C when the viscosity $\eta = 5.90 \times 10^{-4}$ N.sec.m^2 the diffusion rate constant is calculated to be $k_D = 1.1 \times 10^{10}$ sec^{-1}. In view of the gross simplification in the calculation of k_D, by representing the porphyrin and anthraquinone molecules by spheres, we conclude, that k_q is determined by k_D.

There is no effect of the substituent tolyl groups on the quenching rate constant, although the tolyl groups, which are situated above and below the porphyrin ring in a cofacial orientation are expected to hinder the quenching reaction. This confirms the hypothesis, that the quenching rate is limited by diffusion.

We conclude, that anthraquinone appears to be a very efficient quencher for diphenyletioporphyrin. The quenching process appears to be diffusion limited.

Covalently linked system

The charge separation and charge recombination rate constants, k_{CS} and k_{CR}, for AQ-H_2P-AQ in dichloromethane and for AQ-ZnP-AQ in pyridine have been determined by picosecond transient absorption spectroscopy, using the Argonne set-up (see § 4.2). The solubility of the compounds limits the choice of possible solvents. The transient

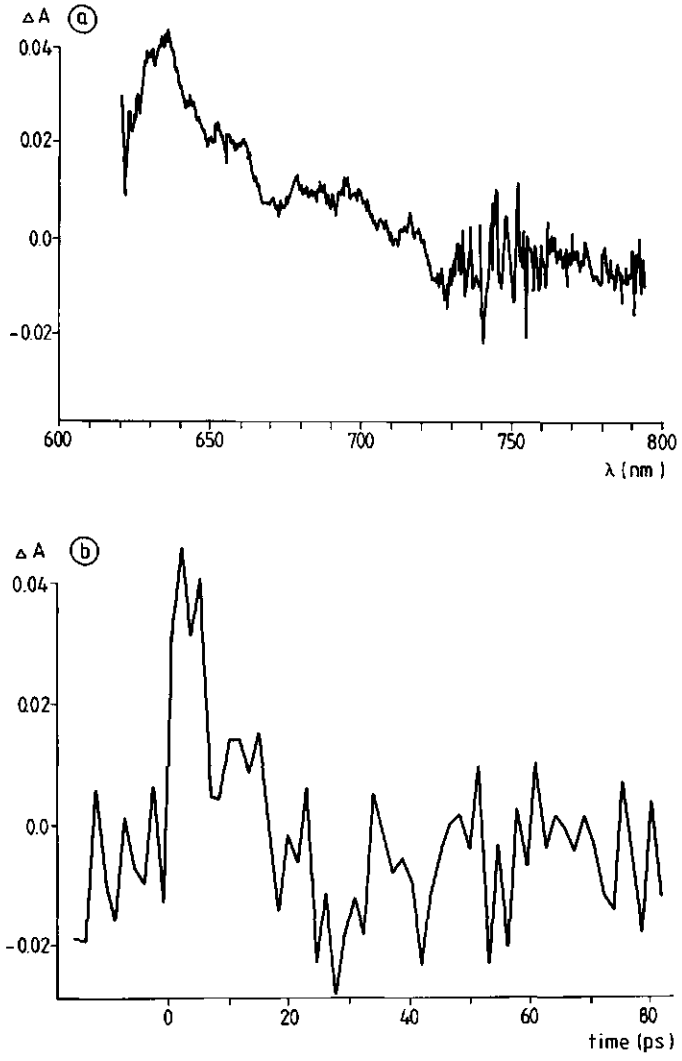

Figure 2: a)Transient absorption difference spectrum of AQ-ZnP-AQ in pyridine 3 ps after a 0.5 ps, 610 nm excitation pulse.
b)Time dependence of the transient absorption difference at 635 nm of AQ-Zn-AQ in pyridine, following a 0.5 ps 610 nm excitation pulse.

absorption spectrum for AQ-H_2P-AQ in dichloromethane after 3 ps is very similar to that for the radical pair DMA-H_2P^+-AQ^- in dichloromethane (fig.2a, § 4.2). The transient absorption spectrum for AQ-ZnP-AQ in pyridine after 3 ps is presented in figure 2a. The transient spectrum has a maximum at 635 nm and is very similar to the spectrum of $ZnTPP^+$, electrochemically generated in dichloromethane [2]. It is, therefore, attributed to the radical pair AQ-ZnP^+-AQ^-. The formation rate constants of the radical pairs AQ-H_2P^+-AQ^- and AQ-ZnP^+-AQ^- are instrument limited (>$3x10^{11}$ sec^{-1}). Both transients decay cleanly to the ground state (see fig.2b for AQ-ZnP-AQ). The radical pair lifetimes are 16.5±1 ps for AQ-H_2P^+-AQ^- in dichloromethane and 6±0.5 ps for AQ-ZnP^+-AQ^- in pyridine. The difference in radical pair lifetimes for AQ-H_2P-AQ and for AQ-ZnP-AQ is attributed to the "inverted effect" (Chapter 2), which predicts a decrease of the ET rate constants with ΔG, the change in free energy for ET, at high exothermicities (ΔG > 0.9 eV). For the recombination steps ΔG = -1.66 eV for AQ-H_2P-AQ and ΔG = -1.49 eV for AQ-ZnP-AQ, so that the recombination ET step for AQ-H_2P-AQ is more exothermic than for AQ-ZnP-AQ, resulting in a larger value of the rate constant for recombination, k_{CR}, for the latter.

Conclusions

AQ-H_2P-AQ and AQ-ZnP-AQ exhibit very fast ET (>$3x10^{11}$ sec^{-1}), which can not be demonstrated by bimolecular fluorescence quenching, which is limited by diffusion rates. To study very fast ET reactions it is necessary to use donor-acceptor complexes, which are held in close proximity by covalent linkages or, alternatively, by electrostatic or ligating interactions, as reported in Chapters 4.2, 5.4, 6 and 7.

References

1. M.D.Newton and N.Sutin, Ann. Rev. Chem. 35 (1984) 437.
2. J.Fajer, D.C.Borg, A.Forman, D.Dolphin and R.H.Freeman, J. Am. Chem. Soc. 92 (1970) 3451.

CHAPTER 5.1

Volume 130, number 6 CHEMICAL PHYSICS LETTERS 24 October 1986

EXCITED-STATE PROPERTIES OF WATER-SOLUBLE PORPHYRIN DIMERS

U. HOFSTRA, R.B.M. KOEHORST and T.J. SCHAAFSMA

Department of Molecular Physics, Agricultural University, De Dreijen 11, 6703 BC Wageningen, The Netherlands

Received 24 June 1986; in final form 9 August 1986

The excited-state properties of heterodimers of tetra(4-carboxyphenyl)porphyrin (TPPC) and tetra(N-methylpyridyl)porphyrin (TMPyP) are studied by absorption and emission spectroscopy, EPR and zero-field ODMR. The excited singlet and triplet states of dimers formed by pairing H_2TPPC with H_2TMPyP or ZnTMPyP are localized on H_2TPPC. The dimers formed by pairing H_2TPPC with CuTMPyP and H_2TMPyP with ZnTPPC or CuTPPC are non-fluorescent due to intramolecular electron transfer.

1. Introduction

The primary donor of bacterial photosynthesis is a bacteriochlorophyll dimer [1]. This has prompted numerous studies on dimers of porphyrins, both as covalently bound dimers [2–11] and as concentration dimers [12–16].

The spectroscopy of concentration dimers, consisting of two different monomers (heterodimers), is complicated by the presence of homodimers and heterodimers in the solution. This problem can be avoided by using a mixture of porphyrin monomers with different sidegroup substituents, favouring the formation of heterodimers.

Porphyrins can be made water-soluble by attaching ionized groups to the porphyrin ring [17]. The porphyrins in this study are tetra(4-carboxyphenyl)porphyrin (TPPC) and tetra(4-N-methylpyridyl)porphyrin (TMPyP) (fig. 1).

We have studied the homodimer of H_2TPPC, formed in solutions of high ionic strength, the heterodimer H_2TPPC–H_2TMPyP and a number of their Zn(II) and Cu(II) derivatives. For $5 < pH < 9$, the carboxyl sidegroups of TPPC and the methylpyridyl sidegroups of TMPyP have four negative and four positive charges, respectively. Preferentially, heterodimers are formed by electrostatic attraction between oppositely charged monomers. Thus, heterodimers can be investigated without interference from homodimers, their formation being prevented by electrostatic repulsion. Under these controlled conditions, no statistical distribution of homo- and heterodimers, such as in solutions of concentration dimers, is found.

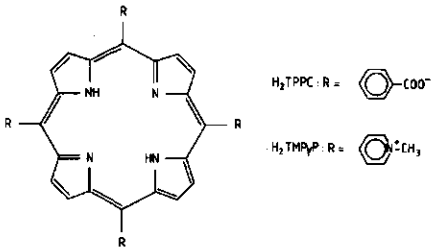

Fig. 1. Molecular structure of H_2TPPC and H_2TMPyP.

In this study, we investigate the different contributions to the intermolecular interactions in the excited singlet and triplet states of the dimers, using absorption and emission spectroscopy, EPR and zero-field magnetic resonance. In all three fluorescent dimers the lowest excited singlet state appears to be localized on the H_2TPPC. The strong quenching of fluorescence or luminescence in some of the heterodimers is attributed to intramolecular electron transfer.

2. Experimental

H_2TMPyP and H_2TPPC were synthesized accord-

ing to published procedures [18,19]. CuTMPyP and ZnTMPyP were prepared from TMPyP free base [20]. To prepare CuTPPC and ZnTPPC, H_2TPPC was dissolved in 30 mM Tris.HCl buffer ($pH = 8$) and treated with excess $CuCl_2$ or $ZnCl_2$. The metalloporphyrin was crystallized by adding acetic acid after completion of the reaction, recrystallized, washed with dilute acetic acid and dried in vacuum.

For spectroscopic studies, we used an aqueous solution containing 75% w/v sucrose and 30 mM Tris.HCl, $pH = 8.5$. The pH was chosen to be well above the $pK = 4.2$ value (H_2O, 25°C) of the carboxyphenylgroup, ensuring easy solubility of the porphyrin. In this solvent, which forms an optically transparent glass at low temperatures, TPPC and TMPyP do not aggregate, as they do in neat H_2O, even at high pH [21,22].

Absorption spectra were recorded using a Uvikon 810 spectrophotometer, fluorescence spectra using a Perkin Elmer LS-5 fluorimeter. The triplet state of a number of monomers and dimers was studied by fluorescence-detected magnetic resonance (FDMR) in zero magnetic field, using a spectrometer previously described in detail [23]. Samples at 4.2 K were optically excited using a 900 W xenon lamp, filtered through a saturated $CuSO_4$ solution, followed by a Schott BG12 filter, or using a cw Ar^+ laser operating at 476.5 or 514.5 nm. The fluorescence fading measurements [24] were performed at 77 and 195 K, using a modified apparatus of the FDMR spectrometer with a mechanical chopper in the excitation light beam.

3. Results

The results of the absorption measurements are listed in table 1. The Soret band (410–430 nm) of H_2TPPC exhibits a blue-shift of 2 nm on addition of a TMPyP compound, whereas the Q bands (500–650 nm) shift to the red. The maximum shift is found at a 1:1 ratio, indicating the formation of a 1:1 complex.

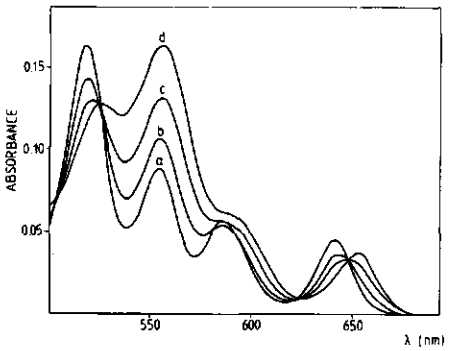

Fig. 2. Absorption spectra of 1.0×10^{-5} M H_2TPPC in 75% w/v sucrose/H_2O/30 mM Tris.HCl; $pH = 8.5$ with (a) 0, (b) 3.8×10^{-6} M, (c) 7.5×10^{-6} M, (d) 1.13×10^{-5} M CuTMPyP.

In pure H_2O, TPPC and TMPyP porphyrins form a distribution of mixed 1:1 accordion-type aggregates [25]. This is not observed in 75% w/v sucrose solution. Fig. 2 shows the changes in the absorption spectrum when titrating a solution of H_2TPPC with increasing amounts of CuTMPyP. Since the latter porphyrin has no absorption bands in the 630–660 nm region, the bands at 641 and 653 nm are well separated and due to H_2TPPC and H_2TPPC–CuTMPyP, respectively. The occurrence of an isosbestic point indicates that a single 1:1 complex is formed. The dimerization constant K_d is found to be $2 \times 10^6\ M^{-1}$. The absorption spectra of H_2TPPC and H_2TMPyP solutions do not exhibit an isosbestic point upon titration, due to overlapping monomer absorption bands.

Table 1
Absorption wavelengths (nm) of free-base porphyrin monomers and dimers at room temperature

Porphyrin	Soret	$Q_{x(1,0)}$	$Q_{x(0,0)}$	$Q_{x(1,0)}$	$Q_{x(0,0)}$
H_2TCPP	420	517	554	586	640
H_2TMPyP	427	518	553	587	643
H_2TPPC–H_2TMPyP	418	521	558	593	650
H_2TPPC–H_2TPPC	420	518	555		644

Table 2
Emission wavelengths [a] (nm) of water-soluble porphyrin monomers and dimers in 75% w/v sucrose in H_2O, $pH = 8.5$; $T = 80$ or 300 K

Porphyrin	$Q_{(0,0)}$		$Q_{(0,1)}$		$I_{Q(0,0)}/I_{Q(0,1)}$		Phosph. 80 K
	80 K	300 K	80 K	300 K	80 K	300 K	
H_2TPPC	639	646	703	711	2.1	2.6	
H_2TMPyP	638	651	702	714	1.0	1.0	
ZnTMPyP	606	622	657	667	1.1	1.0	753
CuTMPyP							705 [b]
H_2TPPC–H_2TMPyP	657	[c]	721	[c]	2.3		
H_2TPPC–H_2TPPC	653	665	723	730	3.9	3.0	
H_2TPPC–ZnTMPyP	650	[c]	706	[c]	2.7		[c]

[a] Excitation in the Soret band. [b] Quartet luminescence. [c] No emission is observed.

The absorption spectrum of H_2TPPC is red-shifted on addition of KCl, due to dimerization, in agreement with earlier findings for similar compounds [12]. The absorption spectra of H_2TMPyP and a 1:1 mixture of H_2TPPC and H_2TMPyP, on the other hand, do not change on addition of KCl.

No emission is found for solutions of heterodimers at room temperature. In frozen solution fluorescence of some dimers is observed, however, which is red-shifted as compared to that of the monomers (table 2). No emission is observed from H_2TPPC–CuTMPyP, H_2TMPyP–ZnTPPC and H_2TMPyP–CuTPPC.

The zero-field splitting (ZFS) parameters D and E of the lowest triplet state of a number of fluorescent dimers were determined from fluorescence-detected magnetic resonance (FDMR) spectra at 4.2 K and from EPR. No triplets could be detected by conventional EPR in non-fluorescent dimers. ZFS values are collected in table 3.

Table 3
Zero-field splitting parameters (in units of 10^{-4} cm^{-1}) measured by FDMR for porphyrin monomers and dimers. Solvent: 75% w/v sucrose/H_2O; 30 mM Tris.HCl, $pH = 8.5$

Porphyrin	λ_{em}(nm) [a]	D	E
H_2TPPC	640	387	66
H_2TMPyP	646	418	41
H_2TPPC–H_2TPPC	655	365	73
H_2TPPC–H_2TMPyP	655	365	67
H_2TPPC–ZnTMPyP	654	376	82

[a] Detection wavelength, bandwidth 10 nm.

Table 4
Triplet state decay constants k_T (in s^{-1}); $T = 77$ K [a]

Porphyrin	k_T(77 K) [b]
H_2TPPC	166
H_2TMPyP	101
H_2TPPC–H_2TMPyP	162

[a] Obtained from fluorescence fading.
[b] Estimated error: ± 10 s^{-1}.

Generally, the D values of the triplet state of dimers are found to be smaller than in the corresponding monomer. The ZFS parameters of the dimer H_2TPPC–H_2TPPC are close to the values for the dimer of tetrakis(5,10,15,20-sulfonatophenyl)-porphyrin [12]. The positions and relative amplitudes of the FDMR transitions of H_2TPPC–H_2TMPyP and H_2TPPC–ZnTMPyP are close to those of the H_2TPPC monomer, but are very different from those of either H_2TMPyP or ZnTMPyP.

Triplet-state decay constants at 77 K are given in table 4, and are independent of temperature up to 195 K. In this temperature range the triplet decay could be described by a single exponential.

4. Discussion

H_2TPPC dimerizes in solution on addition of KCl due to shielding of the negative charges that oppose dimerization; it is therefore the result of van der Waals attraction between the hydrophobic por-

phyrin macrocycles. Although the electrostatic repulsion between the monomer units in H_2TMPyP is expected to be very similar to that in the H_2TPPC dimer, dimerization of H_2TMPyP is not significantly enhanced by increasing the ionic strength of the solution, in contrast to the behaviour of H_2TPPC. This is likely to be due to the delocalization of the positive charge over the pyridinium substituent groups [26] in H_2TMPyP, the result of which is a less complete shielding of the positive charges in H_2TMPyP in the presence of Cl^- ions at positions equivalent to those of K^+ in the H_2TPPC dimer.

In contrast to homodimers, the opposite charges of TPPC and TMPyP in heterodimers are additive to the van der Waals attraction, resulting in considerable stabilization. From ring current shifts in 300 MHz H-NMR spectra, it can be concluded that the dimers have a stacked face-to-face conformation [27]. For such a configuration a simple calculation using a plane-to-plane distance of 3.5 Å yields an electrostatic attractive energy of magnitude comparable to the van der Waals interaction, which here is mainly due to the π-electrons of the porphyrin macrocycle [28].

Strikingly, all emission from the heterodimers at room temperature is quenched. This is attributed to the presence of low-lying charge- transfer states in the dimers at room temperature (table 5, fig. 3).

In frozen solution, the emitting state of the dimers H_2TPPC–H_2TMPyP and H_2TPPC–ZnTMPyP is localized mainly on the TPPC moiety in view of the small shift (10 nm) of the dimer fluorescence with respect to that of the monomeric H_2TPPC. The emission of H_2TMPyP–ZnTPPC in frozen solution is strongly quenched, but the emission of H_2TPPC–ZnTMPyP is not. Fig. 3 represents the low-lying electronic states for both compounds. The strong quenching of the emission can be understood from the presence of a low-lying charge-transfer state in H_2TMPyP–ZnTPPC, which is not present in its isomer H_2TPPC–ZnTMPyP.

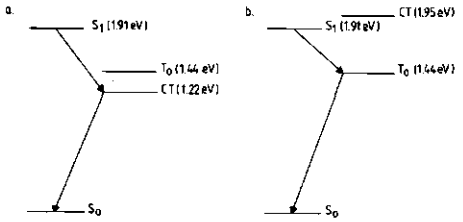

Fig. 3. Energy level scheme of (a) H_2TMPyP–ZnTPPC and (b) H_2TPPC–ZnTMPyP in solid solution. $E = E_{1/2,ox}$ (porph. 1) $- E_{1/2,red}$ (porph. 2). For redox potentials, see table 5. Solvent stabilization neglected.

Table 5
First oxidation and reduction potentials (versus NHE) of porphyrins in aqueous solution

Porphyrin	$E_{1/2,ox}$(V)	$E_{1/2,red}$(V)
H_2TPPS [a]	1.10 [b]	−1.06 [b]
H_2TMPyP	>1.30 [b]	−0.42 [c]
ZnTPPC	0.87 [b]	−1.16 [b]
ZnTMPyP	1.18 [b]	−0.85 [b]
CuTPPC		0.15 [c]
CuTMPyP		0.11 [c]

[a] H_2TPPC could not be measured probably because dimerization occurs at the concentration needed for our cyclic voltammetry measurements ($\approx 10^{-3}$ M). The redox potentials of the anionic systems TPPC and TPPS are very similar [17].
[b] From ref. [17].
[c] Measured in sucrose solution at $pH = 8.5$.

The quenching of the fluorescence of H_2TPPC–CuTMPyP and H_2TMPyP–CuTPPC can be attributed to enhanced intersystem crossing to the triplet state in the presence of a paramagnetic Cu(II) ion and/or to electron transfer. The reduction potentials of CuTMPyP and CuTPPC show that the Cu(II) centre of these porphyrins can be reduced, due to low-lying CT states as has been found for copper(II)-tetra(4-N,N′,N″-trimethylanilinium)porphyrin [29].

There are two contributions to the observed red-shift of the fluorescence of H_2TPPC–H_2TMPyP, H_2TPPC–H_2TPPC and H_2TPPC–ZnTMPyP with respect to the monomer fluorescence of H_2TPPC. The first contribution stems from charge transfer or charge resonance interactions. The oxidation and reduction potentials of these porphyrins show that there are low-lying charge-transfer states in these dimers. The second contribution to the fluorescence red-shift originates from singlet exciton coupling between the excited states of both porphyrin moie-

ties in the dimers. This term should depend on the energy difference between the lowest excited singlet states of both porphyrins in the dimer. In some covalently bound porphyrin dimers, this exciton coupling is responsible for a significant blue-shift of the Soret band in the absorption spectrum [30]. In our complexes this blue-shift can be off-set by the red-shift caused by charge-transfer interactions. A similar effect has been found in the electronic spectra of a stratibisporphyrin [31].

Exciton coupling can explain the smaller emission shift in H_2TPPC–ZnTMPyP as compared to that in H_2TPPC–H_2TMPyP. The difference between the energies of the singlet excited states of ZnTMPyP and H_2TPPC is larger than between those of H_2TMPyP and H_2TPPC in the heterodimer resulting in a larger exciton coupling for the latter.

The similarity between the parameters of the lowest triplet state of H_2TMPyP–H_2TPPC and H_2TPPC–ZnTMPyP and those of the monomeric H_2TPPC indicates that the lowest triplet state is located mainly on H_2TPPC. The triplet-state decay constant of H_2TPPC–H_2TMPyP is very similar to that of H_2TPPC. Therefore, the π–π interactions in the lowest triplet state of the dimer must be very weak. The dimers show a reduction of the D value compared to that of H_2TPPC, which can be explained by some charge-transfer character of the triplet state [32].

Water-soluble porphyrin dimers show various interactions in their excited states, depending on the nature of the peripheral substituent groups and of the central atom. Porphyrins with oppositely charged substituent groups are useful in the study of (selectively) monometallated heterodimers.

References

[1] H. Michel, J. Mol. Biol. 158 (1982) 567.
[2] D. Dolphin, J. Hiom and J.B. Paine III, Heterocycles 16 (1981) 417.
[3] M.R. Wasielewski, in: Molecular biology, biochemistry and biophysics, Vol. 35, ed. F.K. Fong (Springer, Berlin, 1982) p. 234.
[4] J.P. Collman, F.C. Anson, C.E. Barnes, C.S. Bencosme, T. Geiger, E.R. Evitt, R.P. Kreh, K. Meier and R.B. Pettman, J. Am. Chem. Soc. 105 (1983) 2694.
[5] M.A. Bergkamp, C.-K. Chang and T.L. Netzel, J. Phys. Chem. 87 (1983) 4441.
[6] F. Gueckel, D. Schweitzer, J.P. Collman, S. Bencosme, E.R. Evitt and J. Sessler, Chem. Phys. 86 (1984) 161.
[7] J.C. Mialocq, C. Gianotti, P. Maillard and M. Momenteau, Chem. Phys. Letters 112 (1984) 87.
[8] I. Fujita, J. Fajer, C.-K. Chang, C.-B. Wang, M.A. Bergkamp and T.L. Netzel, J. Phys. Chem. 86 (1982) 3754.
[9] B. von Maltzan, Z. Naturforsch. 40a (1985) 389.
[10] J.D. Petke and G.M. Maggiora, Chem. Phys. Letters 97 (1983) 231.
[11] J.E. Hunt, J.J. Katz, A. Svirmickas and J.C. Hindman, J. Am. Chem. Soc. 106 (1984) 2242.
[12] T.K. Chandrasekhar, H. van Willigen and M.H. Ebersole, J. Phys. Chem. 88 (1984) 4326.
[13] G. Bharkar Maiya and V. Krishnan, Inorg. Chem. 24 (1985) 3253.
[14] T.K. Chandrasekhar and H. van Willigen, Chem. Phys. Letters 106 (1984) 237.
[15] E. Ojadi, R. Selzer and H. Linschitz, J. Am. Chem. Soc. 107 (1985) 7783.
[16] H. van Willigen and U. Das, J. Am. Chem. Soc. 107 (1985) 7784.
[17] K. Kalyanasundaram and M. Neumann-Spallart, J. Phys. Chem. 86 (1982) 5163.
[18] D. le Roux, J.-C. Mialocq, O. Anitoff and G. Folcher, J. Chem. Soc. Faraday Trans. II 80 (1984) 909.
[19] A. Adler, F.R. Longo, J.D. Finarelli, J. Goldmacher, J. Asson and L. Korsakof, J. Org. Chem. 32 (1976) 476.
[20] K. Kalyanasundaram and M. Grätzel, Helv. Chim. Acta 63 (1980) 478.
[21] J. Turay, P. Hambright and N. Datta-Gupta, J. Inorg. Nucl. Chem. 40 (1978) 1687.
[22] K. Kano, T. Miyake, K. Uomoto, T. Sato, T. Ogawa and S. Hashimoto, Chem. Letters (1983) 1867.
[23] L. Benthem, Thesis, Landbouwhogeschool, Wageningen (1984).
[24] R. Avarmaa, Mol. Phys. 37 (1979) 441.
[25] T. Shimidzu and T. Iyoda, Chem. Letters (1981) 853.
[26] K. Kalyanasundaram, J. Chem. Soc. Faraday Trans. II 79 (1983) 1365.
[27] U. Hofstra, R.B.M. Koehorst and T.J. Schaafsma, unpublished results.
[28] B.S. Sudhindra and J.H. Fuhrhop, Intern. J. Quantum Chem. 20 (1981) 747.
[29] A. Bettelheim, D. Ozer and R. Harth, J. Chem. Soc. Faraday Trans. I 81 (1985) 1577.
[30] C.K. Chang, Advan. Chem. Ser. 173 (1979) 162.
[31] N.E. Kagan, D. Mauzerall and R.B. Merrifield, J. Am. Chem. Soc. 99 (1977) 5484.
[32] R. Kooyman, Thesis, Landbouwhogeschool, Wageningen (1980).

MAGNETIC RESONANCE IN CHEMISTRY, VOL. 25, 1069-1073 (1987)

Solution Structure of Porphyrin Aggregates Determined by ^{1}H NMR Ring Current Shifts

I. Heterodimers of Oppositely Charged Porphyrins

U. Hofstra,* R. B. M. Koehorst and T. J. Schaafsma
Department of Molecular Physics, Agricultural University, de Dreijen 11, 6703 BC Wageningen, The Netherlands

The solution structures of dimers consisting of negatively charged Zn[tetra(4-carboxyphenyl)porphyrin], ZnTPPC, with positively charged Zn[tetra(4-*N*-methylpyridyl)porphyrin], ZnTMPyP, and with H_2[tetra(4-*N*-methylpyridyl)porphyrin], H_2TMPyP, were determined by ^{1}H NMR ring current shifts. The conformation is not affected by the presence of the metal in the centre of the TMPyP monomer. The dimers have a cofacial conformation with a plane-to-plane separation of 3.1 Å and an in-plane translation of 4.2 Å along the aryl—aryl axis.

KEY WORDS Ring current shifts Heterodimers of oppositely charged porphyrins Solution structure ^{1}H NMR

INTRODUCTION

Dimers of macrocyclic tetrapyrroles play a vital role in the photosynthetic process, a chlorophyll dimer being the primary donor in the bacterial reaction centre. This has prompted many studies of porphyrin dimers, both as covalently linked porphyrin dimers[1,2] and as concentration dimers.[3-5] Concentration heterodimers (i.e. dimers of two unequal molecules) are difficult to study, because the homodimers of both constituents are also present in the solution. This can be avoided by using dimers of oppositely charged water-soluble porphyrins.

In a previous study,[6] we reported on the photophysical properties of hetero-dimers of positively charged tetra(4-*N*-methylpyridyl)porphyrins (TMPyP) and negatively charged tetra(4-carboxyphenyl)porphyrins (TPPC) (Fig. 1). We proposed that in one of these dimers electron transfer occurred. Since the electron transfer should depend on the geometry of these dimers,[7] we have investigated their conformation.

In this paper we present the solution structure of the dimers [ZnTPPC-H_2TMPyP] and [ZnTPPC-ZnTMPyP] as determined by ^{1}H NMR. The large aromatic ring current in the monomeric porphyrin molecule

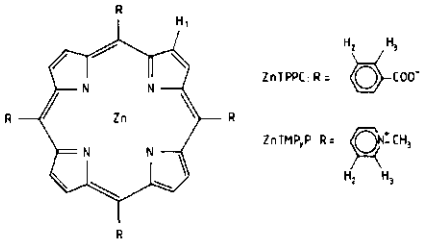

Figure 1. Molecular structure of ZnTPPC and ZnTMPyP. H_2TMPyP has two protons in the centre of the porphyrin ring.

* Author to whom correspondence should be addressed.

0749-1581/87/121069-05$05.00

makes a significant contribution to the chemical shifts of the porphyrin protons. In a porphyrin dimer the ring current chemical shifts are determined by the conformation of the dimer. We have adopted the ring current model of Abraham *et al.*[8] to calculate the conformation of the dimers. The contribution of the porphyrin macrocycle to the ring current shift is treated as the sum of the contributions of four pentagons and four hexagons. The current loops are replaced by equivalent magnetic dipoles located at 0.64 Å above and below the centre of the polygons. The total ring current shift of a nucleus is given by

$$\delta_i = \sum_{k=1}^{8} \mu_H(1-3\cos^2\Theta_{ik})/r_{ik}^3 + \sum_{k=1}^{8} \mu_P(1-3\cos^2\theta_{ik})/r_{ik}^3 + \sum_{k=1}^{4} \mu_A(1-3\cos^2\theta_{ik})/r_{ik}^3 \quad (1)$$

where μ_H, μ_P and μ_A are the dipole moments of the hexagons, the pentagons and the aryl groups, respectively, r_{ik} is the distance of the nucleus i to the origin of the dipole moments and ϕ_{ik} is the angle between the vector r_{ik} and the normal to the polygon k.

At short distances between a proton and the neighbouring porphyrin the equivalent dipole approximation is no longer valid. The ring current shift is then given by

$$\delta = \delta_d g_d[b(d^2-z^2)+c(d^4-z^4)] \quad (2)$$

where δ_d and g_d are the shift and gradient of the shift at the close range boundary at $z = d$, b and d are -0.64 Å and 3.6 Å, respectively, and $c = -(1+2bd)/4z$.[8]

EXPERIMENTAL

The preparation of the porphyrins has been described previously.[6] The TMPyP compounds were used as their

Received 27 May 1987
Accepted 10 August 1987

iodide salts, $H_2TMPyP^{4+} \cdot I^-_4$ and $ZnTMPyP^{4+} \cdot I^-_4$ ZnTPPC was used in the acid form.

For the NMR experiments we used a 4:1 mixture of D_2O and CD_3OD as a solvent. 30 mM non-deuteriated tris(hydroxymethyl)aminomethane (Tris) was added to ionize the carboxyl groups of TPPC ($pK \approx 5$). For the optical experiments non-deuteriated solvents were used. The $D_2O:CD_3OD$ ratio has a large influence on the dimerization constant and on the formation of higher aggregates. An increase of the fraction of D_2O in the solvent mixture results in an increase of the dimerization constants and also in an increase of the formation of higher aggregates.[9] For the compounds reported in this paper the solvent composition could be chosen such that the fraction of dimers was close to 100%.

The ^1H NMR spectra were obtained on a Bruker CXP-300 spectrometer at 295 K. The chemical shifts are quoted relative to TMS. The CD_2HOD peak at 3.39 ppm was used as a reference signal for the determination of the chemical shifts. A Kontron Uvikon spectrometer was used to measure the optical absorption spectra. The absorption differences between monomer solutions and 1:1 mixtures of the porphyrins were measured in a double compartment cuvette as the absorption difference before and after mixing of the two monomer solutions in the cuvette. The total optical path length of the cell was 8.8 mm. At high concentrations ($>10^{-4}$ M), where the double compartment cuvette could not be used owing to the very high absorbance, the monomer absorption data were calculated from the absorption spectra at 5×10^{-5} M.

RESULTS

The dimerization constants of the dimers [ZnTPPC–ZnTMPyP] and [ZnTPPC–H_2TMPyP] were determined optically. The optical absorption spectra of 1:1 mixtures of the monomers in the solvent mixture 4:1 H_2O–CH_3OH were measured over a wide range of monomer concentrations: 5×10^{-7} to 5×10^{-4} M for the ZnTPPC–ZnTMPyP mixture and 5×10^{-7} to 5×10^{-5} M for the ZnTPPC–H_2TMPyP mixture. The maximum concentration attainable for the latter mixture was limited by the solubility of H_2TMPyP. The absorption data of each mixture could be fitted with a single dimerization constant (Fig. 2). Figure 2 shows that the aggregation of ZnTPPC and ZnTMPyP and of ZnTPPC and H_2TMPyP in this concentration range can be described as a dimerization without the need to invoke higher aggregates. The dimerization constants are $6.2 \pm 0.4 \times 10^6$ M^{-1} for [ZnTPPC–ZnTMPyP] and $7 \pm 1 \times 10^6$ M^{-1} for [ZnTPPC–H_2TMPyP]. The errors indicate the range over which the standard deviation of K does not increase by more than 10% from the value yielding the best fit.

The NMR spectrum of a 1:1 mixture of ZnTPPC and ZnTMPyP was taken with a total porphyrin concentration of 1×10^{-3} M. At this concentration 98% of the porphyrins have formed the dimer [ZnTPPC–ZnTMPyP]. The total porphyrin concentration in the case of a 1:1 mixture of ZnTPPC and H_2TMPyP was 1×10^{-4} M; 95% of the porphyrins have then dimerized to [ZnTPPC–H_2TMPyP].

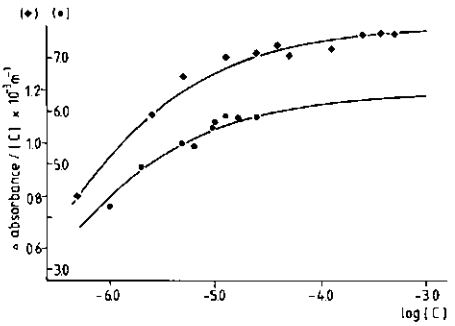

Figure 2. Absorption difference at 560 nm between a 1:mixture of ZnTPPC–ZnTMPyP and the corresponding monomer solutions (◆) and the absorption difference at 515 nm between a 1:1 mixture of ZnTPPC–H_2TMPyP and the corresponding monomer solutions (●) in 4:1 H_2O–CH_3OH, 30 mM Tris. The drawn lines represent the best fit to the data with a single dimerization constant. Top curve (ZnTPPC–ZnTMPyP), $K = 6.2 \pm 0.4 \times 10^6$ M^{-1}; bottom curve (ZnTPPC–H_2TMPyP), $K = 7 \pm 1 \times 10^6$ M^{-1}.

The ^1H NMR spectra of the monomer solutions of ZnTPPC and ZnTMPyP in 4:1 D_2O–CD_3OD and of a 1:1 mixture of these compounds are shown in Fig. 3. Only the low-field regions of the spectra, containing the pyrrole proton resonances and the *meta*- and *ortho*-phenyl proton resonances, are shown. Figure 4 shows the ^1H NMR spectra of solutions of ZnTPPC and of H_2TMPyP in 4:1 D_2O–CD_3OD and of a 1:1 mixture of these compounds. The NMR spectra did not change appreciably on raising the temperature to 340 K. Therefore, under our experimental conditions, in solutions containing monomers and dimers the observed chemical shifts are always an average of the chemical shifts of the monomers and the dimers. The resonances in the

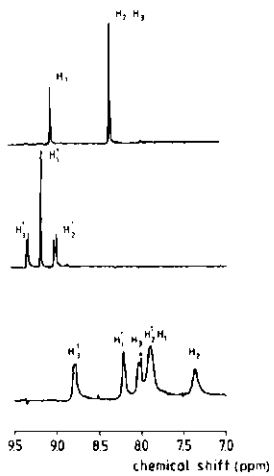

Figure 3. Aromatic region of the ^1H NMR spectra of: (top) 1×10^{-3} M ZnTPPC in 4:1 D_2O–CD_3OD, 30 mM Tris; (centre) 1×10^{-3} M ZnTMPyP in 4:1 D_2O–CD_3OD, 30 mM Tris; (bottom) 5×10^{-4} M 1:1 mixture ZnTPPC–ZnTMPyP in 4:1 D_2O–CD_3OD, 30 mM Tris.

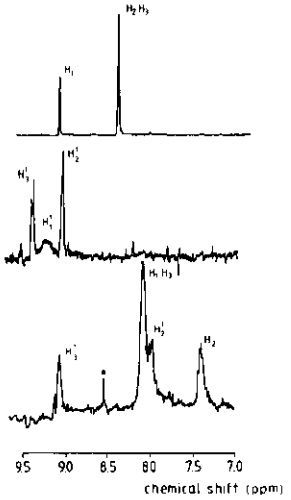

Figure 4. Aromatic region of the ^1H NMR spectra of (top) 1×10^{-3} M ZnTPPC in 4:1 D_2O–CD_3OD, 30 mM Tris; (centre) 1×10^{-4} M H_2TMPyP in 4:1 D_2O–CD_3OD, 30 mM Tris; (bottom) 5×10^{-5} M solution of 1:1 mixture of ZnTPPC–H_2TMPyP in 4:1 D_2O–CD_3OD, 30 mM Tris. The asterisk denotes an artifact due to the solvent.

NMR spectrum of [ZnTPPC-ZnTMPyP] could thus be identified using a titration, varying the concentration ratio of ZnTMPyP and ZnTPPC from 4:1 to 1:4. The same procedure was used for the identification of the resonances of the dimer [ZnTPPC-H_2TMPyP]. In a 1:2 mixture of ZnTPPC and H_2TMPyP the resonance positions of H_2TMPyP were the average of the resonance positions in a 1:1 mixture and those of a monomer solution, whereas the resonance positions of ZnTPPC were the same as in a 1:1 mixture.

We also tried to measure the 1H NMR spectra of the dimer [H_2TPPC-ZnTMPyP]. It appears, however, that at the concentrations needed for the NMR experiments it is mostly higher aggregates that are formed in 1:1 mixtures of H_2TPPC and ZnTMPyP. From experiments at different concentration ratios, when trimers or tetramers are formed, the ring current shifts can be derived for the dimer. These shifts prove to be almost identical with those for [ZnTPPC-H_2TMPyP] and [ZnTPPC-ZnTMPyP], resulting in a very similar dimer conformation.

The chemical shifts of the H-1, H-2 and H-3 protons of the ZnTPPC, ZnTMPyP and H_2TMPyP monomers are presented in Table 1. Table 1 also contains the ring current shift contribution to the observed chemical shifts, as obtained from the difference between the chemical shift of the porphyrins and the reference compounds. The difference between the chemical shifts of the protons in 1:1 ZnTPPC-ZnTMPyP and ZnTPPC-H_2TMPyP mixtures and the chemical shifts of the monomers are presented in Table 2. Because the dimerization is nearly complete, these shifts are taken to be pure dimerization shifts. The experimental ring current shifts for H-1, H-2 and H-3 of both monomers in the dimer follow from the difference between the chemical shifts of these protons in the dimer and in the corresponding monomer.

Table 1. Experimental proton chemical shifts (in ppm) of 1×10^{-3} M solutions of ZnTPPC and ZnTMPyP monomers and of a 1×10^{-4} M solution of H_2TMPyP monomers in 4:1 D_2O–CD_3OD, 30 mM Tris

Compound	Proton[a]	Chemical shift	Ring current shift
ZnTPPC	H-1	9.08	3.22[b]
	H-2	8.39	0.83[c]
	H-3	8.39	0.44[c]
ZnTMPyP	H-1	9.18	3.32[b]
	H-2	9.01	0.88[d]
	H-3	9.35	0.49[d]
H_2TMPyP	H-1	9.25	3.39[b]
	H-2	9.05	0.92[d]
	H-3	9.41	0.56[d]

[a] For numbering of protons see Fig. 1.
[b] Shift with reference to the reference compound cyclohexa-1,2-diene[8].
[c] Reference compound is benzoic acid.
[d] Reference compound is *N*-methylpyridinium iodide.

The chemical shift of the —$N(CH_3)$ protons of ZnTMPyP and H_2TMPyP is 4.88 ppm. In the solvent mixture 4:1 D_2O-CD_3OD, 30 mM Tris, the shifts are difficult to detect owing to the presence of intense proton resonances from CD_2HOD and Tris. The dimerization shift for ZnTMPyP in [ZnTPPC-ZnTMPyP] was determined to be $\Delta\delta = -0.21$ ppm.

Table 2. Differences between the chemical shifts (in ppm) of a 1:1 mixture of 1×10^{-3} M solutions of ZnTPPC with ZnTMPyP and of a 1:1 mixture of 1×10^{-4} M solutions of ZnTPPC with H_2TMPyP in 4:1 D_2O–CD_3OD, 30 mM Tris, and the chemical shifts of the corresponding monomers

Mixture	Proton[a]			Experimental value	Calculated value[b]
	ZnTPPC	ZnTMPyP	H_2TMPyP		
ZnTPPC–ZnTMPyP		H-1		−0.99	−0.90
	H-1			−1.03	−0.90
		H-2		−1.15	−1.11
	H-2			−1.02	−1.11
		H-3		−0.59	−0.63
	H-3			−0.52	−0.63
ZnTPPC–H_2TMPyP			H-1	—[c]	−0.90
	H-1			−1.00	−0.90
			H-2	−1.06	−1.11
	H-2			−0.97	−1.11
			H-3	−0.39	−0.63
	H-3			−0.31	−0.63

[a] For numbering of protons see Fig. 1.
[b] Calculated ring current shifts for H-1 to H-3 in both monomeric components of the dimers are identical, since the equivalent dipoles of both monomers are identical, and because only dimers and no monomers or other aggregates are assumed to be present in solution.
[c] The dimerization shift could not be determined accurately, since the H-1 resonances in the monomer are broadened due to N–H tautomerism. The corresponding dimer resonances are too broad to detect at the maximum obtainable concentration.

DISCUSSION

The changes in the ring current shifts on dimerization are all towards high field, indicating a cofacial orientation of the monomers in the dimers.

The changes in ring current shifts on dimerization are almost identical for the dimers [ZnTPPC-ZnTMPyP] and [ZnTPPC-H_2TMPyP], although the exicted state properties and the redox potentials of the dimers are different. For the investigated dimers the ring current shifts are insensitive to the presence of the metal and the charge of the side groups of the monomeric units of the dimer. Therefore, we used the same values of the equivalent dipole moments for the dimers as for the monomers.

The ring current shifts of the monomers were calculated using the values for the equivalent dipoles previously used by Abraham *et al.*[8] for the ring current shifts of ZnTPP, namely $\mu_H = 17.1$, $\mu_P = 19.3$ and $\mu_A = 27.6$ Å^3. The coordinates of the porphyrins were taken from the x-ray data of H_2TPP.[10] The aryl substituent groups in the monomers were assumed to be perpendicular to the porphyrin plane. The calculated ring current shifts of the monomers were equal to the experimental ring current shifts to within 0.06 ppm. Therefore, we used values of the equivalent dipoles for ZnTPP in the calculation of the conformation of the dimers.

Since the ring current shifts of both monomers in the dimer were found to be nearly equal, a symmetrical orientation of the monomers was assumed. On average, the protons of both monomers sense an identical magnetic field from the ring current of the opposite monomer. Therefore, one can exclude a rotation of one monomer with respect to the other monomer around a common normal to the porphyrin planes in combination with a translation in the plane of the molecules in the average dimer structure. The protons of both monomers in the dimer would exhibit a different ring current shift on dimerization in both a non-parallel or rotated conformation.

For these calculation of both dimer conformations the plane-to-plane distance in the dimer was systematically varied as well as the translation of the monomers in the plane of the molecules with respect to each other. At short intermolecular distances, when an aryl group was very close to the plane of the other porphyrin the rotation angle of the aryl group with respect to the porphyrin plane was varied towards the value of the rotation angle of 63°, as observed in the molecular crystal.[10]

The calculated ring current shifts of H-1, H-2 and H-3 were averaged over all protons of that type on the molecule, as a result of fast exchange. A computer program was used to vary systematically the intermolecular distances, and to calculate the ring current shifts due to the dimerization for each conformation. The distances x and y in the plane of the molecules were varied independently from 0 to 5 Å in 0.1 Å steps and the distance z perpendicular to the porphin plane was varied from 3 to 5 Å in 0.1 Å steps. The calculated dimerization shifts, yielding optimum agreement with experimental shifts, are included in Table 2. The fits for H-3 are not particularly good because in the dimer these protons are

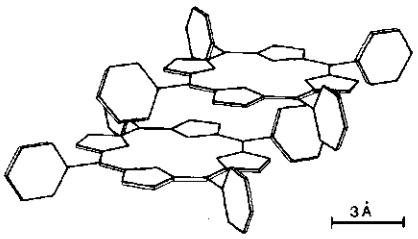

Figure 5. Calculated conformation of the dimers [ZnTPPC–ZnTMPyP] and [ZnTPPC–H_2TMPyP].

fairly near to the edge of the cylinder within which the shifts are described by the approximation formula (2). On the edge of the cylinder the gradient of the chemical shift is not continuous. The same argument explains the discrepancy between the calculated $\Delta\delta = 0.1$ ppm and the experimental dimerization shift $\Delta\delta = -0.21$ ppm for the $N(CH_3)$ protons of ZnTMPyP in [ZnTPPC-ZnTMPyP].

The calculated conformation of the dimers is given in Figs 5 and 6. The plane-to-plane distance is 3.1 Å, whereas the translation amounts to 4.2 Å along the aryl–aryl axis. The calculated shifts are quite sensitive to the shifts in the x and y directions in the plane of the molecule. A 0.5 Å shift in one or both of these directions results in calculated shifts which deviate by 0.1 ppm for H-1 and H-2 from the optimum values quoted in Table 2. The calculated plane-to-plane distance representing the best fit to the NMR data corresponds approximately to the distance of closest approach of the two monomers. It is remarkably short compared with the calculated value of 3.5 to 4.5 Å (Refs. 11–13) in related systems using NMR and EPR. The difference may arise from the electronic interactions in the dimer which are not taken into account in the ring current model, and are expected to decrease the ring current dipole moments of the dimer contituents.

Interestingly, the in-plane translation allows a shorter perpendicular distance, because the steric hindrance of the phenyl groups is decreased. The shift of 4.2 Å is sufficient to decrease the steric hindrance (Fig. 6). At the same time, the increase of the π–π interaction energy more than compensates for the decrease of the coulombic attraction energy between the negatively charged

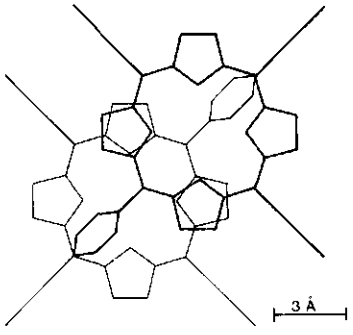

Figure 6. Top view of the calculated conformation of the dimers [ZnTPPC–ZnTMPyP] and [ZnTPPC)H_2TMPyP].

carboxyl group and the positively charged *N*-methylpyridyl group, resulting from the translation.

The precise knowledge of the structure of these dimers has implications for the explanation of the photophysical behaviour of these dimers. Previously, we proposed that electron transfer occurred in the dimer [ZnTPPC-H_2TMPyP].[6] We attributed the difference in photophysical behaviour for the dimer [ZnTMPyP-H_2TPPC], which did not appear to show electron transfer, to the difference between the redox potentials of these dimers. The ^{1}H NMR results show that the structures of these dimers do not depend on the presence of the metal ion in the monomers, therefore excluding the possibility that the difference in photophysical behaviour of these dimers is due to different structures of the dimers.

The calculated plane-to-plane distance in these dimers is short and comparable to the corresponding distance in the bacteriochlorophyll dimer of the bacterial reaction centre.[10] The knowledge of the ground-state conformations of porphyrin dimers and their derivatives is important in order to design model system which efficiently mimic photosynthetic electron transfer.

Acknowledgements

We thank Mr A. van Veldhuizen for running the ^{1}H NMR spectra. This investigation was supported by the Netherlands Foundation for Chemical Research (S.O.N.) with financial aid from the Netherlands Organization for the Advancement of Pure Research (Z.W.O.).

References

1. D. Dolphin, J. Hiom and J. B. Paine, III, *Heterocycles* **66**, 417 (1981).
2. S. G. Boxer, *Biochim. Biophys. Acta* **726**, 265 (1985).
3. G. Bhaskar Maiya and V. Krishnan, *Inorg. Chem.* **24**, 3253 (1985).
4. E. Ojadi, R. Selzer and H. Linschitz, *J. Am. Chem. Soc.* **107**, 7783 (1985).
5. S. Radzki, S. Gaspard and C. Gianotti, *J. Chem. Res. (M)* 3101 (1986).
6. U. Hofstra, R. B. M. Koehorst and T. J. Schaafsma, *Chem. Phys. Lett.* **130**, 555 (1986).
7. R. J. Cave, P. Siders and R. A. Marcus, *J. Phys. Chem.* **90**, 1436 (1986).
8. R. J. Abraham, K. M. Smith, D. A. Goff and Ian-Li Lai, *J. Am. Chem. Soc.* **104**, 4332 (1982).
9. T. Shimidzu and T. Iyoda, *Chem. Lett.* 853 (1981).
10. S. J. Silvers and A. Tulinsky, *J. Am. Chem. Soc.* **89**, 3331 (1967).
11. V. Thanabal and V. Krishnan, *J. Am. Chem. Soc.* **104**, 3643 (1982).
12. R. J. Abraham, K. M. Smith, D. A. Goff and F. W. Bobe, *J. Am. Chem. Soc.* **107**, 1085 (1985).
13. L. Banci, *Inorg. Chem.* **24**, 782 (1984).
14. J. Deisenhofer, O. Epp, K. Miki, R. Huber and H. Michel, *J. Mol. Biol.* **180**, 385 (1984).

CHAPTER 5.3
MAGNETIC RESONANCE IN CHEMISTRY, VOL. 26, 167-172 (1988)

Solution Structure of Porphyrin Aggregates Determined by ^{1}H NMR Ring Current Shifts

II.* Conformations of Dimers and Higher Aggregates of Water-Soluble Porphyrins

R. B. M. Koehorst,† U. Hofstra and T. J. Schaafsma
Department of Molecular Physics, Agricultural University, De Dreijen 11, 6703 BC Wageningen, The Netherlands

The aggregation of the water-soluble porphyrins tetra(4-carboxyphenyl)porphyrin free base (H_2TPPC), tetra(4-*N*-methylpyridyl)porphyrin free base (H_2TMPyP) and their zinc derivatives (ZnTPPC and ZnTMPyP) was studied by ^{1}H NMR and optical absorption spectroscopy. In the solvent H_2O–CH_3OH (4:1), mixing of the anionic H_2TPPC or ZnTPPC with the cationic H_2TMPyP or ZnTMPyP yields various types of 'hetero' aggregates. Only H_2TPPC forms 'homo' aggregates in this solvent. Addition of 1 M KCl results in an increase in the aggregation of H_2TPPC and also enhances the aggregation of ZnTPPC. The structures of the 'hetero' aggregates are stacks of the oppositely charged porphyrins in an alternating order. However, when one of the constituents is H_2TPPC, aggregates having structures of the 'homo' type are also formed. The ^{1}H NMR ring current shifts are accounted for by identical conformations of dimers, and dimer structures in trimers and higher aggregates of the 'hetero' type.

KEY WORDS Ring current shifts Aggregates of oppositely charged porphyrins Solution structure ^{1}H NMR

INTRODUCTION

Porphyrin dimers have been extensively studied to mimick the light-induced electron transfer in photosynthesis, using covalently linked dimers[1,2] and concentration dimers.[3,4] The spectroscopy of concentration dimers of the hetero type, containing two different monomers, is complicated by the presence of homo dimers in the solution. This problem can be avoided by using a mixture of anionic and cationic porphyrins in aqueous solutions.

In Part I,[5] it was demonstrated that tetra(4-carboxyphenyl)porphyrins (TPPC) and tetra(4-*N*-methylpyridyl)porphyrins (TMPyP) (Fig. 1) exclusively form hetero dimers. Light-induced intramolecular electron transfer takes place in some of these dimers.[6] Because the distances and relative orientations of the constituents of a dimer are important parameters in photochemical electron transfer,[7] we have studied the solution conformation of these dimers by ^{1}H NMR. This may provide an answer to the question of whether the difference in photochemical behaviour between the dimers ZnTPPC–H_2TMPyP and ZnTMPyP–H_2TPPC[6] is due to the redox properties of the dimer constituents or to their conformations.

In Part I[5] we reported that the structures of the ZnTPPC–ZnTMPyP and ZnTPPC–H_2TMPyP dimers are the same, although ZnTPPC has different partners in the dimer. This paper reports the ground-state conformations and equilibria of mixed oligomers of anionic and cationic porphyrins and of homo aggregates of H_2TPPC and of ZnTPPC, obtained from ^{1}H ring current shifts and optical spectroscopy.

The negatively charged tetra(4-carboxyphenyl)-porphyrins will be abbreviated to H_2P^{4-} and ZnP^{4-} and the positively charged tetra(4-*N*-methylpyridyl)-porphyrins to H_2P^{4+} and ZnP^{4+}.

EXPERIMENTAL

The preparation of the porphyrins has been described previously.[6] For the NMR experiments we used a 4:1 mixture of D_2O and CD_3OD as a solvent, containing 30 mM of non-deuteriated tris(hydroxymethyl)-aminomethane (Tris) to ionize the carboxyl groups of TPPC ($pK \approx 5$). Non-deuteriated solvents were used for the optical experiments. The ^{1}H NMR spectra were obtained at 300 MHz on a Bruker CXP-300 spectrometer at 295 K. The chemical shifts are quoted relative to TMS. A Kontron Uvikon 810 spectrometer was used for measuring the optical absorption spectra.

To study dimers of the homo type, KCl was added to aqueous solutions of H_2P^{4-} and of ZnP^{4-}, as it is known that anionic porphyrins aggregate at high ionic strength.[8,9]

The following mixtures were studied by ^{1}H NMR: ZnP^{4-}–ZnP^{4+} in the molar ratios 1:1, 2:1 and 1:2 and H_2P^{4-}–ZnP^{4+} in the molar ratios 1:1, 2:1 and 1:2. For the optical absorption measurements 1:1 mixtures of ZnP^{4-}–ZnP^{4+}, ZnP^{4-}–H_2P^{4+}, H_2P^{4-}–ZnP^{4+} and H_2P^{4-}–H_2P^{4+} were used. Optical absorption differences between monomer solutions and 1:1 mixtures

* For Part I, see Ref. 5.
† Author to whom correspondence should be addressed.

0749–1581/88/020167–06$05.00

Received 10 August 1987
Accepted (revised) 21 October 1987

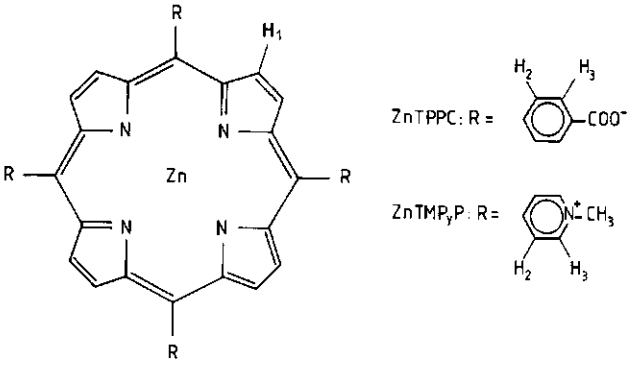

Figure 1. Molecular structure of ZnTPPC and ZnTMPyP. H_2TPPC and H_2TMPyP have two protons in the centre of the porphyrin ring.

of the porphyrins were measured in a double-compartment cuvette as the absorption difference before and after mixing of the two monomer solutions in the cuvette. The optical path length of the cell was 8.8 mm. At high concentrations ($>10^{-4}$ M), where the double-compartment cuvette could not be used owing to the very high absorbance, the monomer absorption data were calculated from the absorption spectra at 5×10^{-5} M.

RESULTS

Optical data

Homo aggregates. The optical absorption spectra of H_2P^{4-} and ZnP^{4-} in 1 M KCl solutions were measured at concentrations ranging from 5×10^{-7} to 1×10^{-3} M. In the absence of KCl, Lambert–Beer's law is valid for ZnP^{4-} over the whole concentration range. The difference between the absorbance at 560 nm with and without KCl, ΔA, was taken to be the absorption difference due to dimerization for ZnP^{4-}. The data were fitted with the equation

$$\Delta A = \Delta\varepsilon([P]/2 + (1 - \sqrt{(1 + 8[P]K_D)})/8K_D) \quad (1)$$

where [P] is the porphyrin concentration, K_D is the dimerization constant and $\Delta\varepsilon = \varepsilon_D - 2\varepsilon_M$, where ε_D and ε_M are the molar absorptivities of the dimer and monomer, respectively. The best fit is shown in Fig. 2. K_D was determined to be 610 ± 30 l mol^{-1}.

For H_2P^{4-} the absorbance at 650 nm in the absence of KCl deviates from Lambert–Beer's law at concentrations higher than 1×10^{-4} M. The absorbances of the H_2P^{4-} monomers at higher concentrations were extrapolated from the values at low concentrations. At porphyrin concentrations from 5×10^{-7} to 1×10^{-4} M the difference between the absorbance at 520 nm with and without 1 M KCl, ΔA, was used to calculate the dimerization constant for H_2P^{4-}, by fitting ΔA to Eqn (1). At higher concentrations the aggregation is not limited to dimerization. As was found for tetra(4-sulphonatophenyl)porphyrin,[8] the data could be fitted with a combination of a dimerization and a tetramerization equilibrium. The difference between the absorbances of H_2P^{4-} at 2.5×10^{-4} and 5×10^{-4} M at 650 nm and the absorbance of dimeric H_2P^{4-}, as extrapolated from the data at low concentrations, was used to calculate the tetramerization constant, K_T, with the equation

$$\Delta A = \Delta\varepsilon'([P]/4 + (1 - \sqrt{(1 + 4[P]K_T)})/8K_T) \quad (2)$$

where $\Delta\varepsilon' = \varepsilon_T - 2\varepsilon_D$ and K_T is the tetramerization constant. K_T was determined to be 500 l mol^{-1}. The calculated and experimental absorption data are shown in Fig. 2.

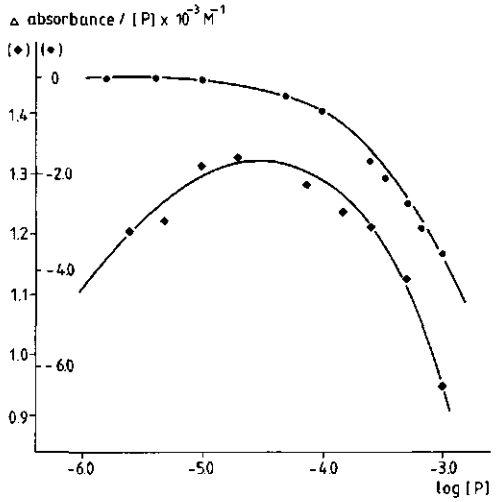

Figure 2. Absorption difference at 560 nm between solutions of ZnP^{4-} in H_2O–CH_3OH (4:1)–30 mM Tris—1 M KCl and the corresponding solutions without KCl (●), and the absorption difference at 650 nm between solutions of H_2P^{4-} in the same solvent and the corresponding solutions without KCl (◆). For H_2P^{4-} the reference absorption of the monomers for concentrations larger than 1×10^{-4} M is calculated from the data at lower concentrations. The lines represent the best fit to the data with a single dimerization constant for ZnP^{4-}, $K_D = 610 \pm 30$ l mol^{-1} (top curve) or with a dimerization constant $K_D = 9.0 \pm 1.0 \times 10^6$ l mol^{-1} and a tetramerization constant $K_T = 500 \pm 200$ l mol^{-1} for H_2P^{4-} (bottom curve).

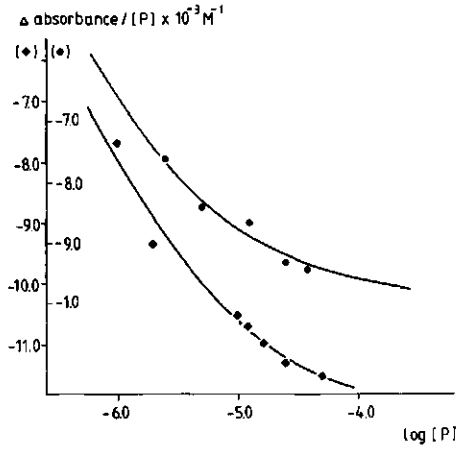

Figure 3. Absorption difference at 520 nm between a 1:1 mixture of H_2P^{4-}–ZnP^{4+} and the corresponding monomer solutions (●) and between a 1:1 mixture of H_2P^{4-}–H_2P^{4+} and the corresponding monomer solutions (◆) in H_2O–CH_3OH (4:1)–30 mM Tris. The lines represent the best fit to the data with a single dimerization constant. Top curve, H_2P^{4-}–ZnP^{4+}, $K_D = 5.7 \pm 2.0 \times 10^6$ l mol^{-1}; bottom curve, H_2P^{4-}–H_2P^{4+}, $K_D = 2.4 \pm 0.2 \times 10^6$ l mol^{-1}.

Hetero aggregates. The absorption differences between 1:1 mixtures of ZnP^{4-}–ZnP^{4+} (at $\lambda = 560$ nm), ZnP^{4-}–H_2P^{4+} (at $\lambda = 560$ nm), H_2P^{4-}–ZnP^{4+} (at $\lambda = 520$ nm) and H_2P^{4-}–H_2P^{4+} (at $\lambda = 520$ nm) and their monomer solutions in the concentration range 5×10^{-7} to 1×10^{-5} M were used to calculate the dimerization constant by fitting the data to the equation

$$\Delta A = \Delta\varepsilon([P] + (1 - \sqrt{(1 + 4[P]K_D)})/2K_D) \quad (3)$$

where [P] is the concentration of each porphyrin constituent and $\Delta\varepsilon = \varepsilon_D - \varepsilon_M$. The fits to the experimental data are shown in Fig. 3.

At higher concentrations we need to invoke larger aggregates for H_2P^{4-}–ZnP^{4+} (1:1) and for H_2P^{4-}–H_2P^{4+} (1:1). The tetramerization constant for H_2P^{4-}–H_2P^{4+} was calculated in an analogous manner to the calculation for H_2P^{4-} in 1 M KCl, from the absorbance at 650 nm, where at concentrations higher than 1×10^{-4} M the molar absorptivity decreases again after an increase on dimerization at concentrations $< 10^{-4}$ M.

Dimerization constants are given in Table 1.

^{1}H NMR data

Homo aggregates. The chemical shifts of the pyrrole protons and the *ortho*- and *meta*-aryl protons of the porphyrin monomers (labelled H-1, H-2 and H-3, respectively, in Fig. 1) are presented in Table 2. The CD_2HOD signal was taken as a reference at 3.39 ppm.

We measured the change in chemical shifts on homo aggregation of H_2P^{4-} and ZnP^{4-} at 1×10^{-3} M porphyrin concentration, with and without 1 M KCl added to the solutions. These results are summarized in Table 3.

Table 1. Hetero dimerization constants (l mol^{-1}) for the 1:1 mixtures of ZnP^{4-}, ZnP^{4+}, H_2P^{4-} and H_2P^{4+}, in H_2O–CH_3OH (4:1)–30 mM Tris and homo dimerization constants of H_2P^{4-} and ZnP^{4-} in H_2O–CH_3OH (4:1)–30 mM Tris–1 M KCl

	ZnP^{4-}	H_2P^{4-}
ZnP^{4+}	$6.2 (\pm 0.4) \times 10^{+6}$	$5.7 (\pm 2.0) \times 10^{+6}$
H_2P^{4+}	$7.0 (\pm 1.0) \times 10^{+6}$	$2.4 (\pm 0.2) \times 10^{+6}$
		30 (±20)[a]
ZnP^{4-}	610 (±30)	
H_2P^{4-}		$9.0 (\pm 1.0) \times 10^{+6}$
		500 (±200)[b]

[a] Tetramerization constant determined for the concentration range 2×10^{-5}–5×10^{-5} M.
[b] Tetramerization constant of H_2TPPC–1 M KCl determined from the optical absorption data at the concentration range from 5×10^{-5} to 1×10^{-3} M.

Table 2. Experimental proton chemical shifts (δ) of 1×10^{-3} M solutions of ZnP^{4-} and ZnP^{4+} and of 1×10^{-4} M of H_2P^{4-} and H_2P^{4+} in D_2O–CD_3OD (4:1)–30 mM Tris

Compound	Proton[a]	δ(ppm)
ZnP^{4-}	H-1	9.08
	H-2	8.39
	H-3	8.39
ZnP^{4+}	H-1	9.18
	H-2	9.01
	H-3	9.35
H_2P^{4-}	H-1	9.11
	H-2	8.41
	H-3	8.41
H_2P^{4+}	H-1	9.25
	H-2	9.05
	H-3	9.41

[a] H-1, H-2 and H-3 are the pyrrole and aryl protons as labelled in Fig. 1.

Table 3. Differences between the chemical shifts of H_2P^{4-} and of ZnP^{4-} at 1×10^{-3} M porphyrin concentration (with and without 1 M KCl added) and the chemical shifts of the monomeric solutions at 1×10^{-4} M ($\Delta\delta$)

Sample	Proton	Δδ(ppm)
H_2P^{4-}	H-1	−0.0; −1.0
	H-2	−0.27
	H-3	−0.01
H_2P^{4-}–1 M KCl	H-1	−1.1; −2.7
	H-2	−1.21
	H-3	−0.20
ZnP^{4-}	H-1	0.0
	H-2	0.0
	H-3	0.0
ZnP^{4-}–1 M KCl	H-1	−1.05
	H-2	−0.73
	H-3	−0.20

The chemical shifts of the solutions at 1×10^{-4} M without KCl were taken to be the chemical shifts of the monomers in the calculation of the chemical shift differences in Table 3, because the absorbances of these solutions follow Lambert–Beer's law up to this concentration. The NMR spectra of ZnP^{4-} in 1 M KCl were taken at concentrations ranging from 2×10^{-4} to 1×10^{-3} M. The differences between the chemical shifts of the pyrrole protons in these solutions and the chemical shifts of the monomer ZnP^{4-} in 1×10^{-4} M solution in the absence of KCl were fitted with an equation similar to Eqn (1). The dimerization constant was calculated to be 590 ± 50 l mol^{-1}. The chemical shifts of ZnP^{4-} in 1 M KCl extrapolated to low porphyrin concentrations are identical with those in the absence of KCl.

Hetero aggregates. Table 4 contains the change in chemical shifts on aggregation, $\Delta\delta$, as obtained from the difference between the chemical shift of the hetero aggregates and the constituent monomers. The resonances in the NMR spectra could be identified using titrations, varying the concentration ratios.

Table 4. Differences between the chemical shifts of porphyrin mixtures and the chemical shifts of the corresponding monomers ($\Delta\delta$) at a total porphyrin concentration of 1×10^{-3} M in D_2O–CD_3OD (4:1)–30 mM Tris, unless stated otherwise

Sample	Proton ZnP^{4-}	Proton ZnP^{4+}	Proton H_2P^{4-}	$\Delta\delta$(ppm)
ZnP^{4-}–ZnP^{4+}	H-1			−1.03
(1:1)		H-1		−0.99
	H-2			−1.02
		H-2		−1.15
	H-3			−0.52
		H-3		−0.59
ZnP^{4-}–ZnP^{4+}	H-1			−0.62
(2:1)		H-1		−1.23
	H-2			−0.59
		H-2		−1.47
	H-3			−0.31
		H-3		−0.85
ZnP^{4-}–ZnP^{4+}	H-1			−1.20
(1:2)		H-1		−0.63
	H-2			−1.15
		H-2		−0.72
	H-3			−0.46
		H-3		−0.34
ZnP^{4+}–H_2P^{4-}		H-1		−1.23
(1:1)			H-1	[b]
		H-2		−1.51
			H-2	−1.77
		H-3		−0.82
			H-3	−0.59
ZnP^{4+}–H_2P^{4-}		H-1		−0.93
(2:1)			H-1	~ −2 (broad)
		H-2		−1.14
			H-2	−1.70
		H-3		−0.58
			H-3	−0.50
ZnP^{4+}–H_2P^{4-}		H-1		−1.18
(1:2)			H-1	[b]
		H-2		−1.48
			H-2	−1.03
		H-3		−0.75
			H-3	−0.30

[a] Total porphyrin concentration 3×10^{-4} M.
[b] In the monomer spectrum the H-1 resonance is already broadened. Aggregation results in further broadening beyond detection.

DISCUSSION

Homo aggregates

As high-field shifts for protons H-1 through H-3 are observed in the ^{1}H NMR spectrum of the porphyrin H_2P^{4-} at 1×10^{-3} M with respect to those at 1×10^{-4} M it is concluded that at 1×10^{-3} M H_2P^{4-} is partly aggregated. This is confirmed by the optical absorption spectra at these concentrations. The optical absorption spectrum of ZnP^{4-} does not change on increasing the concentration from 5×10^{-7} to 1×10^{-3} M. In addition, the NMR spectrum of ZnP^{4-} does not change from 1×10^{-4} to 1×10^{-3} M, and it is therefore concluded that at this concentration no aggregates of ZnP^{4-} are formed. Because only upfield shifts are observed in the NMR spectra of aggregated solutions with respect to the spectra of monomeric solutions, the porphyrin units in the aggregates must have a parallel orientation to each other.

The addition of 1 M KCl to a 1×10^{-3} M solution of H_2P^{4-} results in an increase of the high-field shifts of the H_2P^{4-} protons. The addition of 1 M KCl to a 1×10^{-3} M solution of ZnP^{4-} also results in high-field shifts of the ZnP^{4-} protons. From the data in Table 1 it can be seen that in a 1 M KCl solution ZnP^{4-} has not completely dimerized, whereas in the same solvent aggregates larger than dimers must be formed for H_2P^{4-}.

Corsini and Herrmann[8] published NMR spectra of the anionic tetra(4-sulphonatophenyl)porphyrin free base (H_2TPPS) at concentrations (0.014–0.102 M) much higher than ours. On lowering the temperature of a concentrated sample they observed a splitting of the β-pyrrole proton resonance and ascribed this to N–H tautomerism in the aggregate. We observed a similar splitting of the β-pyrrole resonance of H_2P^{4-} in solutions containing H_2P^{4-} in aggregated form (Table 3). The tautomers in a monomeric solution of H_2P^{4-} exhibit a splitting of only 0.3 ppm. Therefore, we believe that the large splitting observed in the aggregates results from differences in the conformation of the tautomers. The signals do not average at 295 K since the exchange between the species is too slow. No splitting of the phenyl resonances is observed, probably because the difference in dimerization shifts for the phenyl resonances of both types of dimers are smaller than those for the pyrrole protons, and the interconversion is assumed to be fast enough to average out the splitting between the phenyl proton resonances.

Because of the observed splitting of the β-pyrrole resonances we conclude that the N–N axes of the H_2P^{4-} units in the dimer and the oligomer must be parallel to each other. A rotation by 45° of one porphyrin with respect to the other (the phenyl rings oriented such that the molecules fit to each other like a pair of toothed wheels) yields identical aggregated structures in the tautomers, and thus can be excluded. It should be noted that for the hetero dimers [ZnP^{4-}–ZnP^{4+}] and [ZnP^{4-}–H_2P^{4+}] we calculated a conformation in which the N–N axes are also parallel to each other.[5]

Hetero aggregates

From titration experiments we conclude that the observed NMR spectra result from averaging of the resonances of chemically equivalent protons of monomeric and aggregated porphyrin species, owing to exchange of monomers between the different species in solution on a time scale which is fast compared with the chemical shift differences at 300 MHz. As already stated in Part I,[5] the monomeric ring current shifts for the protons H-1 to H-3 are almost identical for the various investigated porphyrins. Further, from the optical absorption data for the 1:1 mixtures of ZnP^{4-} with ZnP^{4+} (see Table 1) it is concluded that ZnP^{4-}–ZnP^{4+} (1:1) contains 98% hetero dimer at 1×10^{-3} M. Therefore, the chemical shifts in the NMR spectra of this mixture are considered to be essentially pure hetero dimer shifts, from which the change in ring current shifts due to dimer formation were calculated.

From the data presented in Table 4 it can be seen that when one equivalent of ZnP^{4-} is added to the mixture ZnP^{4-}–ZnP^{4+} (1:1) the Δδ values of the ZnP^{4-} protons decrease, whereas those of the ZnP^{4+} protons increase; addition of one equivalent of ZnP^{4+} to the same 1:1 mixture yields similar changes in the ring current shifts, i.e. a decrease in Δδ for the ZnP^{4+} protons and an increase in Δδ for the ZnP^{4-} protons. A decrease in Δδ of the protons of the added porphyrin would be predicted when the added porphyrin exchanges on a fast time scale with its corresponding constituent in a [ZnP^{4-}–ZnP^{4+}] dimer. Since the 1:1 solution consists almost completely of dimers, the observed increase in the Δδ values of the minority porphyrin cannot be explained by a shift of the monomer–dimer equilibrium. The most plausible explanation is the formation of trimers with ZnP^{4-} and ZnP^{4+} in an alternating order as the next higher aggregate. Other trimers and also tetramers are excluded based on the following arguments:

i. Addition of an additional equivalent of one porphyrin to the dimer solution does not enhance the formation of the tetramer [ZnP^{4-}–ZnP^{4+}–ZnP^{4-}–ZnP^{4+}].
ii. Trimers and tetramers having an asymmetric composition would imply homo interactions between ZnP^{4-} or ZnP^{4+} monomers. These are energetically unfavourable, as confirmed by the absence of homo dimerization for these zinc porphyrins up to the highest obtainable concentration.

The Δδ values of H_2P^{4-} and ZnP^{4+} in the mixture H_2P^{4-}–ZnP^{4+} (1:1) are larger than expected for a dimer with a conformation close to that of [ZnP^{4-}–ZnP^{4+}].[5] Further, we note that at 1×10^{-3} M the optical absorption differences between H_2P^{4-}–ZnP^{4+} (1:1) and the monomer solutions do not fit a dimerization equilibrium, so that aggregates larger than dimers must be present in solution. Because the factors by which the Δδ values of H_2P^{4-} and ZnP^{4+} in the aggregate have increased with respect to the expected dimer shifts [as determined for the dimers (ZnP^{4-}–ZnP^{4+}) and (ZnP^{4-}–H_2P^{4+})[5]] are not the same, the environment of each porphyrin in the aggregate must be different. In a trimer or tetramer a porphyrin monomer can occupy an 'inner' or an 'outer' position, if we assume a parallel stacking of the monomer units in the trimer or tetramer.

Since we observed homo aggregation of H_2P^{4-} at 1×10^{-3} M even without KCl being added, H_2P^{4-}–ZnP^{4+} (1:1) at high concentrations ($> 1 \times 10^{-4}$ M) might contain aggregates with a 'homo dimer-like' structure of H_2P^{4-} within the aggregate. Because the trimer [ZnP^{4+}–H_2P^{4-}–H_2P^{4-}] and the tetramer [ZnP^{4+}–H_2P^{4-}–H_2P^{4-}–ZnP^{4+}] cannot explain the observed Δδ values of ZnP^{4+} in H_2P^{4-}–ZnP^{4+} (1:1), which are larger than the expected dimer shifts, even higher aggregates must be present.

To prevent homo dimerization of H_2P^{4-}, one equivalent of ZnP^{4+} was added to the mixture H_2P^{4-}–ZnP^{4+} (1:1). As mentioned above, ZnP^{4+} itself does not show homo dimerization. The Δδ values of the added component ZnP^{4+} decreased, but the Δδ values of the H_2P^{4-} protons remained almost the same and were much larger than the expected dimer Δδ value (see Table 4). Therefore the formation of aggregates such as the trimer [ZnP^{4+}–H_2P^{4-}–ZnP^{4+}] and the pentamer [ZnP^{4+}–H_2P^{4-}–ZnP^{4+}–H_2P^{4-}–ZnP^{4+}] might occur in the solution. However, since the decreased shifts of the ZnP^{4+} protons in the 1:2 mixture of H_2P^{4-}–ZnP^{4+} with respect to those in the 1:1 mixture fit perfectly the dimer shifts (as expected for the dimer [H_2P^{4-}–ZnP^{4+}]), aggregates other than the trimer can be excluded. The aggregation shifts of H_2P^{4-} in the 1:1 and the 1:2 mixtures of H_2P^{4-}–ZnP^{4+} are very similar, because in the [ZnP^{4+}–H_2P^{4-}–ZnP^{4+}] trimer in the 1:2 mixture H_2P^{4-} is at the 'inner' position, and in the 1:1 mixture aggregates are present, with homo dimer-like structures of H_2P^{4-}, having ZnP^{4+} at the 'outer' positions and H_2P^{4-} solely at the 'inner' positions. Examples of such aggregates are [ZnP^{4+}–H_2P^{4-}–H_2P^{4-}–ZnP^{4+}], [ZnP^{4+}–H_2P^{4-}–ZnP^{4+}–H_2P^{4-}–H_2P^{4-}–ZnP^{4+}] and [ZnP^{4+}–H_2P^{4-}–ZnP^{4+}–H_2P^{4-}–H_2P^{4-}–ZnP^{4+}–H_2P^{4-}–ZnP^{4+}]. The presence of the above-mentioned large aggregates can very well account for the observed light scattering of H_2P^{4-}–ZnP^{4+} (1:1) at a 1×10^{-3} M porphyrin concentration.

By comparing the aggregation shifts with those for [ZnP^{4-}–ZnP^{4+}],[5] we conclude that the relative orientations and distances of the porphyrins within the trimer [ZnP^{4+}–H_2P^{4-}–ZnP^{4+}] are very similar to those in the dimer [ZnP^{4-}–ZnP^{4+}]. The accuracy of the experimental and calculated data does not allow us, however, to distinguish between a 'zig-zag' stack and a 'skew' stacking. The two 'outer' ZnP^{4+} porphyrins in

the trimer [ZnP^{4+}–H_2P^{4-}–ZnP^{4+}] do not contribute to each other's $\Delta\delta$ values but, as can be seen from the data for the trimer solution (Table 4), they almost double the $\Delta\delta$ values of H_2P^{4-} with respect to the expected dimer shift.

We also attempted to prepare trimers having an 'inner' ZnP^{4+} flanked by two 'outer' H_2P^{4-} units (i.e. [H_2P^{4-}–ZnP^{4+}–H_2P^{4-}]). For this purpose a 2:1 mixture of H_2P^{4-}–ZnP^{4+} was taken with the lowest total porphyrin concentration (3×10^{-4} M) at which the NMR resonances are still detectable. The low concentration was used to prevent the formation of higher aggregates. The increase in the $\Delta\delta$ values of ZnP^{4+} in the mixture H_2P^{4-}–ZnP^{4+} (2:1) with respect to the dimerization shift (as expected for the dimer [H_2P^{4-}–ZnP^{4+}]) can be explained by the formation of the trimer [H_2P^{4-}–ZnP^{4+}–H_2P^{4-}]. However, as the $\Delta\delta$ values of H_2P^{4-} do not decrease with respect to the dimerization shift, as is expected when an equilibrium between monomers, dimers and trimers is assumed, we need to invoke the trimer [H_2P^{4-}–H_2P^{4-}–ZnP^{4+}]. Hence the 2:1 mixture H_2P^{4-}–ZnP^{4+} can be described by the equilibrium

$$[H_2P^{4-}] + [H_2P^{4-}\text{–}ZnP^{4+}] \rightleftharpoons [H_2P^{4-}\text{–}H_2P^{4-}\text{–}ZnP^{4+}]$$
$$[H_2P^{4-}\text{–}ZnP^{4+}\text{–}H_2P^{4-}].$$

Obviously, despite the relatively low concentration (3×10^{-4} M), homo dimerization of H_2P^{4-}, which contributes to the observed chemical shifts, cannot be prevented.

CONCLUSIONS

From the observed chemical shifts of aggregates we conclude that the hetero dimers [ZnP^{4-}–ZnP^{4+}], [ZnP^{4-}–H_2P^{4+}] and [H_2P^{4-}–ZnP^{4+}] have the same conformation. Our results for the excited state[6] can now be ascribed to the redox properties of the dimer constituents, because the conformation of the hetero dimer is found to be independent of the presence of a zinc atom in either one or both porphyrins.

Trimers [ZnP^{4+}–H_2P^{4-}–ZnP^{4+}] are produced quantitatively in H_2P^{4-}–ZnP^{4+} (1:2) solutions. In the ZnP^{4-}–ZnP^{4+} (2:1 and 1:2) solutions, monomers and dimers, as well as trimers, are present. The formation of aggregates is probably decreased by the presence of a fifth ligand on the zinc atoms.

Aggregates of which H_2P^{4-} is one of the constituents may contain homo dimer-like structures of H_2P^{4-}, in addition to the alternation of cationic and anionic porphyrins present in aggregates of ZnP^{4-}–ZnP^{4+} and ZnP^{4-}–H_2P^{4+}.

A knowledge of the precise conformation of the dimers is crucial for studies of electron-transfer processes in photosynthetic model systems. These dimers can be covalently linked to electron-donor (D) and -acceptor (A) groups, thus creating [D-P^{4-}–P^{4+}-A] systems which are easily accessible for modification owing to their modular design. Their [P^{4-}–P^{4+}] centre part closely resembles the primary donor of the bacterial reaction centre.[10]

Acknowledgements

We thank Mr A. van Veldhuizen of the Organic Chemistry Department for recording the ^{1}H NMR spectra. This investigation was supported by the Netherlands Foundation for Chemical Research (SON) with financial aid from the Netherlands Organization for the Advancement of Pure Research (ZWO).

REFERENCES

1. D. Dolphin, J. Hiom and J. B. Paine, III, *Heterocycles* **66**, 417 (1981).
2. S. G. Boxer, *Biochim. Biophys. Acta* **726**, 265 (1985).
3. G. Bhaskar Maiya and V. Krishnan, *Inorg. Chem.* **24**, 3253 (1985).
4. E. Ojadi, R. Selzer and H. Linschitz, *J. Am. Chem. Soc.* **107**, 7783 (1985).
5. U. Hofstra, R. B. M. Koehorst and T. J. Schaafsma, *Magn. Reson. Chem.* in press.
6. U. Hofstra, R. B. M. Koehorst and T. J. Schaafsma, *Chem. Phys. Lett.* **130**, 555 (1986).
7. R. J. Cave, P. Siders and R. A. Marcus, *J. Phys. Chem.* **90**, 1436 (1986).
8. A. Corsini and O. Herrmann, *Talanta* **33**, 335 (1986).
9. R. F. Pasternack, *Ann. N.Y. Acad. Sci.* **206**, 614 (1973).
10. J. Deisenhofer, O. Epp, K. Miki, R. Huber and H. Michel, *J. Mol. Biol.* **180**, 385 (1984).

CHAPTER 5.4

Extension of watersoluble porphyrin dimers towards modular model systems for photoinduced electron transfer.

5.4.1 Introduction

A new four component modelsystem for photoinduced electron transfer (ET) was designed, consisting of an electrostatically bonded porphyrin dimer (P_1-P_2), as described in §§ 5.1-5.3 with an electron donor molecule (D) covalently attached to P_1 and an electron acceptor molecule (A) similarly attached to P_2. The resulting D-P_1-P_2-A system allows multi-step ET: ET within the dimer from P_1 to P_2 is followed by ET from D to P_1 and from P_2 to A. The model system resembles the photosynthetic reaction centre, containing a bacteriochlorophyll dimer as the primary donor, an electron acceptor pheophytin and an electron donor cytochrome c [1]. Experiments on an ultrafast timescale suggest, that the primary step in the photosynthetic reaction centre is charge separation within the primary donor, followed by ET to pheophytin and subsequently to a quinone and ET from cytochrome c to the primary donor [2,3].

The porphyrin dimer in the model system consists of oppositely charged watersoluble porphyrins. One porphyrin constituent is a derivative of a tetrafold negatively charged porphyrin, tetracarboxyphenylporphyrin (TPPC), the other porphyrin is a derivative of a tetrafold positively charged porphyrin, tetramethylpyridiniumporphyrin (TMPyP). TPPC and TMPyP form heterodimers in aqueous solution [4-6]. Dimers with different central atoms in the porphyrin ring, Zn or H_2, can be created by combining differently substituted porphyrins: ZnTPPC-ZnTMPyP, H_2TPPC-H_2TMPyP, ZnTPPC-H_2TMPyP and H_2TPPC-ZnTMPyP [4-6].

It was the purpose of this investigation to extend the Zn- and H_2-porphyrins with extra donor and acceptor groups to allow for multi-step electron transfer in the dimers. As secondary donor N,N-dimethylaniline (DMA) was attached to H_2TPPC and to ZnTPPC via a diether

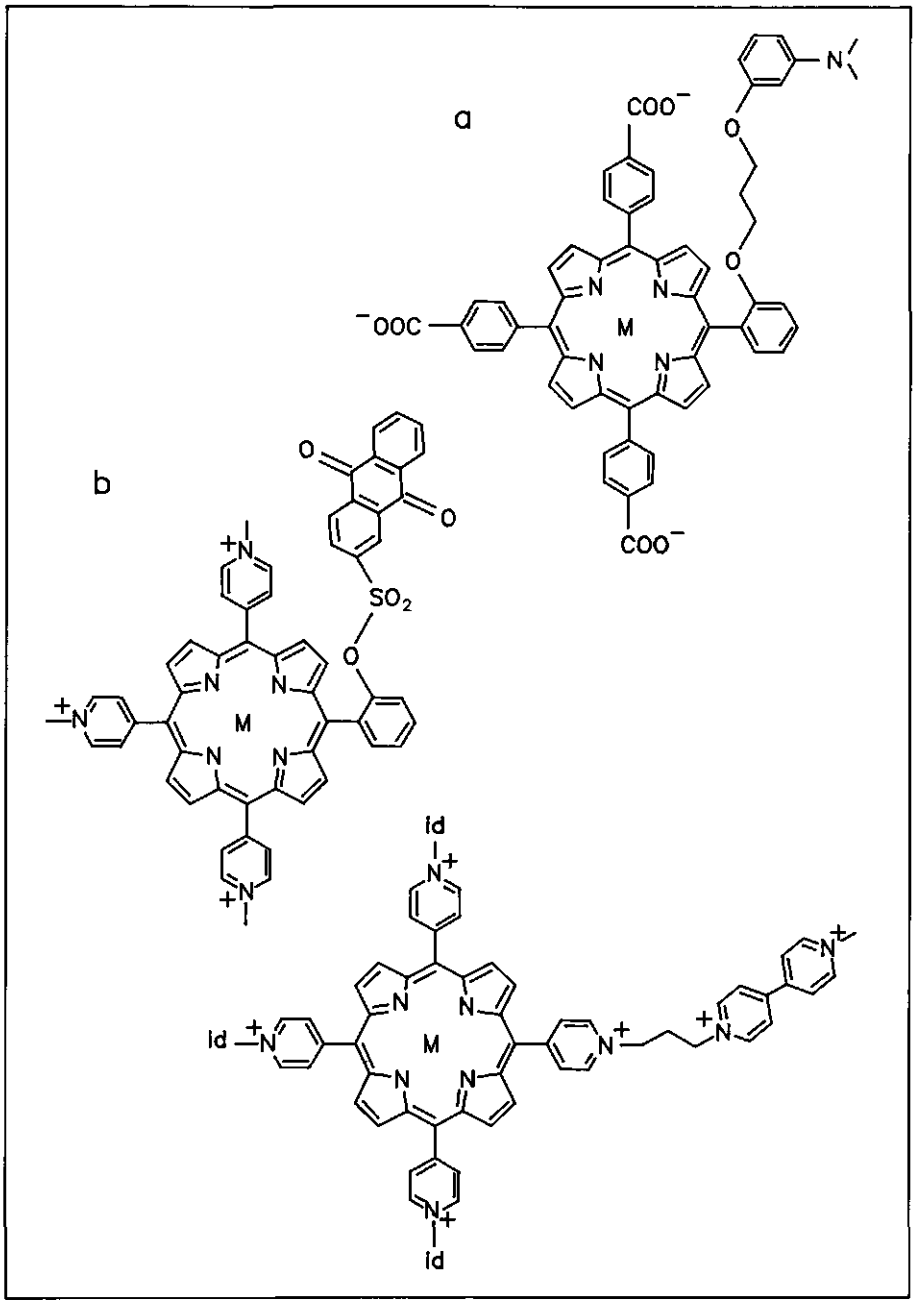

Figure 1: Molecular structure of substituted watersoluble porphyrins. (a) DMA-ZnTPPC (M = Zn) and DMA-H_2TPPC (M = H_2); (b) ZnTMPyP-AQ (M = Zn) and H_2TMPyP-AQ (M = H_2); (c) ZnTMPyP-$(MV)_4$ (M = Zn).

bridge, $-O-(CH_2)_3-O-$, at the ortho position of the phenyl group. Anthraquinone (AQ) was attached to H_2TMPyP and ZnTMPyP as secondary acceptor via a sulfonyloxy bridge, $-O-SO_2-$ at the meta position of the pyridinium group w.r.t. the position of attachment of the latter group to the porphyrin. Four methylviologen (MV) groups were linked to ZnTMPyP at the N-atom of each pyridinium group via a propyl chain $-(CH_2)-(CH_2)-(CH_2)-$ as secondary acceptors. The substituted porphyrins are presented in figure 1.

5.4.2 Experimental

The symmetrical tetra-(4-carboxyphenyl)porphyrins and tetra-4-N-methylpyridyl)porphyrins were prepared as described in ref.4.

DMA-H_2TPPC was prepared from a bifunctional tetra-arylporphyrin, containing one ortho-hydroxyphenyl group and three para-carbomethoxy phenylgroups. This asymmetrical porphyrin was synthesized, using the mixed aldehyde condensation [7,8]. Three equivalents of para-carbomethoxybenzaldehyde and one equivalent of ortho-hydroxybenzaldehyde were reacted with four equivalents of pyrrole. The desired porphyrin was purified by column chromatography on silica, using $CHCl_3$ as eluent. The substitution of the aliphatic chain was performed with 1,3-dibromopropane [9], resulting in 5-(3-bromopropyloxy-phenyl)-10,15,20-tri(para-carbomethoxyphenyl)-porphyrin. The substitution of DMA and the saponification of the carbomethoxyester groups were achieved in one step by adding the porphyrin to a 1 M solution of potassium 3-(N,N-dimethylamino)phenolate in DMSO and stirring the solution overnight. The reaction mixture was diluted with water and neutralized with acetic acid. The crystallized porphyrin was dissolved in aqueous 1 M NaOH and neutralized with acetic acid. The material obtained in this manner is pure DMA-H_2TPPC, as confirmed by ^{1}H NMR and optical absorption spectra.

H_2TMPyP-AQ was obtained from its pyridyl analog by methylation with

methyliodide in DMF [10]. The pyridyl porphyrin was synthesized in a one step mixed aldehyde condensation, using 4-pyridincarbaldehyde, pyrrole and 2-(2'-anthraquinonesulfonyloxy)benzaldehyde (a kind gift of dr.G.M.Sanders and Mr.M.van Dijk of the Organic Chemistry Department). The crude products were repeatedly chromatographed on silica, using as eluent $CHCl_3$ with increasing amounts of pyridine up to 10 %. The second porphyrin fraction contains the desired mono-anthraquinone substituted pyridylporphyrin. The purity of this compound was checked by ^1H NMR and optical absorption spectra. The solubility of the final product after methylation, H_2TMPyP-AQ, is too low to measure its ^1H NMR spectrum. The ability of H_2TMPyP-AQ to form heterodimers with anionic TPPC's was verified by optical absorption spectroscopy.

The metallated derivatives, DMA-ZnTPPC and ZnTMPyP-AQ, were prepared, using an aqueous $ZnCl_2$ solution [4].

To synthesize ZnTMPyP-$(MV)_4$ a mixture of free base tetra(4-pyridyl)porphyrin and 50 fold excess 1,3-dibromopropane in DMF was stirred for 36 hrs at 80 °C, resulting in the fourfold quaternized porphyrin, which was filtered and washed with acetone. A mixture of this porphyrin and 1-methyl-4-(4'-pyridyl)pyridinium (synthesized according to ref.11) was stirred for 60 hrs at 80 °C. The solution was subsequently treated with $ZnCl_2$ to produce the zinc porphyrin. The solvent was distilled off and the product was dissolved in a 9:1 ethanol/water mixture and purified by repeated gel filtration on Sephadex LH-20.

Instrumentation for the fluorescence decay measurements and for the transient absorption measurements is described in chapter 3.

5.4.3 Unsubstituted dimers

Photoinduced electron transfer may occur in the dimers from TPPC to TMPyP due to the favourable oxidation and reduction potentials of the porphyrin constituents. The four negative charges on the TPPC

sidegroups decrease the oxidation potentials and the positive charges on the TMPyP's facilitate their reduction (Table I).

ET has been investigated by fluorescence quenching experiments for several porphyrin dimers. The results are summarized in Table I, also containing the free energy for the ET processes:

$\Delta G = E_{ox}(D) - E_{red}(A) - E_{S_1} + \Delta G(\epsilon)$, where E_{S_1} is the energy of the lowest excited singlet state of the dimer, calculated from the absorption spectrum of the dimer. $\Delta G(\epsilon)$ is the electrostatic contribution to ΔG. For the H_2O/CH_3OH solvent mixture at room temperature, which has a high dielectric constant ($\epsilon \simeq 70$), $\Delta G(\epsilon)$ is small (Chapter 2, eqs.7,9) and has been neglected.

Table I: Redoxpotentials[a] and fluorescence quenching[b] for the dimers at 300 K and at 80 K.

compound	E_{ox} (V)	E_{red} (V)	E_{S_1} (eV)	ΔG 300K	ΔG 80K	quenching[c] 300K	quenching[c] 80K
H_2TPPC-H_2TMPyP	0.87	-0.64	1.91	-0.40	+0.10	x	-
H_2TPPC-ZnTMPyP	0.87	-0.85	1.91	-0.19	+0.31	x	-
ZnTPPC-H_2TMPyP	0.60	-0.64	1.91	-0.67	-0.17	x	x
ZnTPPC-ZnTMPyP	0.60	-0.85	2.05	-0.60	-0.10	x	x

a: The redoxpotentials of the dimers have been determined from the oxidation potentials[a] of H_2TPPC and ZnTPPC and the reduction potentials[a] of H_2TMPyP and ZnTMPyP vs SCE in 4:1 H_2O/CH_3OH, 30 mM HCO_3^-, pH 8.5. The redoxpotentials were measured on a PAR model 173 potentiostat with a PAR model 179 coulometer, using a SCE reference electrode and platinum working electrodes. The potential was AC modulated at 100 Hz.

b: The fluorescence quenching has been measured for 1×10^{-5} M solutions of the dimers in 75 % w/v sucrose in H2O, 30 mM Tris, pH 8.5.

c: x indicates > 95 % quenching.

ΔG for the frozen solution at 80 K is more positive than at room temperature, because the solvent molecules can not reorient their dipoles, following a change of the local electric field accompanying the ET reaction in the dimer. The energy of the reaction products is, therefore, higher than for the liquid solution at 300 K. The contact-ion approximation [12] was used to calculate the change in free energy, that occurs upon decreasing the dipolemoment, μ, of the dimer: $\Delta G(\epsilon) = -(\mu^2/a^3).(\epsilon-1)/(2\epsilon+1)$. The average distance a between the dipole centres is 5.2 Å [5]. The charge is assumed to be completely transferred, resulting in μ = e.a . Taking ϵ = 3 to 9 for the apolar frozen solution $\Delta G(\epsilon)$ = +0.4 to +0.6 eV. As can be seen from Table II, where $\Delta G(\epsilon)$ = +0.5 eV is taken, with this correction term for ΔG ET can still occur for ZnTPPC-ZnTMPyP and for ZnTPPC-H_2TMPyP in frozen solution, but not for H_2TPPC-H_2TMPyP and for H_2TPPC-ZnTMPyP. This prediction remains valid, taking into account, that values of ϵ for the frozen solvent and μ for the contact-ion pair can only be estimated.

Table II: First oxidation and reduction potentials[a] vs SCE of substituted watersoluble porphyrins in 4:1 H_2O/CH_3OH, 30 mM HCO_3^-, pH 8.5

compound	E_{ox} (V)	E_{red} (V)
DMA-H_2TPPC	0.63	
H_2TMPyP-AQ		-0.55
ZnTMPyP-AQ		-0.50
ZnTMPyP-$(MV)_4$		-0.52

a: For experimental details see Table I.

In solutions of the dimer H_2TPPC-ZnTMPyP in 4:1 H_2O/CH_3OH at room temperature porphyrin cation radicals were detected in low yield by microsecond transient absorption measurements (figure 2). A long-lived transient species with an absorption maximum of 740 nm is detected,

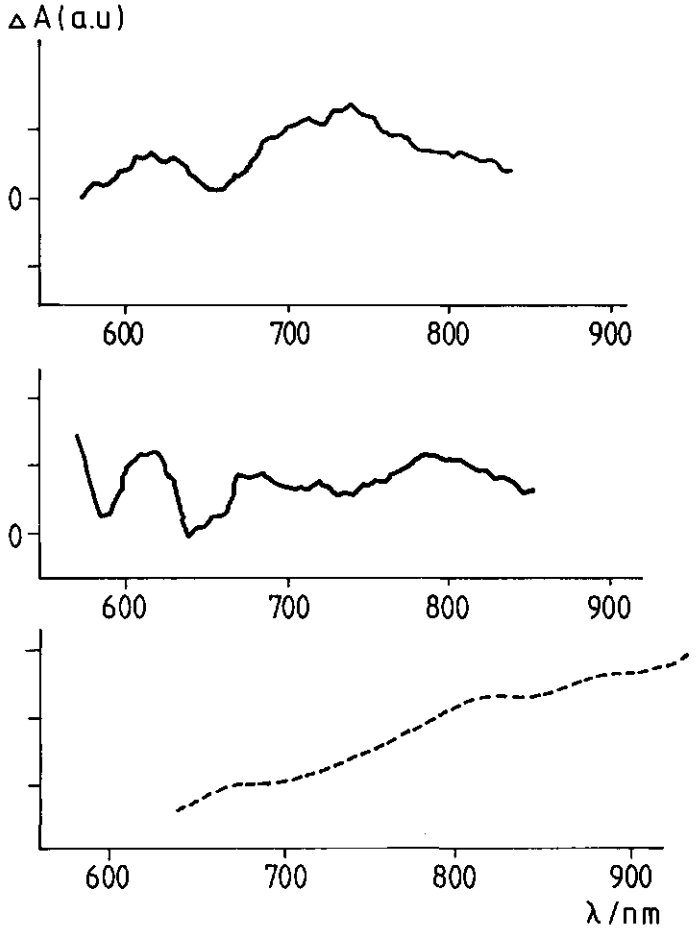

Figure 2: (a)Transient absorption difference spectrum with 5 nm intervals at 100 μsec after the laserpulse of $4x10^{-5}$ M. H_2TPPC and $4x10^{-5}$ M ZnTMPyP in 4:1 H_2O/CH_3OH, 30 mM HCO_3^-.
(b)Transient absorption difference spectrum with 5 nm intervals at 300 μsec of $4x10^{-5}$ M H_2TPPC in 4:1 H_2O/CH_3OH, 30 mM HCO_3^-.
(c)T-T absorption spectrum of ZnTMPyP from ref.14.

which can not be ascribed to a T-T absorption. The T-T absorption difference spectra for H_2TPPC and for ZnTMPyP are presented in figures 2b and 2c and the T-T absorption for the dimer is expected to be only slightly shifted w.r.t. that for H_2TPPC, because also the S_0-S_1 absorption spectrum is only 10 nm shifted w.r.t. that for monomeric H_2TPPC. The long-lived transient is identified as $ZnTMPyP^-$, which absorbs at 740 nm in methanol [13]. The formal negative charge of $ZnTMPyP^-$ is not the true charge, because the four positive charges on the pyridinium groups are not included. The decay of the transient is not exponential in the first part of the curve. The decay after a few hundred microseconds can be fitted with a single lifetime of 1.0 ms. The long lifetime and the low yield of the transient $ZnTMPyP^-$ species indicate, that it is not part of a radical pair state in the dimer. We propose, that the $ZnTMPyP^-$ radical is formed in the dimer after the first electron transfer step: H_2TPPC^*-ZnTMPyP -> H_2TPPC^+-$ZnTMPyP^-$ and escapes from the dimer before charge recombination. The decay of $ZnTMPyP^-$ is caused by bimolecular processes. The H_2TPPC^+ cation radical is not observed, probably due to very fast bimolecular quenching of this species or because its spectrum is hidden under other absorption bands.

In solutions of another dimer ZnTPPC-H_2TMPyP in 4:1 H_2O/CH_3OH the H_2TMPyP^- anion radical is detected at ≈ 740 nm.

In frozen 75% w/v sucrose in H_2O solutions of ZnTPPC-ZnTMPyP and ZnTPPC-H_2TMPyP at 77 K, where ET may occur, as follows from the data in Table I, only triplet species, resulting from monomeric porphyrins were detected in low yield; no products of electron transfer reactions were observed.

5.4.4 Substituted watersoluble porphyrins

The redoxpotentials of the substituted watersoluble porphyrins were investigated to determine, which secondary ET steps after the primary charge separation within the dimer are energetically favourable (Table II). Two secondary ET steps may occur:

$D\text{-}P_1^+\text{-}P_2^-\text{-}A \rightarrow D\text{-}P_1^+\text{-}P_2\text{-}A^- \rightarrow D^+\text{-}P_1\text{-}P_2\text{-}A^-$ or

$D\text{-}P_1^+\text{-}P_2^-\text{-}A \rightarrow D^+\text{-}P_1\text{-}P_2^-\text{-}A \rightarrow D^+\text{-}P_1\text{-}P_2\text{-}A^-$

The oxidation potential of DMA at 0.63 V indicates, that DMA is a favourable secondary electron donor for H_2TPPC, but not for ZnTPPC (Table I). The reduction potential of AQ with a sulfonyloxygroup is higher than without this linking group (E_{red}= 0.8 V, Chapter 6). In these compounds AQ is a suitable secondary electron acceptor for ZnTMPyP and for H_2TMPyP (Table I).

ET in the substituted watersoluble porphyrin monomers was investigated by fluorescence lifetime measurements (Table III)

Table III: Fluorescence lifetimes[a] (nsec) of substituted watersoluble porphyrins in 4:1 H_2O/CH_3OH, 30 mM HCO_3^-.

compound	α_1	τ_1	α_2	τ_2	α_3	τ_3
H_2TPPC	0.12	3.49	0.88	10.71		
DMA-H_2TPPC	0.19	3.24	0.26	10.61	0.55	0.79
H_2TMPyP	0.33	1.83	0.67	6.25		
H_2TMPyP-AQ	0.41	1.34	0.59	5.98		
ZnTPPC		1.92				
DMA-ZnTPPC	0.52	1.83	0.48	0.56		
ZnTMPyP		1.31				
ZnTMPyP-AQ	0.48	1.39	0.52	1.10		
ZnTMPyP-$(MV)_4$	0.54	0.33	0.46	0.16		

a: Excitation wavelength: 590 nm (CR 590 dye laser); detection at 657 nm (free base porphyrins) or 701 nm (zinc porphyrins). Oxazine in methanol was used as reference compound to deconvolute the fluorescence decays by the instrumental respons. Further experimental details, see Chapter 3.

The data of Table III show, that the fluorescence lifetimes of ZnTMPyP and H_2TMPyP are both significantly shorter than those for ZnTPPC and H_2TPPC, respectively. Substitution of a DMA or an AQ group results in an additional fluorescence component, except for H_2TMPyP, for which one component becomes shorter. Apparently, the fluorescence lifetimes of the majority of the substituted porphyrins can be described as resulting from two conformations: (i) an interacting conformation, where quenching occurs and (ii) a non-interacting conformation, for which the fluorescence lifetime is similar to that for the unsubstituted porphyrin. Only for ZnTMPyP-$(MV)_4$ both fluorescence lifetimes are significantly shortened, probably because this compound has four substituent groups, so that non-interacting conformations do not occur.

The fluorescence lifetimes of the watersoluble porphyrins are shortened upon substitution of an electron donor or acceptor to the porphyrin. The fluorescence quenching is however much smaller than for the porphyrin dimers (>95 %). It is concluded, that ET from DMA to the porphyrin or from the porphyrin to AQ is slower than between the porphyrin constituents of the dimers. The short plane-to-plane distance in the dimer (3.1 Å) results in a relatively large orbital overlap and, consequently, in a large electronic coupling V for the dimer, favouring fast ET. This process is expected to be the first ET step in the substituted dimers. The energy diagrams for DMA-H_2TPPC-H_2TMPyP-AQ and DMA-H_2TPPC-ZnTMPyP-AQ are given in figure 3.

The substituted dimer DMA-H_2TPPC-ZnTMPyP was investigated by microsecond transient absorption measurements. At long times a transient is observed, which is ascribed to a radical species, as for H_2TPPC-ZnTMPyP. The transients at 570 µsec for both dimers are shown in figure 4. The transient absorption band at 740 nm, which was ascribed to $ZnTMPyP^-$ is identical for both dimers. The transient at 510 nm in the spectrum of H_2TPPC-ZnTMPyP is probably also due to $ZnTMPyP^-$. A new transient at 480 nm in the spectrum of DMA-H_2TPPC-ZnTMPyP is attributed to DMA^+, which has a intense broad band centered at 480 nm [15]. Due to the relatively low ET recombination rate constant within the dimer, DMA-H_2TPPC-ZnTMPyP may dissociate in solution into

DMA^+-H2TPPC and $ZnTMPyP^-$.

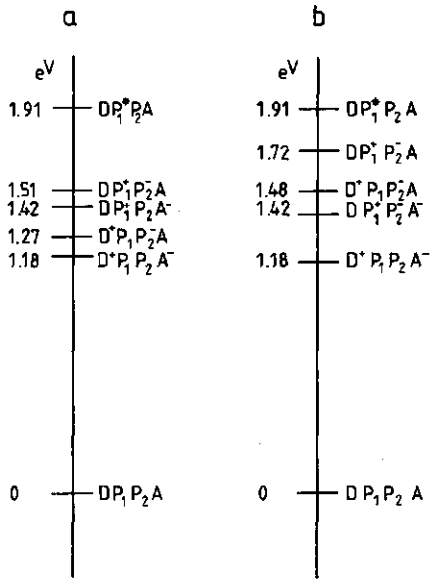

Figure 3: Energy level digrams for (a) DMA-H_2TPPC-H_2TMPyP-AQ and (b) for DMA-H_2TPPC-ZnTMPyP-AQ, both indicated as DP_1P_2A. No correction for coulombic interactions was made.

These preliminary experiments on substituted watersoluble porphyrin dimers show that it is energetically possible to generate a D^+-P_1-P_2-A^- state if the porphyrin dimer is H_2TPPC-ZnTMPyP, to which DMA and AQ are covalently bound via an ether bridge and a sulfonyloxy bridge respectively, DMA functioning as secondary donor and AQ as secondary acceptor.

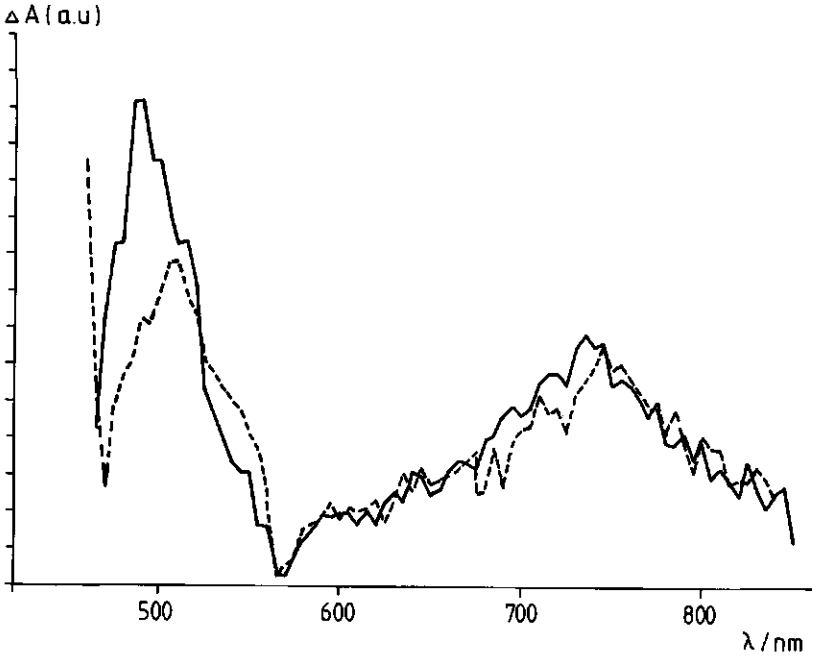

Figure 4: Transient absorption difference spectrum with 5 nm intervals at 570 μsec after the laser pulse of $4x10^{-5}$ M H_2TPPC and $4x10^{-5}$ M ZnTMPyP (----) and of $4x10^{-5}$ M DMA-H_2TPPC and $4x10^{-5}$ M ZnTMPyP (——).

References

1. J.Deisenhofer, O.Epp, K.Miki, R.Huber and H.Michel, J. Mol. Biol. 180 (1984) 385.
2. S.R.Meech, A.J.Hoff and D.A.Wiersma, Chem. Phys. Lett. 121 (1985) 287.
3. W.W.Parson, Ann. Rev. Biophys. Bioeng. 11 (1982) 57.
4. U.Hofstra, R.B.M.Koehorst and T.J.Schaafsma, Chem. Phys. Lett. 130 (1986) 555.
5. U.Hofstra, R.B.M.Koehorst and T.J.Schaafsma. Magn. Res. Chem. 25 (1987) 1069.
6. R.B.M.Koehorst, U.Hofstra and T.J.Schaafsma, Magn. Res. Chem. 26 (1988) 167.
7. R.G.Little, J.A.Anton, P.A.Loach and J.A.Ibers, J. Heterocyclic. Chem. 12 (1975) 343.
8. A.Shamim, P.Worthinton and P.Hambright, J. Chem. Soc. Pak. 3 (1981) 1.
9. R.G.Little, J. Heterocycl. Chem. 15 (1978) 203.
10. D.LeRoux, J.-C.Mialocq, O.Anitoff and G.Folcher, J. Chem. Soc. Faraday Trans. 2 80 (1984) 909.
11 M.-P. Pileni, A.M.Braun and M.Grätzel, Photochem. Photobiol. 31 (1981) 423.
12. G.J.Kavarnos and N.Turro, Chem. Rev. 86 (1986) 401.
13. S.Baral, P.Neta and P.Hambright, Radiat. Phys. Chem. 24 (1984) 245.
14. K.Kalyanasundaram and M.Neumann-Spallart, J. Phys. Chem. 86 (1982) 5163.
15. T.Shida and W.H.Hamill, J. Chem. Phys. 44 (1966) 2369.

Photoinduced electron transfer in donor-porphyrin-acceptor model systems and their components.

6.1 Introduction

Triads, i.e. donor-porphyrin-acceptor (DPA) compounds, are attractive as photosynthetic modelsystems, because the first electron transfer (ET) step is followed by a secondary forward ET step, thereby decreasing the recombination rate of the positive and negative charges [1,2]. We investigated the photoinduced ET in several donor-porphyrin and porphyrin-acceptor compounds with the purpose of designing a triad DPA model system. By investigating the redoxpotentials and the fluorescence quenching by ET in a series of two-component donor-porphyrin and porphyrin-acceptor compounds the possible ET pathways were determined for the triad.

The modelsystems consist of tetraphenylporphyrin, H_2TPP or ZnTPP, (1, 11) covalently linked to an electron donor, N,N-dimethylaniline (DMA) or to an electron acceptor, anthraquinone (AQ) or phthalimide (PHT). The functional groups, substituting one phenyl group of H_2TPP or ZnTPP, are collected in figure 1. In the majority of the compounds the functional groups are linked by an ether bridge, only in the compounds 5 and its zinc analog 15 the porphyrin and the AQ group are linked with a sulfonyloxy bridge.

Because the donor-acceptor distance and the conformation of the compounds are expected to have a large effect on the ET rate constants, the solution conformations of these compounds were investigated by ^{1}H NMR to study the relation between the average ground state conformation and the ET rate constant.

The ET rate constants were calculated from the excited singlet state lifetimes, which were determined from the fluorescence decay curves, as measured by the time-correlated single photon counting technique. By using this method it is assumed, that the other decay constants, i.e. the radiative decay constant, the intersystem crossing decay constant and the interconversion decay constant, are equal to

1,11:
2,12:
3,13:
4,14:
5,15:
6,16:
7,17:
8,18:
9,19:
10,20:

Figure 1: Molecular structures of the functional groups of the model compounds based on H_2TPP (2-10) and ZnTPP (12-20). The functional groups replace a phenyl group of H_2TPP or ZnTPP.

those for the reference compounds. This assumption is justified, because the donor and the acceptor only have a very weak interaction at the typical donor-acceptor distances of the investigated compounds.

6.2 Experimental

To obtain the N,N-dimethylaniline linked porphyrins 6 and 9 5-(2-hydroxyphenyl)-10,15,20-triphenylporphyrin and 5-(4-hydroxyphenyl)10,15,20-triphenylporphyrin were synthesized and purified following published procedures [3]. Addition of excess 1,3-dibromopropane to a solution of a hydroxyphenylporphyrin in the presence of one equivalent of anhydrous K_2CO_3 yielded almost quantitatively the corresponding (3-bromo,1-propoxy)phenylporphyrin [4]. Purification of the porphyrins was performed by column chromatography on silica (Merck Silicagel 60) with $CHCl_3$ as the eluent. The (3-bromo-1-propoxy)phenylporphyrin was added to excess potassium 3-(N,N-dimethylamino)phenolate (Merck, zur Synthese) in DMSO and stirred overnight. The product was crystallized by adding water to the solution. The desired DMA-linked porphyrins, 6 and 9 were purified by column chromatography on silica, using toluene/2% methanol as eluent. The purity was checked by optical spectra and ^{1}H NMR.

To prepare the phthalimide linked porphyrins 7 and 8 excess commercially available N-(3-bromopropyl)phthalimide (EGA Chemie) was added to a solution of the proper hydroxyphenylporphyrin in the presence of one equivalent of anhydrous K_2CO_3 and the solution was stirred overnight. The product was crystallized by adding water to the solution. Pure 7 and 8 were obtained by column chromatography on silica, using toluene as the eluent as confirmed by the optical and ^{1}H NMR spectra.

The anthraquinone linked porphyrin, 3 was prepared from 2 which was synthesized by the mixed aldehyde condensation method [3]. 2 was

dissolved in 48 % HBr in water and the solution was refluxed overnight. The partially hydrolyzed porphyrins and the remaining starting material were separated by column chromatography on silica, using toluene as the eluent. The third purple fraction, the largest fraction of the four, contained the desired (2-methoxy-5-hydroxy)phenylporphyrin. The anthraquinone moiety was linked to the porphyrin by adding excess 2-(bromomethyl)anthraquinone (Fluka, purum) to a solution of the porphyrin in DMF in the presence of one equivalent of anhydrous K_2CO_3 and stirring overnight. After crystallization of the product 3 by the addition of water it was purified by column chromatography on silica with toluene.

For the preparation of 5 (2-methoxy-5-hydroxy)phenylporphyrin was reacted with excess 2-anthraquinone-sulfonylchloride in pyridine. 5 was purified by column chromatography on silica with $CHCl_3$ as the eluent. The purity of 3 and 5 was checked by optical spectroscopy and ^1H NMR.

For the preparation of 10 (2-hydroxy-5-methoxy)phenylporphyrin was reacted with 1,3 dibromopropane in DMF in the presence of anhydrous K_2CO_3. After stirring overnight the porphyrin mixture was crystallized by adding water to the solution and chromatographed on silica, using $CHCl_3$ as eluent. The desired 2-(3-bromo-1-propoxy)-5-methoxy)phenylporphyrin was eluted as the first compound from the column. 750 mg of this compound in 100 ml 48 % HBr in water was refluxed during four hours, yielding the hydrolyzed product after neutralizing the solution with aqueous sodium hydroxyde. The porphyrin mixture was chromatographed on silica, using $CHCl_3$, and pure (2-(3-bromo-1-propoxy),5-hydroxy)phenylporphyrin was obtained. DMA was linked to the porphyrin and the product was purified as described above for 6 and 9. The product was reacted with excess 2-(2-bromoethyl)anthraquinone in DMF in the presence of one equivalent of K_2CO_3 and stirred overnight. After crystallization by adding excess water the final product 10 was purified by column chromatography on silica, using $CHCl_3$ as eluent. The purity was checked by optical spectroscopy and ^1H NMR.

The zinc porphyrins 11-20 were prepared from their free base analogs by standard procedures.

6.3 Determination of the solution structures by ^{1}H NMR

The average ground state conformations of these model systems were determined from their ^{1}H NMR spectra by fitting the calculated ring current shifts (rcs's) to the experimental rcs's, using the double-dipole method of Abraham et al.[5]. The principles of this method are described in §4.2. In the previous calculations, §§4.2 and 5.2, the conformations were generated by varying the position and orientation of the substituent w.r.t. the porphyrin over a wide range of translations and rotations. For the present calculations the method has been improved w.r.t. that in §4.2 by introducing the conformations from a molecular design program [6]. A starting porphyrin conformation was taken from the crystallographic data of tetraphenylporphyrin [7]. The substituents are attached to the molecule by taking fragments from the databank of the program and the total structure is optimized by minimizing the total energy of the molecule. This structure is used as a starting conformation. Subsequently, new conformations are generated by rotating over the linking bonds. The rcs's for these conformations are calculated and the conformation, yielding optimal agreement between calculated and experimental rcs's is chosen as the best fit.

The average conformations for 8 and 18 were investigated in acetone (AC) and in tetrahydrofuran (THF) (Tables I and II). The calculated donor-acceptor conformations are presented in figure 2. The centre-to-centre distances for 8 are r = 6.8 Å in AC and r = 8.8 Å in THF. The centre-to-centre distances are significantly smaller for 18: r = 5.4 Å in AC and r = 5.9 Å in THF. The shorter donor-acceptor distances in the more polar solvent acetone can be explained by assuming that charge transfer interactions between donor and acceptor contribute to the ground state interaction energy of the compounds. Charge transfer interactions are larger in more polar solvents and increase with increasing donor-acceptor distances, thereby enhancing a more folded conformation in acetone than in tetrahydrofuran.

From the calculated conformation it appears that the Zn-atom of 18 is ligated by the N-atom of phthalimide. The conformation of 18 can only be fitted by assuming an equilibrium between ligated and non-

Table I: Experimental[a] and calculated ring current shifts, δ_{exp} and δ_{calc}, (ppm) of the phthalimide linked compounds 8 and 18 in aceton (AC) and in tetrahydrofuran (THF).

	8 (AC)		8 (THF)		18 (AC)		18 (THF)	
proton[b]	δ_{exp}	δ_{calc}	δ_{exp}	δ_{calc}	δ_{exp}	δ_{calc}	δ_{exp}	δ_{calc}
α	+0.15	+0.22	+0.04	+0.08	+0.04	+0.05	+0.06	+0.06
β	-0.64	-0.74	c	-0.20	-0.81	-0.93	-0.72	-0.72
γ	-0.81	-1.25	c	-0.97	-1.16	-1.28	-0.61	-0.62
1,4	-0.76	-0.81	-0.07	-0.07	-0.92	-1.25	-0.39	-0.40
2,3	-0.71	-0.53	+0.01	+0.01	-0.60	-0.79	-0.31	-0.31

a: The reference compound to calculate the ring current contribution to the chemical shift is N-(3-bromopropyl)phthalimide. The chemical shifts for the α-protons have been corrected by subtracting the chemical shift induced by the Br-atom and adding the -O-phenyl shift [8].

b: For numbering of the protons see figure 1.

c: The resonances could not be assigned.

Table II: Torsion angles, Ψ, for the phthalimide-linked porphyrins 8 and 18 in AC and THF.

compound	Ψ(1-2-3-4)	Ψ(2-3-4-5)	Ψ(3-4-5-6)	Ψ(4-5-6-7)	Ψ(5-6-7-8)
8 (AC)	+77°	+160°	-8°	-156°	+54°
8 (THF)	-63°	+160°	+97°	+84°	-126°
18 (AC)	+91°	+160°	-133°	+124°	+14°
18 (THF)	+91°	+160°	-137°	+121°	+14°

a: The numbering of the atoms is as follows:

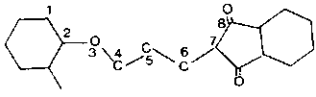

ligated phthalimide. In the ligated conformation the N-atom assumes a sp^3 configuration and the plane of the phthalimide molecule is bent away from the porphyrin.

H2PHTA_THF

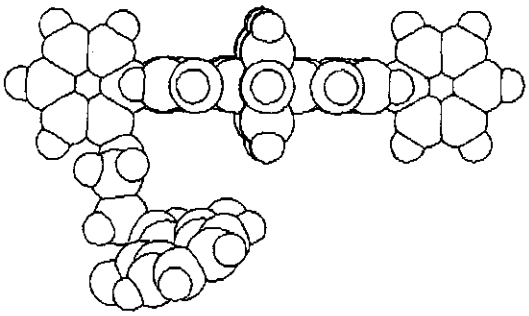

*H2PHTA_AC.DAT

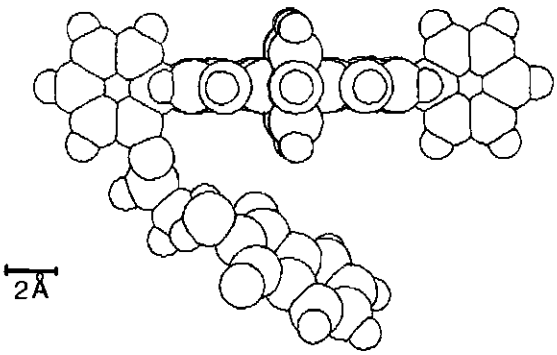

Figure 2: Conformation of 8 in AC (a) and in THF (b).

The conformations for 3 and for 5 were also determined in AC and in THF (Tables III and IV). The calculated centre-to-centre distances are 13.4 Å and 13.6 Å for 3 in AC and in THF, respectively. For 5 the

calculated distance is 8.9 Å in THF. The anthraquinone group in 3 and 5, which is substituted to the meta position of a phenyl group of H_2TPP, appears to be at a large centre-to-centre distance from the porphyrin. In 3 the anthraquinone group is folded further away from the porphyrin plane, resulting in a smaller distance for the latter molecule (figure 3).

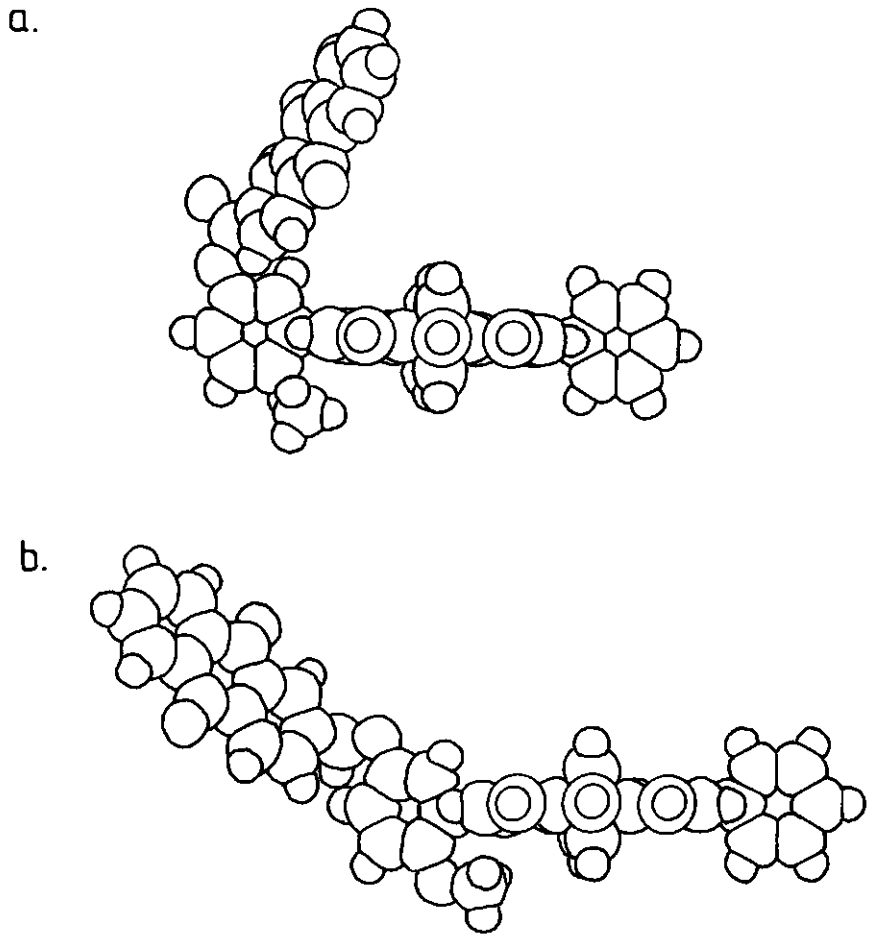

Figure 3: Conformation of 3 (a) and 5 (b) in THF.

Table III: Experimental[a] and calculated ring current shifts, δ_{exp} and δ_{calc}, (ppm) of the anthraquinone linked compounds 3 and 5 in 1:1 acetone/$CDCl_3$[b] (ACC) and tetrahydrofuran (THF).

	3 (ACC)		3 (THF)		5 (AC)	5 (THF)	
proton[c]	δ_{exp}	δ_{calc}	δ_{exp}	δ_{calc}	δ_{exp}	δ_{exp}	δ_{calc}
1	+0.27	+0.20	+0.27	+0.21	-0.18	-0.05	-0.23
3	+0.16	+0.13	+0.27	+0.27	+0.18	+0.15	+0.22
4	+0.02	+0.08	+0.03	+0.11	-0.15	-0.10	-0.15
5	-0.05	+0.02	-0.02	+0.03	-0.35	-0.17	-0.20
6	+0.06	+0.01	-0.04	+0.02	-0.09	-0.12	-0.16
7	+0.06	+0.01	-0.04	+0.02	-0.09	-0.12	-0.16
8	-0.05	+0.02	-0.02	+0.03	-0.35	-0.17	-0.20

a: The reference compound to calculate the ring current contribution to the chemical shift for 3 is 2-methylanthraquinone, where the chemical shift for the methyl protons is corrected for the O-phenyl [8]. The reference compound for 5 is 2-(sulfonyloxy-anthraquinone) benzaldehyde in $CDCl_3$.

b: The solubility in pure acetone is too low for the NMR experiments.

c: For numbering of the protons see figure 1

Table IV: Torsion angles for the anthraquinone-linked porphyrins 3 and 5 in 1:1 AC/$CDCl_3$ (ACC) and THF.

compound	Ψ(1-2-3-4)	Ψ(2-3-4-5)	Ψ(3-4-5-6)	Ψ(4-5-6-7)
3 (ACC)	-170°	+109°	-88°	-174°
3 (THF)	-170°	+110°	-87°	-174°
5 (THF)	-3°	-70°	+7°	+178°

a: The numbering of the atoms is as follows:

for 3:

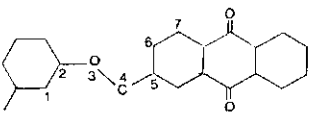

for 5:

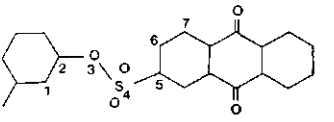

For porphyrin-substituent systems with a long linking chain the above described method for calculating the conformation by fitting the calculated rcs's to the experimental rcs's is very time-consuming, because the number of possible torsion angles increases steeply with the number of bonds in the chain. For 6, having six bonds in the chain, the conformation was calculated by varying the position and the orientation of DMA with respect to the porphyrin to reach optimal

Table V: Experimental[a] and calculated ring current shifts, δ_{exp} and δ_{calc}, (ppm) of the dimethylaniline linked compound 6 in THF.

proton[b]	δ_{exp}	δ_{calc}	conformation[c]
α	+0.17		Z = 6.2 Å
β	-0.64		X = 3.0 Å
γ	-1.02		Y = 4.7 Å
2	-0.44	-0.37	
4	-0.08 (-0.92)[d]	-0.14	Φ_1 = 39°
5	-0.68	-0.68	Φ_2 = -87°
6	-0.97 (-0.13)[d]	-0.95	Φ_3 = -90°

a: The ring current shifts have been calculated from the experimental chamical shifts by subtracting the literature values for 3-(3-phenyloxy)propoxy-N,N-dimethylaniline [8].

b: For numbering of the protons see figure 1.

c: Z is the translation of DMA perpendicular to the porphyrin plane; X and Y are the translations in the plane of the porphyrin: X is the direction of the phenyl-phenyl axis, containing the phenyl group to which the propyl group is substituted. Φ_1 is the rotation about the axis perpendicular to the porphyrin plane; Φ_2 is the rotation angle about the long axis of the DMA molecule; Φ_3 is the rotation angle about the axis perpendicular to that.

d: The assignment of the ^{1}H NMR resonances for the protons 4 and 6 of DMA is not unambiguous. The alternative assignment does, however, not lead to a good fit of the calculated to the experimental ring current shifts.

agreement between the calculated and the experimental rcs's and checking the possibility of the calculated conformation afterwards with a hard-sphere molecular model (Table V).

The porphyrin-DMA centre-to-centre distance is found to be 8.3 Å in THF.

The conformations for the molecules with flexible connecting chains that are calculated from the ^{1}H NMR spectra are average conformations on the NMR timescale. When these conformations are used to calculate the distance dependence of the ET rate constants, it must be remembered that there may exist some conformations with very short donor-acceptor distances. Although they hardly contribute to the average conformation, these conformations may strongly contribute to the ET rate constant. This problem is most severe for compounds with long, relatively flexible chains, like 8, 18, 6 and 16.

6.4 Redoxpotentials and fluorescence lifetime measurements.

The redoxpotentials of the model systems were investigated to determine the possibility for ET in these compounds (Table VI).

Using the redoxpotentials in dichloromethane (DCM) from Table VI the change in free energy upon electron transfer, ΔG, is calculated from the following expression (Chapter 2):

$$\Delta G = E_{ox}(D) - E_{red}(A) - E_S - e^2/\epsilon r - (e^2/2)(1/r_D+1/r_A)(1/\epsilon_R-1/\epsilon),$$

where $E_{ox}(D)$ is the oxidation potential of the donor and $E_{red}(A)$ is the reduction potential of the acceptor. E_S is the energy of the lowest excited singlet state of the porphyrin, calculated from the absorption spectrum of the model system. r is the centre-to-centre donor-acceptor distance, ϵ_R is the dielectric constant of dichloromethane and ϵ is the dielectric constant of the solvent, in which the ET is measured.

Considering the phthalimide-substituted compounds 8 and 18, no shortening of the fluorescence lifetimes w.r.t. those for the

Table VI: Oxidation and reduction potentials (V) in CH_2Cl_2 vs SCE of some covalently linked porphyrin-acceptor and porphyrin-donor systems.

compound	$E_{ox}(2)$	$E_{ox}(1)$	$E_{red}(1)$	$E_{red}(2)$	$E_{ox}(1)-E_{red}(1)$
3	1.23	1.00	-0.86	-1.17	1.86
5		1.00a	-0.75b		1.75
8		1.00a	-1.26c		
6	1.17	0.83	-1.19		2.02
13	1.06	0.79	-0.79	-1.60	1.58
16	1.04	0.78	-1.84		2.62
18	1.05	0.78	-1.26	-1.40	2.04

a: Taken as the oxidation potential of H_2TPP in H_2TPP-AQ.

b: Taken as the reduction potential of AQ in sulfonyloxy linked diphenylporphyrin-anthraquinone (§ 4.2)

c: Reduction potential of phthalimide in 18.

Table VII: Fluorescence lifetimes, τ_1 and τ_2, and ΔG for 18 and the reference compound 11 in AC and in THF.

	11					18				
solvent	α_1	τ_1 (ns)	α_2	τ_2 (ns)	ΔG (eV)	α_1	τ_1 (ns)	α_2	τ_2 (ns)	k_{ET} (sec^{-1})
THF	0.29	1.3	0.71	2.0	-0.31	0.23	1.3	0.77	1.9	$<1x10^7$
AC	0.19	1.3	0.81	2.2	-0.35	0.73	1.0	0.27	1.5	$4.0x10^8$

reference compound 1 was found for 8: τ = 12.4 ns in Tol and τ = 12.2 ns in AC, whereas for 1 τ = 12.1 ns in Tol and τ = 12.3 ns in AC. ET from the excited singlet state of the porphyrin to the phthalimide can apparently not occur as a fluorescence quenching mechanism, because the process is endothermic for 8, both in Tol (ΔG = +0.52 eV) and in AC (ΔG = +0.07 eV).

The fluorescence lifetimes in AC and THF and the ΔG values for 18, the zinc substituted analog of 8, are presented in Table VII. Note the shortening of the lifetimes w.r.t. those of the reference compound 11.

The anthraquinone-substituted compounds 3 and 5 appear to have very different values of ΔG for the formation of the radical pair P^+-AQ^-, due to the effect of the sulfonyloxy group on the reduction potential of AQ. The fluorescence lifetimes for 3 and 5 have been compared with those for the reference compound 2 in toluene (Tol), tetrahydrofuran (THF), acetone (AC) and acetonitril (AN) (Table VIII).

Table VIII: Fluorescence lifetimes, τ, and ΔG for 3 and 5 and for the reference compound 2[a].

	2	3			5		
solvent	τ (ns)	ΔG (eV)	τ (ns)	k_{ET} (sec^{-1})	ΔG (eV)	τ (ns)	k_{ET} (sec^{-1})
Tol	12.5	+0.33	12.6	0	+0.01	6.5	7.4×10^7
THF	12.6	-0.14	12.8	0	-0.32	0.5[c]	1.9×10^9
AC	12.7	-0.28	9.7	2.4×10^7	-0.42	0.4[d]	2.5×10^9
AN	12.3	-0.33	5.0[b]	1.2×10^8	-0.45	-	

a: The fluorescence lifetime of 4, which contains also sulfonyloxy linkages, are within 0.2 ns of those for 2.

b,c,d: The average of two experimentally found lifetimes has been taken; b: α_1=0.17, τ_1=2.8 ns, α_2=0.83, τ_2=5.3 ns; c: α_1=0.64, τ^1=0.2 ns, α_2=0.32, τ_2=1.0 ns; d: α_1=0.97, τ_1=0.1 ns, α_2=0.03, τ_2=11.6 ns

For the dimethylaniline-substituted compound 6 the fluorescence is also quenched. ΔG for the formation of the radical pair DMA^+-P^- and the fluorescence lifetimes for 6 are given in Table IX.

Table IX: Fluorescence lifetimes, τ, and ΔG for 6.

	2		6				
solvent	τ (ns)	ΔG (eV)	α_1	τ_1 (ns)	α_2	τ_2 (ns)	k_{ET}[a] (sec^{-1})
Tol	12.5	+0.11			1.0	12.1	0
DCM	9.3	-0.13	0.09	3.1	0.91	9.1	2.2×10^7
AC	12.7	-0.17	0.93	3.3	0.07	12.4	2.1×10^8
AN	12.3	-0.19	0.97	1.5	0.03	11.8	5.9×10^8

a: For biexponential decays k_{ET} for both conformations has been calculated and the average k_{ET} is given.

6.5 Discussion

For all compounds the shortening of the fluorescence lifetimes is found to increase with ΔG, indicating that electron transfer is the mechanism for the fluorescence lifetime shortening in these compounds. The photoexcited porphyrin can act as donor to AQ and to THF, but also as electron acceptor to DMA. Contrary to the former process, the latter has received only little attention (see, however, ref.9). The ET process is in the Marcus normal region of the k_{ET} vs. ΔG curve (see Chapter 2, fig.4). An irregularity is found for 18, for which the excited state lifetimes for 18 are shortened in acetone, but not in tetrahydrofuran, although from the values for ΔG in these solvents ET is expected to occur in both solvents. If we omit the Coulomb attraction term $-e^2/\epsilon.r$ from the expression for ΔG, the values are ΔG = +0.02 eV in THF and ΔG = -0.22 eV in AC. A Coulombic attration energy

-0.33 eV was calculated for the radical pair $ZnTPP^+$-PHT^- in THF, using r = 5.4 Å (Table I). From the data of Table VI we conclude, that the ET process is actually endothermic for 18 in THF and, therefore, it follows, that at these short distances the macroscopic monopole-monopole approximation for the calculation of the Coulombic attraction energy leads to a overestimation of this term.

The excited singlet state lifetime for 5 is much shorter than for 3 in the same solvent. The effect of the sulfonyloxy bridge appears to be two-fold. The first effect concerns the value of ΔG for the ET reaction. The sulfonyloxy bridge favours the reduction of the anthraquinone and increases the exothermicity of the forward ET step. Since the ET rate constant strongly increases with ΔG in the "normal region" the ET rate constant for 5 is expected to be higher than that for 3 in the same solvent, as was indeed found experimentally (Table VIII).

A second effect appears from comparing k_{ET} for 3 in acetonitril with k_{ET} for 5 in THF. ΔG is equal for both ET steps, but the ET reaction for 5 is 25 x faster than for 3. Several explanations are possible for this effect. It might be thought that the difference could be explained by the smaller porphyrin-anthraquinone distance for 5 than for 3 (Table II). The distance dependence of the ET rate constant is given by $k_{ET} = k_0.e^{-\alpha(r-r_0)}$ (Chapter 2). Taking r_0, the distance of closest approach as 3 Å and using α = 1.1 $Å^{-1}$, r(3) = 12.7 Å and r(5) = 8.9 Å , k_{ET} for 5 is calculated to be 31 x as large as for 3, comparable with the experimental data. There is, however, evidence unvalidating this explanation. In § 5.2 a through-bond ET mechanism was found for ET from photoexcited porphyrin to AQ for o,m-DMA-H_2P-AQ, where AQ is linked to the porphyrin in the same manner as for 5. Assuming a through-bond mechanism the difference in ET rate constants for 3 and 5 can no longer be explained by the distance dependence of k_{ET}, because both compounds have three bonds of comparable lengths in the bridge between the porphyrin and the AQ group. We propose that the difference is caused by the nature of the bridges between the porphyrin and AQ. For 5 the coupling through the bond by a superexchange mechanism is assumed to be larger than for 3, because the energy B to place an electron in the bridge is smaller for the

$-O-SO_2-$ bridge than for the $-O-CH_2-$ bridge. Upon insertion of an electron in the bridge the electron can be accomodated by a double-bonded oxygen atom :

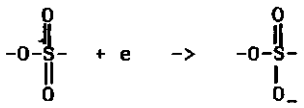

It is therefore conceivable that the energy to transfer the electron to an empty solvent orbital is lower for the sulfonyloxy bridge than for the ether bridge. The electron coupling term V, which is proportional to $e^{-\ln(B)}$ (Chapter 2) is larger, thereby increasing k_{ET}.

6.6 Donor-porphyrin-acceptor triads.

The donor-porphyrin and the porphyrin-acceptor compounds can be combined to form donor-porphyrin-acceptor, D-P-A, triads. The oxidation potential of the donor in the triad should be lower than that of the porphyrin and the reduction potential of the acceptor should be higher than that of the porphyrin, so that the radical pair with the lowest energy in the triad is D^+-P-A^-.

For the porphyrin we chose H_2TPP in stead of ZnTPP, because it has a higher oxidation potential than the electron donor DMA. ZnTPP is not suitable as photosensitizer, because its oxidation potential is comparable to that for DMA, so that both the primary ET from DMA to photoexcited ZnTPP* and the secondary ET from DMA to the $ZnTPP^+$, formed after the primary ET from ZnTPP* to an acceptor can not occur.

PHT is not suitable as electron acceptor to H_2TPP, because the reduction potentials of PHT and H_2TPP are similar (Table II). Therefore we chose AQ as electron acceptor. The resulting triad 10, DMA-H_2TPP-AQ, has DMA and AQ linked to the same phenyl group to ensure, that both functional groups are above and below the plane of the porphyrin macrocycle.

The triad 10 has, in principle, two electron pathways:

i) DMA-H_2TPP*-AQ -> DMA^+-H_2TPP^--AQ -> DMA^+-H_2TPP-AQ^-.

ii) DMA-H_2TPP*-AQ -> DMA-H_2TPP$^+$-AQ$^-$ -> DMA$^+$-H_2TPP-AQ$^-$

ΔG in acetone for the primary step in i) is -0.17 eV and -0.49 eV for the secondary step. For ii) the values for ΔG are -0.28 eV and -0.38 eV.

The ET rate constants for 6 are larger than for 3 in acetone and acetonitril (Table VIII and IX). We expect, therefore that pathway i) will occur for DMA-H_2TPP-AQ. To check, whether the rate constant for the primary ET is equal to that for 6, the fluorescence quantum yields for 10 were compared with those for 3 and 6 (Table X).

Table X: Fluoresence quantum yields[a,b], Φ_f^r, for 3, 6 and 10.

	3	6	10
solvent	Φ_f^r	Φ_f^r	Φ_f^r
Tol	1.03	0.99	1.08
THF	0.95	0.75	0.76
DCM	0.48	0.88	0.43
AC	0.78	0.29	0.27

a: Fluorescence quantum yields are given relative to those for 2.

b: Estimated error is 10 %.

The data of Table X show, that the fluorescence quenching of the triad 10 is almost equal to that for one of the two-component molecules 3 and 6, indicating that the substitution of both substituents to the same phenyl group does not influence the excited state decay kinetics, e.g. by allowing less conformations than for the two-component molecules. An interesting feature from Table X is that the ET pathway can be influenced by the solvent. In dichloromethane the fluorescence quantum yield of 10 is equal to that of 3, whereas in acetone and THF the fluorescence quantum yield of 10 is equal to that of 6, indicating that in dichloromethane the ET pathway is from the photoexcited porphyrin to the anthraquinone, whereas in THF and acetone the ET

pathway is from DMA to the photoexcited porphyrin.

References

1. T.A.Moore, D.Gust, P.Mathis, J.-C.Mialocq, C.Chachaty, R.V.Bensasson, E.J.Land, D.Doizi, P.A.Liddell, W.R.Lehman, G.A.Nemeth and A.L.Moore, Nature 307 (1984) 630.
2. M.R.Wasielewski, M.P.Niemczyk, W.A.Svec and E.B.Pewitt, J. Am. Chem. Soc. 107 (1985) 5562.
3. R.G.Little, J.A.Anton, P.A.Loach and J.A.Ibers, J. Heterocycl. Chem. 12 (1975) 343.
4. R.G.Little, J. Heterocycl. Chem. 15 (1978) 203.
5. R.J.Abraham, K.M.Smith, D.A.Goff and Ian-Li-Lai, J. Am. Chem. Soc. 104 (1982) 4332.
6. Chem-X, released by Chemical Design Ltd., Oxford, England.
7. S.J.Silvers and A.Tulinsky, J. Am. Chem. Soc 89 (1967) 3331.
8. H.Gunther, NMR Spektroskopie, Georg Thieme Verlag, Stuttgart, (1983).
9. A.Harriman and R.J.Hosie, J. Photochem. 15 (1981) 163.

CHAPTER 7

Electron transfer in paramagnetic porphyrin dimers.

7.1 Introduction

Fluorescence quenching of diamagnetic compounds by paramagnetic species at close distance is a well-known phenomenon [1-7]. The term paramagnetic quenching comprises several quenching mechanisms, i.e. electron transfer [5], energy transfer [6,7] and catalyzed intersystem crossing [2-4]. It is the purpose of this paper to clarify the quenching mechanisms through which a paramagnetic porphyrin affects the excited state kinetics of a diamagnetic porphyrin, complexed or covalently linked to the paramagnetic moiety. All three quenching mechanisms can in principle be operative.

Electron transfer (ET) can occur between H_2- or Zn-porphyrins and Cu(II)-porphyrins [5], in view of the redoxpotentials of the monomer constituents of the dimers.

Energy transfer (ENT) can occur between several electronic states of the dimer. This process has been assumed to take place in dimers, of Zn-porphyrin and Cu(II)-porphyrin from the Zn-porphyrin lowest excited singlet state to the Cu(II)-porphyrin doublet state [6,7] and from the Zn-porphyrin triplet state to the tripdoublet state of the Cu(II)-porphyrin [8-10]. In dimers of H_2-porphyrin and Cu(II)-porphyrin ENT from the Cu(II)-porphyrin tripdoublet state to the H_2-porphyrin triplet state has been observed [11].

Catalyzed intersystem crossing (CISC) by nitroxide radicals [2] and transition metals [3,4] has been reported to result in triplet quenching. In Cu(II)-porphyrins the very fast decay of the excited doublet states is due to exchange coupling between between metal d- and porphyrin π-electrons [12]. In a similar manner a paramagnetic Cu(II)-ion can effect the intersystem crossing rates, $S_1 \rightarrow T_0$ and $T_0 \rightarrow S_0$, in a nearby diamagnetic porphyrin. Several factors are operative in the interaction between a paramagnetic Cu(II)-ion and a porphyrin triplet state. The exchange and dipolar interactions in the spin hamiltonian, $J.S_1.S_2$ and $S_1.D.S_2$, respectively (where S_1 is the

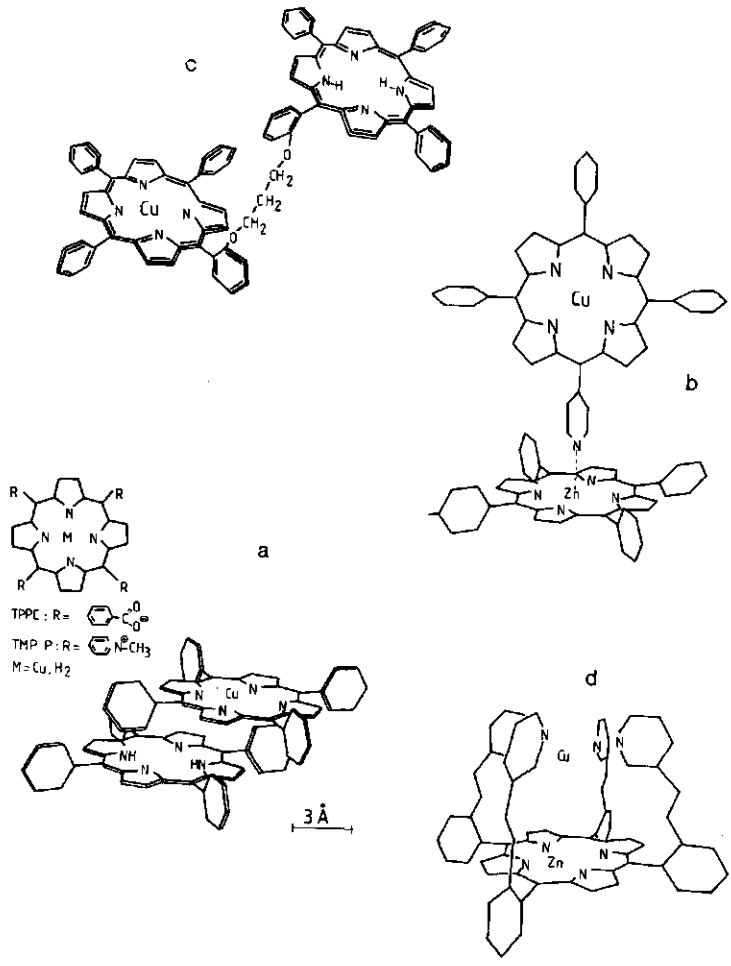

Figure 1 : Molecular structure of a) dimer of tetracarboxyphenylporphyrin and tetramethylpyridiniumporphyrin. For the structure of this dimer see § 5.2; b) Zn-tetraphenylporphyrin, ligated with Cu-4-pyridyl-porphyrin, ZnTPP-CupPyP; in ZnTPP-CumPyP the 4-pyridyl group is replaced by a 3-pyridyl group; c) diether linked tetraphenylporphyrins; the linking chain can be either located at the ortho position of the phenyl groups: o,o H_2TPP-CuTPP, or at the para position: p,p H_2TPP-CuTPP, d) ZnTNP with a Cu^{2+} ion captured by the four nicotinamide groups.

triplet spin on the porphyrin and S_2 is the doublet spin of Cu(II)) can mix the $T_0(m_s=0)$ sublevel of the porphyrin triplet with the $T_0(m_s=\pm1)$ sublevels in the presence of a magnetic field. These interactions do not mix sublevels of T_0 with singlet states, however, and therefore do not contribute to the intersystem crossing from the singlet to the triplet manifold and vice versa. For particular geometries the antisymmetric exchange term $H = \alpha\ S_1 x S_2$ may mix the singlet and triplet states of the porphyrin [13].

The static triplet state properties of a free base or a zinc porphyrin are also expected to be affected by the presence of a nearby Cu(II)-porphyrin or a Cu(II)-ion. The dipolar spin-spin and exchange interactions between the triplet spin of an excited free base or zinc porphyrin and the doublet spin of a nearby Cu(II)-ion change the zero field splitting (zfs) parameters of the diamagnetic porphyrin [14], e.g. in a dimer of Cu-porphyrin and H_2- or Zn-porphyrin.

We have investigated the effects of a nearby Cu(II)-porphyrin on the excited state kinetics and magnetic properties of the lowest excited triplet state of H_2- and Zn-porphyrins in three types of porphyrin dimers 1) oppositely charged watersoluble porphyrin dimers, consisting of negatively charged tetracarboxyphenylporphyrins and positively charged tetramethylpyridiniumporphyrins, H_2TPPC-CuTMPyP and H_2TMPyP-CuTPPC [5], 2) diether-linked tetraphenyl dimers, denoted as H_2TPP-CuTPP and 3) a novel type of dimers, in which Cu-5-pyridyl, 10,15,20-triphenylporphyrin is ligated to ZnTPP, denoted as ZnTPP-CuPyP. For comparison also the photophysical properties were investigated of a zinc porphyrin, Zn-α,α',α'',α'''-tetra(o-nicotinamidophenyl)-porphyrin (ZnTNP), to which Cu(II) is ligated by four nicotinamide substituent groups [15-17]. The structures of all porphyrins are presented in figure 1.

7.2 Experimental

Tetraphenylporphyrin and pyridylporphyrins were synthesized by the condensation of aldehydes and pyrroles [18,19]. The diether-linked porphyrin dimers were synthesized according to the method of Little

[20]. The synthesis of the tetracarboxyphenylporphyrins and the tetramethylpyridiniumporphyrins has been described in ref.5. Metallated derivatives were prepared by conventional procedures. ZnTNP was synthesized according to the method of Elliot [15]. The purity of the porphyrins was checked by thin layer chromatography, UV-Vis absorption spectroscopy and ^{1}H NMR.

The fluorescence and phosphorescence quenching experiments were carried out on a Perkin Elmer LS 5 spectrometer. The fluorescence detected magnetic resonance (FDMR) spectra were measured on a previously described apparatus [21], using a cw argon-ion laser (Coherent Radiation CR 4) as light excitation source and a 0.25 m Spex monochromator and a RCA C 31034 A photomultiplier at the detection side . This apparatus was also used for the fluorescence fading experiments, in which the observed decay rates were extrapolated to zero light intensity to yield the triplet decay rate constants [22] and for phosphorescence lifetime measurements, using chopped light excitation.

The fluorescence lifetimes were detected on a single photon counting apparatus [23], using 100 ps, 514 nm pulses for excitation.

The ESR spectra were recorded on a X-band VARIAN E-6 spectrometer, using a liquid nitrogen flow cryostat for low temperature measurements and a 150 W Xe lamp for light excitation.

7.3 Zn-porphyrin with a nearby Cu(II)-ion

The influence of a Cu(II)-ion on the excited state kinetics of a Zn-porphyrin was investigated for ZnTNP (figure 1d). The pyridyl groups of this porphyrin can capture a Cu(II)-ion. In the complex Cu(II) is four-fold ligated to the four nitrogen atoms of the nicotinamide groups and is thereby kept at a close distance to the porphyrin plane (≈ 5.9 Å [17]). We investigated the fluorescence decay and the fluorescence quantum yield of this complex (Table I).

The static quenching process in this complex is very efficient. The observed fluorescence is from uncomplexed ZnTNP, as is shown by the

Table I: Fluorescence lifetimes, τ_f, (10^{-9} sec) and relative quantum yields, ϕ_f^r, of $5x10^{-6}$ M ZnTNP in 9:1 CH_2Cl_2/CH_3OH at room temperature in the presence of increasing amounts of $CuCl_2$.

concentration $CuCl_2$	τ_f	ϕ_f^r
0	2.23	1
$5x10^{-6}$ M	2.02	0.09 [a]
$2.5x10^{-5}$ M	b	<0.001 [a]

a: Fluorescence quantum yield relative to that in the absence of $CuCl_2$.
b: Fluorescence yield is too low to determine the lifetime.

fluorescence lifetimes. At $2.5x10^{-5}$ M $CuCl_2$ the fluorescence of ZnTNP is completely quenched and all ZnTNP molecules are complexed by Cu(II). The fluorescence and phosphorescence of the complex is also quenched in frozen solution at 77 K.

The efficient paramagnetic quenching of the porphyrin fluorescence has also been found for capped porphyrins, in which a paramagnetic ion is captured by a crown ether [3,24].

As the operative mechanism for the ZnTNP fluorescence quenching we propose electron transfer from the excited singlet state of ZnTNP to the Cu(II)-ion (figure 2a). If we approximate the oxidation potential of ZnTNP by that of ZnTPP (E_{ox}= 0.71 V vs SCE in dichloromethane [25]) and use the standard reduction potential of Cu(II) (E_{red}= 0.158 V [26]), the free energy of the ET process, neglecting electrostatic interactions is ΔG = -1.29 eV and thus the ET reaction is strongly exothermic. From the charge-separated state, indicated as P^+-Cu^- in figure 2a, at 0.79 eV the complex is unable to recombine to the triplet state ^{3}P-Cu (at 1.58 eV, as follows from the observed phosphorescence wavelength).

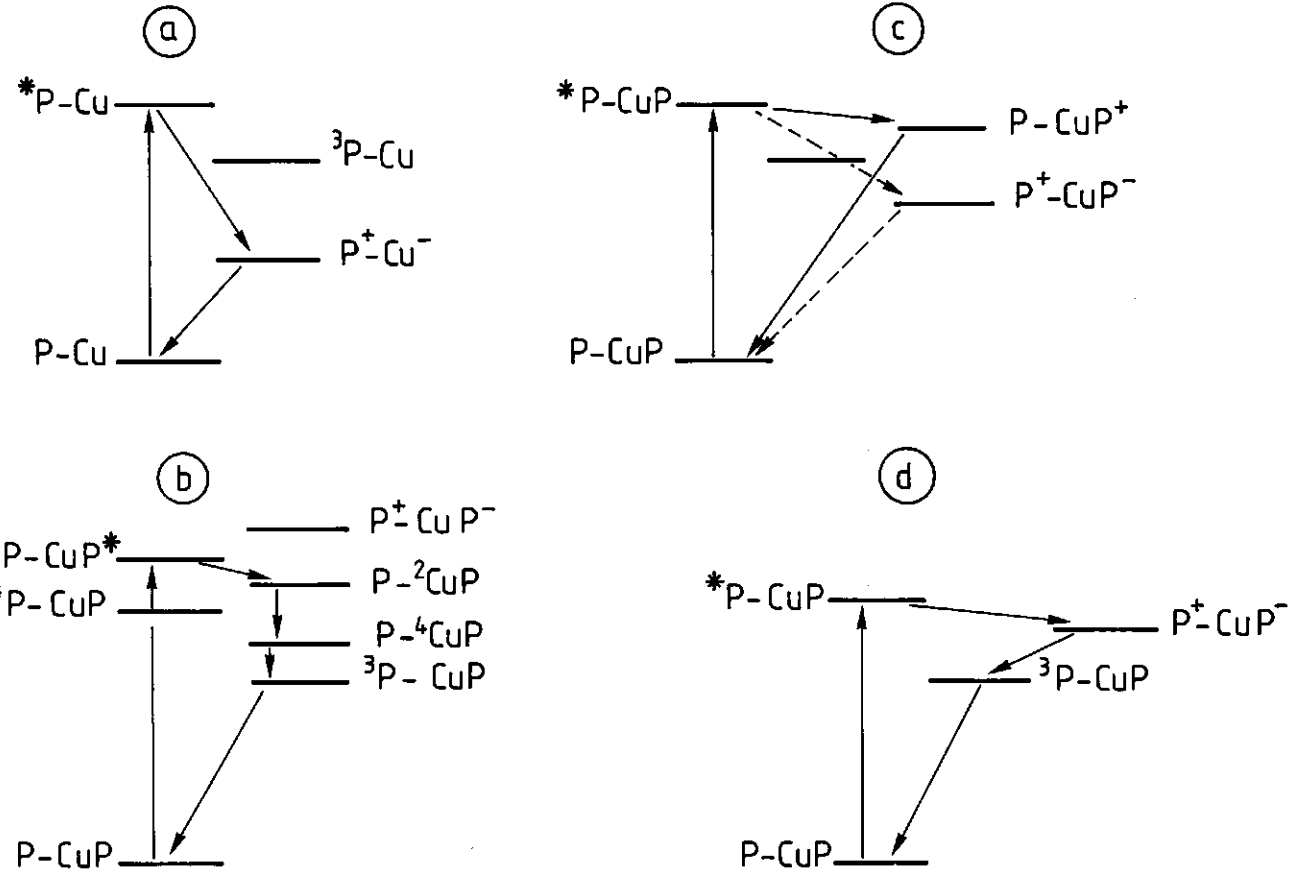
a
*P-Cu
3P-Cu
P+-Cu-
P-Cu
c
*P-CuP
P-CuP+
P+-CuP-
P-CuP
b
P+-Cu P-
P-CuP*
*P-CuP
P-2CuP
P-4CuP
3P-CuP
P-CuP
d
*P-CuP
P+-CuP-
3P-CuP
P-CuP

Figure 2 : Decay pathways for a) ZnTNP-Cu^{2+}; b) H_2TPPC-CuTMPyP (drawn lines) and H_2TMPyP-CuTPPC (dashed lines); c) o,o H_2TPP-CuTPP; d) ZnTPP-CupPyP and ZnTPP-CumPyP.
For clarity reasons the zinc and free base porphyrins have been abbreviated as P and the Cu-porphyrins as CuP.

7.4 Oppositely charged porphyrin dimers

In dimers of watersoluble porphyrins consisting of negatively charged tetracarboxyphenylporphyrin and positively charged tetramethylpyridiniumporphyrin, H_2TPPC-CuTMPyP and H_2TMPyP-CuTPPC the fluorescence from the diamagnetic porphyrin, as well as the luminescence from the quartet state of the Cu(II)-porphyrins is quenched, both at room temperature and at 77 K in frozen solution in 75 % w/v sucrose in H_2O, 30 mM tris(hydroxymethyl)aminomethane (Tris). Also no transient absorption at a microsecond timescale due to the triplet state of the H_2-porphyrin was observed.

We suggest that the mechanism for the emission quenching in these dimers is electron transfer within the dimer (figure 2b). The oxidation- and reduction potentials of the H_2- and Cu(II)-porphyrins are given in Table II.

Table II: Oxidation and reduction potentials vs NHE for H_2- and Cu(II)-porphyrins in aqueous solution.

compound	E_{ox} (V)	E_{red} (V)
H_2TPPC	1.11[a]	-1.06[c,d]
CuTMPyP	1.36[b]	-0.70[b]
H_2TMPyP	>1.30[c]	-0.40[a]
CuTPPC	0.77[b,d]	-1.05[b,d]

a: measured by AC voltammetry vs SCE and converted to values vs NHE by adding 0.24 V.

b: from ref.27. ; c: from ref.28; d: taken from the values for the corresponding tetrakis(4-sulfonylphenyl)porphyrin.

From the data in Table II and the energy of the lowest singlet state, E_{S_1} we calculated ΔG for formation of the charge-separated state. For the dimer H_2TPPC-CuTMPyP ΔG = -0.13 eV and for the dimer H_2TMPyP-CuTPPC ΔG = -0.74 eV. ET as a fluorescence quenching mechanism is therefore energetically possible for both dimers (figure 2b).

7.5 Covalently linked porphyrin dimers

The tetraphenylporphyrins in the covalently linked dimers are linked via a diether chain substituted at the ortho- or para positions of a phenyl group, resulting in o,o H_2TPP-CuTPP and p,p H_2TPP-CuTPP [29].

The fluorescence of H_2TPP in these dimers at room temperature is not quenched.

ET can not occur in these dimers, because of the unfavourable oxidation and reduction potentials of H_2TPP and CuTPP (H_2TPP: E_{ox}= 0.95 V in CH_2Cl_2, E_{red}= -1.05 V in DMSO; CuTPP: E_{ox}= 0.90 V in CH_2Cl_2 and E_{red}= -1.20 V in DMSO (vs SCE [25]). The S_1 state of H_2TPP is at 1.92 eV, resulting in ΔG = +0.23 eV for the formation of H_2TPP^+-$CuTPP^-$ and ΔG = +0.03 eV for the formation of H_2TPP^--$CuTPP^+$, neglecting Coulomb attraction within the charge-separated state, which is very small at the donor-acceptor distance in these dimers [30]. The values of ΔG for ET in toluene are even more positive, if the redoxpotentials are corrected for the solvent.

At low temperature in frozen solution CuTPP luminesces from the tripquartet state [31]. A quenching of this luminescence at 77 K in o,o- and p,p H_2TPP-CuTPP was observed (Table III), whereas the H_2TPP fluorescence quantum yield remains unchanged.

The quenching of the tripquartet emission confirms measurements at room temperature for o,o H_2TPP-CuTPP, which showed, that energy transfer from the tripdoublet state of CuTPP to the H_2TPP triplet state (figure 2c) occurred, as evident from an increased triplet-triplet absorption for H_2TPP [11]. We observed this quenching for the o,o linked dimer, but not for its p,p analog, implying that the the ave-

Table III Luminescence lifetimes, τ_L, (sec) and relative quantum yields, ϕ_L^r, of CuTPP in diether linked H_2TPP-CuTPP dimers in toluene/2% pyridine at 77 K.

	compound	τ_L	ϕ_L^r a
	CuTPP	6.0×10^{-4} b	1
p,p	H_2TPP-CuTPP		1.2±0.2
o,o	H_2TPP-CuTPP	6.9×10^{-4} c 1.4×10^{-4} c	0.15±0.05

a: The quantum yields relative to CuTPP monomer.

b: In methylcyclohexane [32].

c: Biexponential quartet state luminescence.

rage interchromophore distance for the o,o linked dimer in frozen solution is smaller than for the p,p linked dimer. The effect of varying the substitution site on the quenching apparently differs from that for ZnTPP-CuTPP and ZnTPP-Mn(III)TPP at room temperature. For these compounds the ZnTPP fluorescence quenching at room temperature was observed to be larger for p,p ZnTPP-CuTPP and p,p ZnTPP-Mn(III)TPP dimers, than for the o,o analogs, which was ascribed to a larger orbital overlap between the monomer units in the p,p linked dimers [6]. The difference in substitution site dependence can be explained by the fact that the latter experiments were performed at room temperature, when p,p dimers fold more easily during the excited state lifetime than o,o dimers, thereby reducing the effective interchromophore distance for the p,p dimers. The average ground state conformation of the p,p linked dimer corresponds, however, to a complete unfolding, as follows from the NMR data [33]. This unfolded conformation is frozen in at low temperature, largely preventing ENT by orbital overlap of the monomeric units for p,p H_2TPP-CuTPP in the present study.

Triplet to doublet ENT, involving CuTPP in a porphyrin dimer has also been proposed as a quenching mechanism for the triplet state of

ZnTPP in diamide linked ZnTPP-CuTPP dimers [8,9].

ENT from CuTPP to the triplet state of H_2TPP in o,o H_2TPP-CuTPP can be expected to affect the relative populating rates of the triplet sublevels of H_2TPP. The decay rate constants of the triplet state of H_2TPP in these porphyrin dimers were investigated at T = 4.2 K, when spin-lattice relaxation between the triplet sublevels can be neglected [34]. From fluorescence fading experiments [22] the decay rate constants and the relative population rates of the triplet sublevels of the H_2TPP moiety in H_2TPP-CuTPP dimers were determined (Table IV).

As is evident from Table IV, there is no significant effect of the dimer configuration or of the introduction of Cu(II) on the decay rate constants of T_0. The relative populating rate p_z of the o,o linked dimers has considerably decreased w.r.t. H_2TPP, however. This result can be rationalized by realizing, that the excitonic splitting of the S_1 and S_2 states in particular in the o,o dimers decreases the S_2 - T_0 energy difference. Therefore, p_x and p_y, which are predominantly determined by the coupling of the T_0 spin states with the S_2 state

Table IV: Decay rate constants of the lowest triplet state T_0 of H_2TPP, k_x, k_y and k_z, (sec^{-1}) and relative population rates, p_x, p_y and p_z, of the triplet sublevels $|x\rangle$, $|y\rangle$ and $|z\rangle$ of diether linked H_2TPP-CuTPP dimers, $2x10^{-5}$ M in toluene at 4.2 K. Excitation wavelength: 514 nm; emission wavelength: 644 nm. The data are extrapolated to zero light intensity.

compound	k_y [a]	k_x [a]	k_z [a]	p_x [b]	p_y [b]	p_z [b]
H_2TPP [c]	180	480	46	0.51	0.37	0.12
p,p-H_2TPP-H_2TPP [c]	196	508	46	0.52	0.33	0.15
p,p-H_2TPP-CuTPP	100	498	38	0.43	0.50	0.06
o,o-H_2TPP-H_2TPP [c]	161	462	d	0.52	0.48	0
o,o H_2TPP-CuTPP	186	429	26	0.61	0.39	<0.01

a: experimental error ±10%; b: experimental error ±20%;

c: values in benzene/1%pyridine [29].

d: not quoted in view of large experimental error.

(§ 4.1), increase with respect to p_z.

Within experimental error we found no effect of energy transfer from CuTPP on the relative populating rates of the H_2TPP sublevels.

To study the influence of the covalently linked CuTPP on the static triplet state properties of H_2TPP the fluorescence detected magnetic resonance (FDMR) spectra were recorded. The zfs parameters D and E of the T_0 state turned out not to be changed in these dimers, but a linebroadening of the FDMR bands was observed. For o,o H_2TPP-CuTPP a line broadening of 10±2 MHz w.r.t. the linewidth of 50 MHz of monomeric H_2TPP was observed, whereas the FDMR peaks are not broadened for p,p H_2TPP-CuTPP. For the o,o dimer the average centre-to-centre distance, r, between the porphyrin rings is 2.1 nm and for the p,p dimer 2.7 nm [33]. A simple calculation of the magnitude of the average dipolar broadening yields D = 7.2 MHz for r = 2.1 nm and D = 3.4 MHz for r = 2.7 nm, supporting the assumption, that the linebroadening may be ascribed to the dipolar perturbation of the triplet state of H_2TPP by the Cu(II) doublet spin.

7.6 Ligated porphyrin dimers

The excited state kinetics of ZnTPP were investigated for porphyrin dimers, in which a monopyridylporphyrin is ligated to ZnTPP (figure 1b). The pyridylporphyrins are Cu(II)-5-(4-pyridyl)10,15,20-triphenyl porphyrin, CupPyP, and Cu(II)-5-(3-pyridyl)10,15,20-triphenylporphyrin, CumPyP. Like pyridine, the pyridyl group of pyridylporphyrin can serve as a ligand to ZnTPP, as shown by the ligand shift of the fluorescence spectrum of ZnTPP [35] at low temperature upon addition of the pyridylporphyrin, CuPyP (figure 3). Since the solvent should not be able to ligate to ZnTPP, the experiments were done in toluene, which was dried over sodium wire. As judged from the red shift of the Q-bands in the fluorescence excitation spectra at room temperature of ZnTPP in the presence of increasing amounts of CuPyP the equilibrium constant is similar to that for the ligation of pyridine to ZnTPP ($K = 2300 \pm 400\ M^{-1}$ at room temperature [36]). In a slowly frozen solu-

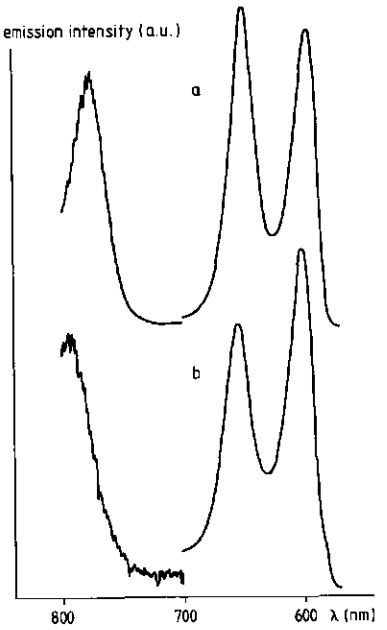

Figure 3 : Emission spectra of $3x10^{-6}$ M ZnTPP a) without and b) with $3x10^{-6}$ M CupPyP in n-octane, T = 77 K; Excitation wavelength: 422 nm.

Table V : Fluorescence lifetimes[a], $\tau_{1,2}$, (10^{-9} sec) and relative fluorescence amplitudes, $\alpha_{1,2}$ of $3x10^{-5}$ ZnTPP in toluene[b] in the presence of pyridine and CumPyP.

	temp.(°C)	non-ligated		ligated	
ligand		α_1	τ_1	α_2	τ_2
-	19	1.0	2.0		
$1x10^{-2}$ M pyridine	-10	0.51	1.82	0.49	1.43
$3x10^{-4}$ M CumPyP	-10	0.22	2.06	0.78	0.092
	19	0.50	2.05	0.50	0.088

a: Excitation wavelength 514.5 nm; detection at 613 ± 20 nm.

b: The solutions were deaerated by flushing oxygen-free argon through the solution during 15 minutes.

tion the ligation at 100 K is complete for a 1:1 mixture of $1x10^{-4}$ M solutions of ZnTPP and CuTPP.

The effect of CumPyP on the fluorescence lifetime of ZnTPP was compared with that of pyridine (Table V). Ligation by pyridine has only a minor effect on the fluorescence lifetime of ZnTPP. Two lifetimes are found for the mixture of ZnTPP and CumPyP, the longest of which equals the lifetime of ZnTPP, indicating that the ligation equilibrium does not shift during the excited state lifetime of ZnTPP. The formation rate constant for the ligated complex ZnTPP-CumPyP in the excited state is therefore smaller than the fluorescence decay rate constant for ZnTPP. The shortest lifetime is assigned to ZnTPP-CumPyP. At lower temperature the amplitude of the shorter component increases, since the ligation equilibrium constant increases at decreasing temperature.

The fluorescence and phosphorescence quantum yields in frozen solutions were determined relative to ZnTPP ligated with pyridine (Table VI). For comparison this table also contains quantum yields for ZnTPP ligated with other metallopyridylporphyrins.

As can be seen from Table VI ligation of PdpPyP to ZnTPP in stead of a small pyridine group does not influence the fluorescence and the phosphorescence quantum yields of ZnTPP. In ZnTPP-PdpPyP energy transfer from ZnTPP to PdpPyP can not occur due to the unfavourable energy levels. In ZnTPP-NipPyP energy transfer occurs from ZnTPP triplet state to the d-d* manifold of NipPyP. The d-d* states in Ni-porphyrins are known to cause a very efficient decay of excited Ni-porphyrins to the ground state [37]. In ZnTPP-H_2pPyP efficient energy transfer occurs from ZnTPP to H_2pPyP, as follows from the fluorescence excitation spectra of H_2pPyP. There is only a small effect of the substitution position (meta or para) of the porphyrin at the pyridylgroup relative to the pyridyl N-atom, although the dimer structures for ZnTPP-CumPyP and ZnTPP-CupPyP are expected to be different.

The triplet decay constants for ZnTPP as monomer and in the dimers ZnTPP-H_2pPyP and ZnTPP-CupPyP were determined from the phosphorescence lifetimes at 77 K (Table VII). As is evident from this table, there is again no significant effect of the presence of Cu(II) in the ligand

Table VI: Fluorescence and phosphorescence quantum yields (ϕ_f^r, ϕ_p^r, resp.) of ZnTPP ligated with pyridylporphyrins relative to the yields of ZnTPP ligated with pyridine in dry toluene at 100 K.

ligand	ϕ_f^r	ϕ_p^r	ϕ_p^r/ϕ_f^r
pyridine	1	1	1
CupPyP	0.57	1.3	2.3
CumPyP	0.55	1.0	1.8
NipPyP	0.98	0.04	0.04
MnpPyP	0.07	<0.04	<0.57
PdpPyP	1.03	1.03	1
H_2pPyP	<0.04	<0.04	

Table VII: Phosphorescence lifetimes[a], τ_p, (10^{-3}sec) of $2x10^{-4}$ M ZnTPP in toluene at 77K in the the presence of several pyridyl ligands[b].

compound	τ_p
ZnTPP	77
ZnTPP-Py	18
ZnTPP-CupPyP	21
ZnTPP-H2pPyP	19

a: Excitation with 80 mW light at 476 nm, using a cw CR4 Ar ion laser by light-on light-off measurement; detection at 798 nm.

b: The concentration of the ligands is: 1 vol% pyridine, $2x10^{-4}$ M CupPyP and $2x10^{-4}$ M H_2pPyP, respectively.

on the lifetime of the ZnTPP T_0 state. The observed decrease of the triplet lifetime in the presence of various ligands is obviously entirely due to ligation of the pyridylgroup to ZnTPP.

The influence of CuPyP on the excited state kinetics and on the static triplet properties of ZnTPP was also investigated by ESR. The light-minus-dark ESR spectrum of the dimer was compared with that of a mixture of non-interacting ZnTPP and CuTPP at the same concentration (figure 4). The influence of CuPyP on the triplet ESR spectrum is observed in the linebroadening of the H_x, H_y and H_z-peaks ($\delta\Delta H_z \approx$ 22 G).

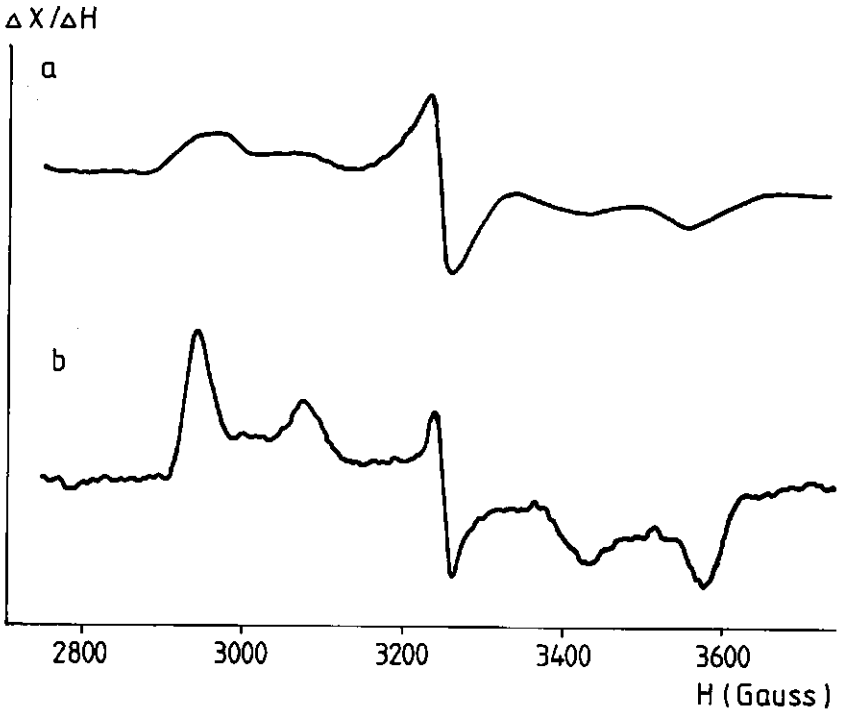

Figure 4 : Light modulated ESR spectra of a) $1x10^{-4}$ M ZnTPP/ $2x10^{-4}$ M CupPyP and b) $1.5x10^{-4}$ M ZnTPP/$3x10^{-4}$ M CuTPP in toluene both at 108 K. Excitation with 150 W Xe lamp, chopped at 20 Hz with lock-in detection. Microwave frequency 9.1 GHz, power 5 mW; field modulation amplitude 25 G.

The coupling with the Cu(II)-spin does not lead to a simple splitting of triplet ESR lines, probably because the principle axes of the dipolar and the anisotropic exchange tensors, describing the interaction between the Cu(II) spin and the ZnTPP T_0 spins need not be coincident with the triplet axes of the ZnTPP. For a perpendicular orientation of the dimer, as in figure 1b, the Zn-Cu distance is 1.02 nm, since the Zn-pyridyl-N distance is 0.25 nm [38], and the pyridyl-N-Cu distance is 0.77 nm, as determined from the crystallographic data of H_2TPP [39]. A simple calculation for the dipolar linebroadening due to the Cu(II) doublet spin, using the Van Vleck equation [40] yields a broadening of 18.5 G at a Zn-Cu distance of 1.02 nm, which compares well with the experimentally observed 22 G.

The signal at g = 2 in the light-minus-dark difference ESR spectrum has increased in the dimer w.r.t. that in the reference solution, containing the separate compounds at the same concentrations and exhibits ^{14}N hyperfine coupling of Cu(II)-porphyrin.

We will consider the three possible mechanisms mentioned in § 7.1 for the quenching of the fluorescence of ZnTPP in ZnTPP-CumPyP and ZnTPP-CupPyP, explaining also the observed high ϕ_p^r/ϕ_f^r ratio: (i) energy transfer from the ZnTPP singlet state to the CuPyP singdoublet state followed by energy transfer from the CuPyP tripdoublet state to the ZnTPP triplet state. The second process explains the high ϕ_p^r/ϕ_f^r ratio for the dimer, (ii) enhanced intersystem crossing due to the paramagnetic Cu(II)-ion and (iii) electron transfer from the donor ZnTPP to the acceptor CuPyP.

ad (i): If energy transfer occurs from ZnTPP to CuPyP the absorption spectrum of ZnTPP is expected to be observed in the excitation spectrum of the quartet emission of CuPyP. The second ENT step would be observed in the phosphorescence excitation spectrum of ZnTPP. Both effects are not observed and therefore energy transfer is considered to be not operative as quenching mechanism for the ZnTPP fluorescence.

ad (ii): The triplet decay rate constant of ZnTPP is not enhanced by the ligand CuPyP (Table VII). Enhanced intersystem crossing from the excited singlet state to the triplet state is therefore unlikely to

occur.

ad (iii): The large g = 2 signal and the observation of the Cu(II)-porphyrin signal in the light-minus-dark ESR spectrum indicate electron transfer as a possible mechanism. Cu(II)pPyP is observed in the light-minus-dark ESR spectrum at g = 2, because after ET CupPyP is reduced to diamagnetic Cu(I)pPyP, decreasing the amount of paramagnetic Cu(II)pPyP in the solution. This ESR signal is superimposed on that of the $ZnTPP^+$-kation. The high ratio of ϕ_p^r/ϕ_f^r (Table VI) for ZnTPP in the dimer can be explained by efficient singlet-triplet mixing in the charge-separated state, similarly as observed for closely-spaced porphyrin-anthraquinone molecules (§ 4.4). The energy of the radical pair state is at 1.84 eV, if we use E_{ox}(ZnTPP) = 0.71 V in CH_2Cl_2 vs SCE [25] and E_{red}(CuPyP) = -1.13 V vs SCE in DMSO (from E_{red}(CuTPP) = -1.20 and a correction of 70 mV for the 4-pyridyl group [41]). The ET process is exothermic with ΔG = -0.21 eV. The energy of the radical pair is higher than that of the triplet state (E_T= 1.58 eV) and recombination via the triplet state can therefore occur (figure 2d).

7.7 Conclusion

In paragraph 7.1 three possible mechanisms were given through which a Cu(II)-porphyrin may influence the excited state kinetics of a H2- or Zn-porphyrin. From the preceding paragraphs we conclude, that if electron transfer is energetically possible, it is this mechanism through which the fluorescence is quenched. Electron transfer occurs in dimers of watersoluble porphyrins H_2TPPC-CuTMPyP and H_2TMPyP-CuTPPC and in the dimers ZnTPP-CumPyP and ZnTPP-CupPyP. In the latter dimers recombination to the triplet state is energetically possible and is indeed observed. In the diether liked tetraphenylporphyrins, in which electron transfer is energetically unfavourable, energy transfer occurs from CuTPP to the H_2TPP triplet state.

The influence of the doublet spin of the Cu(II) atom on the static triplet state properties of the H_2- and Zn-porphyrins is reflected in the dipolar linebroadening of the FDMR- and ESR spectra for

ZnTPP-CupPyP and o,o H_2TPP-CuTPP. In H_2TPPC-CuTMPyP and H_2TMPyP-CuTPPC no triplet states could be detected due to efficient ET in the dimer and in p,p H_2TPP-CuTPP the interchromophore distance is too large to observe any line broadening.

references

1. V.A.Kuzmin and A.S.Tatikolov, Chem. Phys. Lett. 53 (1978) 606.
2. R.A.Caldwell and R.E.Schwerzel, J. Am. Chem. Soc. 94 (1972)1035.
3. G.Blondeel, A.Harriman, G.Porter and A.Wilowska, J.Chem.Soc, Faraday Trans.2, 80 (1984) 867.
4. G.Porter and M.Wright, Discuss. Faraday Soc. 27 (1959) 18.
5. U.Hofstra, R.B.M.Koehorst, T.J.Schaafsma, Chem. Phys. Lett. 130 (1986) 555.
6. R.L.Brookfield, H.Ellul and A.Harriman, Faraday Trans. 2 (1985) 1837.
8. F.P.Schwarz, M.Gouterman, Z.Muljiani and D.H.Dolphin, Bioinorg. Chem 2 (1972) 1.
9. J.C.Mialocq, C.Gianotti, P.Maillard, H.Momenteau, Chem. Phys. Lett. 112 (1984) 87.
10. S.Konishi, M.Hoshino and M.Imamura, J. Phys. Chem. 87 (1983) 1490.
11. O.Ohno, Y.Ogasawara, M.Asano, Y.Kajii, Y.Kaizu, K.Obi and H.Kobayashi, J. Phys. Chem. 91 (1987) 4269.
12. R.L.Ake and M.Gouterman, Theor. Chim. Acta, 15 (1969) 20.
13. C.P.Keijzers, Electron Spin Res. 10B (1987) 1.
14. C.Kollmar and H.Sixl, Mol. Phys. 45 (1982) 1199.
15. M.Elliot, J.Chem.Soc.,Chem. Comm. 399 (1978).
16. M.J.Gunter, L.N.Mander, G.McLaughlin, K.S.Murray, K.J.Berry, P.E.Clarke, D.A.Buckingham, J. Am. Chem. Soc. 102 (1980) 1470.
17. D.A.Buckingham, J. Am. Chem. Soc. 100 (1978) 2899.
18. R.G.Little, J.A.Anton, P.A.Loach and J.A.Ibers, J. Heterocyclic. Chem. 12 (1975) 343.
19. A.Shamim, P.Worthinton and P.Hambright, J. Chem. Soc. Pak. 3 (1981) 1.
20. R.G. Little, J. Heterocyclic Chem. 15 (1978) 203.

21. S.J.van der Bent, P.A.de Jager and T.J.Schaafsma, Rev. Sci. Instr. 47 (176) 117.
22. R.Avarmaa, Mol. Phys. 37 (1979) 441.
23. A.van Hoek, J.Vervoort, A.J.W.G.Visser, J. Biochem. Biophys. Meth. 7 (1983) 243.
24. N.M.Richardson and I.O.Sutherland, Tetrahedr. Lett. 26 (1985) 3739.
25. D.G.Davis in "The Porphyrins", D.Dolphin ed., Academic Press, New York (1978), Vol 5, p. 127.
26. CRC Handbook of Chem. and Phys., CRC Press Inc., Bota Raton (1982).
27. A.Harriman, M.C.Richoux and P.Neta, J. Phys. Chem. 87 (1983) 4957.
28. K.Kalyanasundaram and M.Neumann-Spallart, J. Phys. Chem. 80 (1982) 5163.
29. L.Benthem, Ph.D.Thesis, Wageningen (1984).
30. G.J.Kavarnos and N.J.Turro, Chem. Rev. 86 (1986) 401.
31. M.Gouterman in "The Porphyrins", D.Dolphin ed., Academic Press, New York (1978), Vol 3, p.1.
32. A.Harriman, J.Chem.Soc., Faraday Trans. 1, 77 (1981) 369.
33. L.Benthem, R.B.M.Koehorst and T.J.Schaafsma, Magn. Res. Chem. 23 (1985) 732.
34. I.Y. Chan in "Triplet State ODMR Spectroscopy", R.H.Clarke ed., Wiley, New York (1982), p. 1.
35. R.Humphry-Baker and K.Kalyanasundaram, J. Photochem. 31 (1985) 105.
36. C.B.Storm, H.Turner and M.B.Swann, Inorg. Chem. 23, 2743 (1984).
37. A.Harriman, J.Chem.Soc.,Faraday Trans. 1 76 (1980) 1978.
38. R.J.Abraham, G.R.Bedford and B.Wright, Org. Magn. Res. 18 (1982) 45.
39. S.J.Silvers and A.Tulinsky, J. Am. Chem. Soc. 89 (1967) 3331.
40. A.Carrington and A.D.McLachlan, Introduction to Magnetic Resonance Harper Row, New York, (1969).
41. P.Worthington, P.Hambright, R.F.X.Williams, J.Reid, C.Burnham, A.Shamim, J.Turay, D.M.Bell, R.Kirkland, R.G.Little, N.Datta-Gupta and U.Eisner, J. Inorg. Biochem. 12 (1980) 281.

CHAPTER 8

Summary

This Thesis describes investigations on photoinduced electron transfer (ET) for several compounds, serving as model systems of the natural photosynthesis. In addition, the properties of the systems, e.g. the conformation in solution and the electronic properties of the photoexcited states are treated.

Chapter 2 discusses present theories of photoinduced electron transfer. The following factors appear to effect the electron transfer rate constants:

- donor-acceptor distance
- nature of the linking chain
- conformation of donor and acceptor
- spin dynamics
- change in free energy, ΔG, of the process
- solvent

Chapter 3 describes optical and magnetic resonance experiments to study the electronic properties, the conformations and the electron transfer rates in the model systems.

In this Thesis three different classes of donor-acceptor compounds, containing porphyrins as light-sensitive compounds are treated in detail.

Chapter 4 describes the properties of sulfonyloxy-linked porphyrin-anthraquinone compounds and the porphyrin moiety. The electronic properties of the porphyrin (free base diphenyletioporphyrin) were examined by fluorescence detected magnetic resonance (FDMR). The triplet state properties and the optical absorption spectra of the diphenyletioporphyrin could be rationalized by applying the four-orbital model of Gouterman. In frozen n-octane at 4.2 K the porphyrin in the two sites exhibits different degrees of configuration interaction, indicating that the medium around the molecule exerts a strong effect on the properties of the excited states. The electron transfer from this porphyrin to covalently linked anthraquinone appeared to be very fast for three porphyrin-anthraquinone compounds, in which the

anthraquinone-2-sulfonyloxy group is substituted at a phenylgroup of the porphyrin at the ortho-, meta-, or para-postion. Forward ET in these compounds in CH_2Cl_2 occurred in less then 3 picoseconds after photoexcitation. If the two molecules are not closely folded, so that the through-space electronic coupling is small, ET is most likely to occur through the sulfonyloxy linking bridge. The sulfonyloxy bridge can easily accomodate an electron, enhancing the participation of the empty orbitals of the bridge in a superexchange coupling through the bridge. This illustrates the effect of the nature of the bridge on the electron transfer. In one of the porphyrin-anthraquinone compounds a high triplet yield is found, resulting from a singlet-triplet conversion in the charge-separated state. The same process occurs in natural photosynthesis and is then caused by spin-dephasing due to hyperfine interactions and different g-values. From the triplet ESR spectrum the mechanism of the singlet-triplet conversion for the model compound appears to be different and is attributed to spin-orbit coupling within the charge-separated state. In § 4.3 the covalently linked porphyrin-anthraquinone systems were compared with the freely diffusing systems. The electron transfer rate in the freely diffusing system appears to be diffusion-limited.

Chapter 5 focusses on another class of porphyrin complexes in which electron transfer occurs, namely dimers of oppositely charged water-soluble porphyrins. Heterodimers with two different central atoms can easily be formed by combining different positively and negatively charged porphyrins, resulting in a modular system, of which the energetics can easily be varied by varying the central atoms on the two porphyrin constituents of the dimers. In § 5.1 it is shown that the lowest excited triplet state for those dimers that do not exhibit ET, is localized on one of the constituents of the dimer and has a partly charge transfer character. §§ 5.2 and 5.3 report the structure of the dimers in solution as investigated by ^1H NMR. From ring current shift calculations the porphyrin macrocycles turn out to be at a very close distance (3.1 Å) and shifted along the aryl-aryl axis over 4.2 Å optimizing the interaction between the porphyrin monomers. For some dimers also higher aggregates can be formed with an interchromophore

orientation equal to that in the dimers. §§ 5.1 and 5.4 discuss the observed relation between the fluorescence quenching, caused by electron transfer, with the energetics of these complexes. The porphyrins were extended with extra donor and acceptor groups to separate the charges after the initial formation after photoexcitation of the dimer.

These water-soluble porphyrin dimers are interesting for further research for two reasons: (i) They form oriented stacks of alternatingly charged porphyrins and (ii) their behaviour (ET or not) can be controlled by the central atoms in the components.

Chapter 6 discusses the third class of donor-acceptor compounds that were studied in this work. These were flexibly linked donor-tetraphenylporphyrin-acceptor triads and their components. The average ground-state conformations of these compounds could be determined from ^{1}H NMR by ring current shift calculations. The rate constants for forward ET are found to increase with increasing values of the change in free energy ΔG: the ΔG value for forward ET for these compounds are shown to be in the Marcus normal region. The nature of the bridge is found to be very important, because it affects the redoxpotentials of the acceptor anthraquinone and contributes to the electronic coupling between donor and acceptor via a superexchange mechanism through the bridge.

In chapter 7 the quenching of the fluorescence of a free base or zinc porphyrin by a paramagnetic copper porphyrin was studied for different dimers. In dimers of oppositely charged porphyrins and in dimers consisting of zinc tetraphenylporphyrin ligated by the pyridyl group of copper pyridyltriphenylporphyrine, electron transfer acts as quenching mechanism of the fluorescence of the diamagnetic porphyrin. In covalently linked free base and copper tetraphenylporphyrin electron transfer is energetically forbidden and energy transfer occurs from the copper porphyrin to the triplet state of the free base porphyrin.

SAMENVATTING

Dit proefschrift beschrijft onderzoek naar lichtgeïnduceerde electron overdracht in een aantal modelverbindingen waarmee de eerste stappen van het natuurlijk fotosyntheseproces kunnen worden nagebootst. Verder worden de fysisch-chemische eigenschappen van deze verbindingen, zoals de conformatie in oplossing en de electronische eigenschappen van de aangeslagen toestanden, behandeld.

Hoofdstuk 2 behandelt de theoretische concepten, waarmee momenteel electron-overdracht wordt beschreven. De volgende factoren zijn voor dat proces van belang:

- de donor-acceptor afstand
- de aard van de verbinding tussen donor en acceptor
- de conformatie van donor en acceptor
- de spin toestand van donor en acceptor
- de vrije energie verandering (ΔG) van het proces
- het medium, waarin het proces zich afspeelt

Hoofdstuk 3 beschrijft optische en magnetische resonantie experimenten om de electronische eigenschappen, de conformaties en de electron overdrachtssnelheden te bestuderen.

In dit proefschrift worden drie soorten donor-acceptor verbindingen in detail behandeld. Alle drie hebben ze een porfyrinemolecuul als lichtgevoelig molecuul:

Hoofdstuk 4 beschrijft de eigenschappen van porfyrine-anthrachinon verbindingen, waarin beide moleculen via een sulfonyloxy-brug verbonden zijn, alsmede de eigenschappen van het porfyrine molecuul. De electronische eigenschappen van het porfyrine (vrije base difenyletioporfyrine) werden onderzocht met fluorescentie gedetecteerde magnetische resonantie (FDMR). De triplet eigenschappen en de optische absorptiespectra van het difenyletioporfyrine konden worden gerationaliseerd met behulp van de vier-orbitalen theorie van Gouterman. In bevroren n-octaan bij 4.2 K bevindt het porfyrine zich in twee verschillende sites en vertoont in deze sites een verschillende mate van configuratie interactie, hetgeen er op wijst, dat het medium rond dit molecuul een groot effect heeft op de eigenschappen van de aangeslagen toestanden. De electron-overdracht van dit porfyrine naar

een covalent gebonden anthrachinon molecuul bleek zeer snel te zijn in drie verbindingen, waarin de anthrachinon-2-sulfonyloxy groep respectievelijk is gelocaliseerd op de ortho-, meta- of parapositie van een fenyl groep van het porfyrine. De ladingsscheiding in deze verbindingen in CH_2Cl_2 vond plaats minder dan 3 picoseconden na excitatie met een lichtpuls.

Als de moleculen niet gevouwen zijn, zodat de electronische koppeling door de ruimte slechts gering is, vindt electron overdracht waarschijnlijk door de verbindende sulfonyloxy brug plaats. Deze brug heeft een electronenzuigende werking, zodat de deelname van lege orbitalen van de brug in een superexchange koppeling door de brug bevorderd wordt. Dit illustreert het effect van de brug op de electron overdracht. Voor één van de porfyrine-anthrachinon verbindingen wordt een hoge triplet opbrengst gevonden, die veroorzaakt wordt door een singlet-triplet overgang in de ladingsgescheiden toestand. Hetzelfde proces vind in de natuurlijke fotosynthese plaats, maar wordt dan veroorzaakt door spin-defasering tengevolge van hyperfijnkoppeling en verschil in g-waarden van de radicalen. Uit het triplet ESR spectrum werd afgeleid, dat de singlet-triplet overgang voor deze modelverbinding het gevolg was van spin-baan koppeling in de ladingsgescheiden toestand. In § 4.3 werden de covalent gebonden porfyrine-anthrachinon verbindingen vergeleken met de systemen, waarin deze moleculen vrij in oplossing zijn. De electron overdrachtssnelheid voor de vrije systemen blijkt gelimiteerd te worden door de diffusiesnelheid in oplossing.

Hoofdstuk 5 richt de aandacht op een andere klasse porfyrine complexen, waarin electron-overdracht optreedt, namelijk dimeren van wateroplosbare porfyrines. Heterodimeren met twee verschillende centrale atomen kunnen gemakkelijk gevormd worden door twee verschillende, tegengesteld geladen, porfyrines bij elkaar te voegen. Dit resulteert in een modulair systeem, waarvan de energieën eenvoudig gevarieerd kunnen worden door de centrale atomen van de twee porfyrines in het dimeer te variëren. In § 5.1 wordt aangetoond dat de laagste aangeslagen triplet toestand van de dimeren waarin geen electron-overdracht optreedt, gelocaliseerd is op een van beide porfyrines en een gedeeltelijk charge transfer karakter heeft. In §§ 5.2 en 5.3 wordt de

structuur van de dimeren in oplossing gerapporteerd, zoals deze bepaald is met ^{1}H NMR. Berekeningen van de kringstroom bijdrage aan de chemische verschuivingen in het NMR spectrum laten zien dat de porfyrines zeer dicht op elkaar zitten (3.1 Å) en 4.2 Å verschoven zijn langs de aryl-aryl as, waardoor de interactie tussen de porfyrine monomeren geoptimaliseerd is. Voor sommige dimeren kunnen hogere aggregaten gevormd worden, waarin de onderlinge orientatie identiek is aan die in de dimeren. §§ 5.1 en 5.4 behandelen het waargenomen verband tussen de fluorescentie doving, die veroorzaakt wordt door electron-overdracht, en de verandering in vrije energie die bij electron-overdracht optreedt, voor deze complexen. De porfyrines werden nog uitgebreid met extra donor- en acceptor groepen om de ladingen verder te scheiden na de initiële ladingsscheiding na fotoexcitatie van de dimeren.

Deze wateroplosbare porfyrines zijn interessant voor verder onderzoek om twee redenen: (i) Ze vormen georienteerde lagen ('stacks') van afwisselend geladen porfyrines en (ii) hun gedrag, namelijk of er wel of niet electron overdracht optreedt, kan worden gecontroleerd door middel van de centrale atomen van de componenten.

Hoofdstuk 6 behandelt een derde klasse van donor-acceptor verbindingen die in dit proefschrift aan de orde komen. Het gaat hier om donor-porfyrine-acceptor triaden, die via een flexibele keten met elkaar verbonden zijn, en hun componenten. De gemiddelde conformatie in oplossing van deze verbindingen kon worden bepaald uit de ^{1}H NMR spectra met behulp van berekeningen van de kringstroom bijdrage aan de chemische verschuiving. De snelheidsconstanten die de ladingsscheiding beschrijven bleken toe te nemen met ΔG: de ΔG waarden voor ladingsscheiding voor deze verbindingen bleken in het normale gebied te liggen van de Marcus curve. De aard van de brug bleek zeer belangrijk te zijn, omdat hij zowel de redoxpotentialen van donor en acceptor beinvloedt als bijdraagt aan de electronische koppeling via een superexchange mechanisme door de brug.

In hoofdstuk 7 wordt de fluorescentie doving van een vrije base of een zink porfyrine door een Cu(II)-porfyrine bestudeerd voor verschillende typen dimeren. In dimeren van tegengesteld geladen porfyrines en

in dimeren die bestaan uit zink tetrafenylporfyrine, geligandeerd door de pyridyl groep van Cu(II)-pyridyltrifenylporfyrine vormt electron overdracht het mechanisme voor de fluorescentie doving. In covalent gebonden vrije base en Cu(II)-tetrafenylporfyrines is de electron overdracht energetisch verboden en treedt energie-overdracht op van het Cu(II)-porfyrine naar de triplet toestand van het vrije base porfyrine.

Ulbert Hofstra werd op 20 april 1958 geboren te Balk (Gaasterland). In 1976 legde hij het eindexamen VWO af aan de Christelijke Scholengemeenschap "Menso Alting College" te Hoogeveen en begon aan de studie Scheikunde aan de Vrije Universiteit te Amsterdam. In 1980 behaalde hij het kandidaatsexamen. De doctoraalstudie omvatte Fysische Chemie (hoofdvak), Anorganische Chemie (eerste bijvak) en Electronica (tweede bijvak). Tevens haalde hij de eerste graads onderwijsbevoegdheid in de scheikunde.

In januari 1984 studeerde hij af, kwam in dienst van Z.W.O. en begon op de vakgroep Moleculaire Fysica van de Landbouwuniversiteit het onderzoek dat tot dit proefschrift leidde.